FIELDIANA

Geology

NEW SERIES, NO. 40

Sauropterygia from the Middle Triassic of Makhtesh Ramon, Negev, Israel

Olivier Rieppel
Jean-Michel Mazin
Eitan Tchernov

February 26, 1999
Publication 1499

PUBLISHED BY FIELD MUSEUM OF NATURAL HISTORY

Information for Contributors to Fieldiana

General: *Fieldiana* is primarily a journal for Field Museum staff members and research associates, although manuscripts from nonaffiliated authors may be considered as space permits.

The Journal carries a page charge of $65.00 per printed page or fraction thereof. Payment of at least 50% of page charges qualifies a paper for expedited processing, which reduces the publication time. Contributions from staff, research associates, and invited authors will be considered for publication regardless of ability to pay page charges, however, the full charge is mandatory for nonaffiliated authors of unsolicited manuscripts. Three complete copies of the text (including title page and abstract) and of the illustrations should be submitted (one original copy plus two review copies which may be machine copies). No manuscripts will be considered for publication or submitted to reviewers before all materials are complete and in the hands of the Scientific Editor.

Manuscripts should be submitted to Scientific Editor, *Fieldiana,* Field Museum of Natural History, Chicago, Illinois 60605-2496, U.S.A.

Text: Manuscripts must be typewritten double-spaced on standard-weight, 8½- by 11-inch paper with wide margins on all four sides. If typed on an IBM-compatible computer using MS-DOS, also submit text on 5¼-inch diskette (WordPerfect 4.1, 4.2, or 5.0, MultiMate, Displaywrite 2, 3 & 4, Wang PC, Samna, Microsoft Word, Volkswriter, or WordStar programs or ASCII).

For papers over 100 manuscript pages, authors are requested to submit a "Table of Contents," a "List of Illustrations," and a "List of Tables" immediately following title page. In most cases, the text should be preceded by an "Abstract" and should conclude with "Acknowledgments" (if any) and "Literature Cited."

All measurements should be in the metric system (periods are not used after abbreviated measurements). The format and style of headings should follow that of recent issues of *Fieldiana.*

For more detailed style information, see *The Chicago Manual of Style* (13th ed.), published by The University of Chicago Press, and also recent issues of *Fieldiana.*

References: In "Literature Cited," book and journal titles should be given in full. Where abbreviations are desirable (e.g., in citation of synonymies), authors *consistently* should follow *Botanico-Periodicum-Huntianum* and *TL-2 Taxonomic Literature* by F. A. Stafleu & R. S. Cowan (1976 *et seq.*) (botanical papers) or *Serial Sources for the Biosis Data Base* (1983) published by the BioSciences Information Service. Names of botanical authors should follow the "Draft Index of Author Abbreviations, Royal Botanic Gardens, Kew," 1984 edition, or *TL-2.*

References should be typed in the following form:

CROAT, T. B. 1978. Flora of Barro Colorado Island. Stanford University Press, Stanford, Calif., 943 pp.

GRUBB, P. J., J. R. LLOYD, AND T. D. PENNINGTON. 1963. A comparison of montane and lowland rain forest in Ecuador. I. The forest structure, physiognomy, and floristics. Journal of Ecology, **51:** 567–601.

LANGDON, E. J. M. 1979. Yagé among the Siona: Cultural patterns in visions, pp. 63–80. In Browman, D. L., and R. A. Schwarz, eds., Spirits, Shamans, and Stars. Mouton Publishers, The Hague, Netherlands.

MURRA, J. 1946. The historic tribes of Ecuador, pp. 785–821. In Steward, J. H., ed., Handbook of South American Indians. Vol. 2, The Andean Civilizations. Bulletin 143, Bureau of American Ethnology, Smithsonian Institution, Washington, D.C.

STOLZE, R. G. 1981. Ferns and fern allies of Guatemala. Part II. Polypodiaceae. Fieldiana: Botany, n.s., **6:** 1–522.

Illustrations: Illustrations are referred to as "figures" in the text (not as "plates"). Figures must be accompanied by some indication of scale, normally a reference bar. Statements in figure captions alone, such as "× 0.8," are not acceptable. Captions should be typed double-spaced and consecutively. See recent issues of *Fieldiana* for details of style.

All illustrations should be marked on the reverse with author's name, figure number(s), and "top."

Figures as submitted should, whenever practicable, be 8½ by 11 inches (22 × 28 cm) and may not exceed 11½ by 16½ inches (30 × 42 cm). Illustrations should be mounted on boards in the arrangement to be obtained in the printed work. This original set should be suitable for transmission to the printer as follows: Pen and ink drawings may be originals (preferred) or photostats; shaded drawings must be originals, but within the size limitation; and photostats must be high-quality, glossy, black and white prints. Original illustrations will be returned to the corresponding author upon publication unless otherwise specified.

Authors who wish to publish figures that require costly special paper or color reproduction must make prior arrangements with the Scientific Editor.

Page Proofs: *Fieldiana* employs a two-step correction system. The corresponding author will normally receive a copy of the edited manuscript on which deletions, additions, and changes can be made and queries answered. Only one set of page proofs will be sent. All desired corrections of type must be made on the single set of page proofs. Changes in page proofs (as opposed to corrections) are very expensive. Author-generated changes in page proofs can only be made if the author agrees in advance to pay for them.

♾ **This paper meets the requirements of ANSI/NISO Z39.48-1992 (Permanence of Paper).**

FIELDIANA

Geology

NEW SERIES, NO. 40

Sauropterygia from the Middle Triassic of Makhtesh Ramon, Negev, Israel

Olivier Rieppel

Department of Geology
Field Museum of Natural History
Roosevelt Road at Lake Shore Drive
Chicago, Illinois 60615
U.S.A.

Jean-Michel Mazin

Laboratoire de Géobiologie
Université de Poitiers
Faculté des Sciences Fondamentales et Appliquées
40, Avenue du Recteur Pineau
86022 Poitiers
France

Eitan Tchernov

Department of Evolution, Systematics, and Ecology
Hebrew University
Givat-Ram
Jerusalem 91904
Israel

Accepted March 31, 1998
Published February 26, 1999
Publication 1499

PUBLISHED BY FIELD MUSEUM OF NATURAL HISTORY

ISSN 0096-2651
PRINTED IN THE UNITED STATES OF AMERICA

Table of Contents

List of Illustrations

List of Tables

Sauropterygia from the Middle Triassic of Makhtesh Ramon, Negev, Israel

Olivier Rieppel **Jean-Michel Mazin** **Eitan Tchernov**

Abstract

The Sauropterygia of the Middle Triassic Muschelkalk of Makhtesh Ramon, Negev, are reviewed, and their evolutionary and paleobiogeographic history is reconstructed on the basis of cladistic analysis of their interrelationships. The fauna includes cyamodontoid placodonts (*?Psephosaurus*) as well as Eosauropterygia such as possible pachypleurosaurs, *Simosaurus* sp., at least three diagnosable taxa of *Nothosaurus* (*Nothosaurus* cf. *N. giganteus, N. haasi* n. sp., and *N. tchernovi*), and one lariosaur (*Lariosaurus stensioei*).

The use of cyamodontoids for historical biogeographic analysis remains impeded because the diagnosis of lower Muschelkalk taxa (*?Psephosaurus, Cyamodus*) remains incomplete. The taxic composition of the eosauropterygian fauna, as well as the pattern of cladistic relationships of its nothosaurian components, indicates paleobiogeographic affinities of the Makhtesh Ramon fauna with the Germanic and Alpine realm, supporting the hypothesis of a Burgundian Gate that connected the Germanic basin with the southern branch of the developing Neotethys during upper Anisian and Ladinian times.

Refined analysis of *Nothosaurus* documents the occurrence of the sister species *N. haasi* n. sp. and *N. tchernovi* at Makhtesh Ramon, which provides evidence for dichotomous speciation and habitat partitioning within the intraplatform basin habitat characteristic of the northern Gondwanan shelf (southern margin of the developing southern branch of the Neotethys) during Anisian and Ladinian times.

Introduction

The first sauropterygian fossil reported from Palestine (Israel) was a right humerus of *Nothosaurus* from the Wady Ayun Musa northeast of the Dead Sea (Cox, 1924). Cox's (1924) work focused mainly on invertebrates, and he found the Trans-Jordan Trias to yield a "fauna remarkable for its unique association of 'Alpine' and 'German' elements" (Cox, 1932, p. 93). The occurrence of vertebrate fossils in the Middle Triassic deposits of Makhtesh Ramon in the Negev (Fig. 1), southern Israel, was first signaled by Shaw (1947). A vertebra collected in the area by J. Wahrmann in 1949 was described by Swinton (1952). Further collections from Makhtesh Ramon were reported by Brotzen (1955), who identified what he believed to be the earliest occurrence of a cyamodontoid placodont of the genus *Psephosaurus,* along with bones and teeth "of numerous nothosaurian and other reptiles" (Brotzen, 1955, p. 404). In the same year, Peyer (1955) exhibited tetrapods from Makhtesh Ramon at the annual meeting of the Swiss Paleontological Society, including a skull fragment and ilium of a large *Nothosaurus* and vertebrae of the prolacertilian *Tanystropheus.* The stratigraphy of the Makhtesh Ramon Muschelkalk was reviewed by Brotzen (1957) in a study that also included the formal description of two cyamodontoid placodonts, namely *Psephosaurus mosis* and *P. picardi.* The following years witnessed a series of papers by the late Professor G. Haas systematically describing the vertebrate fossils from the Muschelkalk of Makhtesh Ramon (Haas, 1959, 1969, 1975: Placodontia; Haas, 1963: *Micronothosaurus stensioei*; Haas, 1980: *Nothosaurus tchernovi*; Haas, 1981: *Simosaurus*).

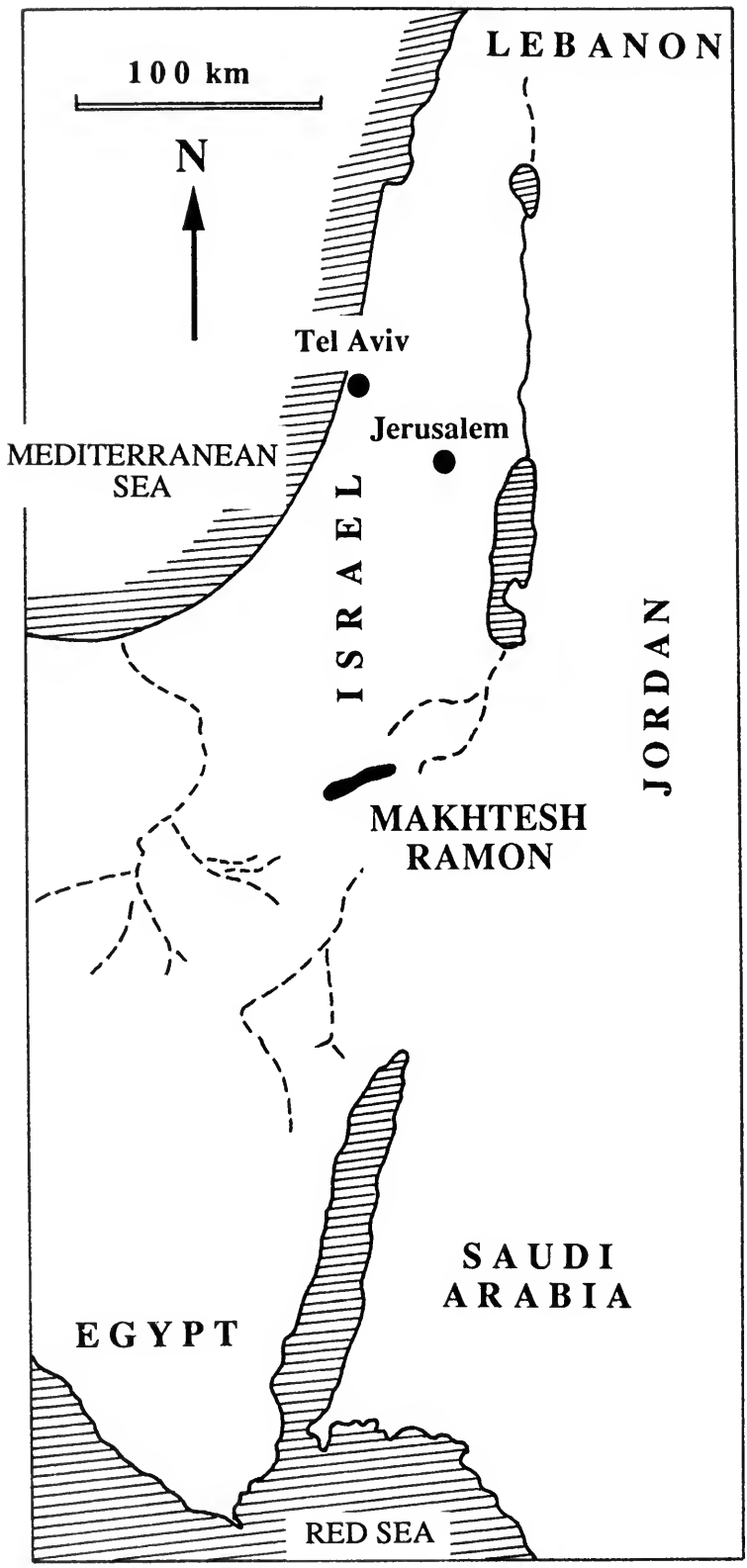
100 km
N
LEBANON
Tel Aviv
Jerusalem
MEDITERRANEAN SEA
ISRAEL
JORDAN
MAKHTESH RAMON
SAUDI ARABIA
EGYPT
RED SEA

During a visit to the Hebrew University of Jerusalem (HUJ), one of us (J.-M. M.) surveyed the extensive collections of vertebrate remains from Makhtesh Ramon that had accumulated since Haas's work and selected a portion of the material, which was taken out on loan to Paris to be prepared using acid. This material forms the core of the present descriptions, to which was added other, less well-preserved and/or prepared material that is diagnostic, and a review of previously described taxa.

Geological Provenience of the Material

The marine Middle Triassic (Muschelkalk) of Makhtesh Ramon in the Negev was deposited in a basin that formed by rapid subsidence of a previously continental area (Freund et al., 1975; Hirsch, 1984). The boundary of the subsiding basin ran across the central and northern Negev (Freund et al., 1975). Subsidence preceded the onset of rifting in late Anisian times along what was to become the North African coast, and which crossed the present Levant coast and Syria to reach the margin of the Neotethys Ocean (Garfunkel & Derin, 1984; May, 1991). The result of these events, initiating the opening of the southern branch of the Neotethys (Sengör et al., 1984), was an embayment of the Neotethys that was centered in Israel and southwestern Syria (May, 1991; Fig. 2). Triassic strata in Israel reach a thickness of 500 to 1,100 m and are particularly well exposed at the Makhtesh Ramon locality in the Negev, located in the center of the Triassic–Jurassic "low" (Freund et al., 1975).

Unfortunately, stratigraphic control on the provenience of the sauropterygians within these deposits is rather poor (Brotzen, 1955, 1957; Peyer, 1955), most of them having been picked up from the float. However, revision of the stratigraphy of the Middle Triassic deposits at Makhtesh Ramon by Parnes (1962, 1965, 1975, 1986; Parnes et al., 1985; Zak, 1986) provides some indication of the age of the horizons from which the material described here is derived (Fig. 2).

In his initial approach to the biostratigraphy of the Makhtesh Ramon exposures, Parnes (1962) associated the occurrence of *?Psephosaurus mosis* Brotzen, 1957, *Nothosaurus* sp., and *Tanystropheus* with that of *Beneckeia levantina* in his "level 3." The occurrence of *?P. picardi* Brotzen, 1957, *?Psephosaurus* spp., *Placodus,* and *Nothosaurus* spp. was associated with that of *Israelites (Hungarites) ramonensis, Protrachyceras wahrmani,* and *Pr. curionii* var. *ramonensis* in "level 5." Translated into his latest revisions (Parnes, 1986; see also Parnes et al., 1985), these associations with invertebrate index fossils place the occurrence of *?P. mosis* in the *Levantina* level of the Gevanim Formation of late Pelsonian (early late Anisian) time (Middle Member of the Gevanim Formation, upper Bithynian, upper lower Anisian, according to Druckman, 1974). The type section at Makhtesh Ramon is 68 m thick (Druckman, 1974). In the following descriptions, these deposits will colloquially be referred to as *Beneckeia* beds.

By contrast, *?P. picardi, ?Psephosaurus* spp., *Placodus,* and *Nothosaurus* spp., as indeed the bulk of the sauropterygian material here described, with the exception of *?P. mosis* and possibly the *Nothosaurus* fragment HUJ-Pal. 223, derive from the middle and upper part of the Fossiliferous Limestone Member of the Saharonim Formation of late Anisian (middle and late Illyrian) and early Ladinian (Fassanian) age. Druckman (1974) assigns these deposits to the Lower Member of the Saharonim Formation, straddling the Anisian–Ladinian boundary; the type section at Makhtesh Ramon is 45 m thick. In the following descriptions, these deposits will colloquially be referred to as *Ceratites* beds.

The occurrence of *?P. mosis,* collected by Brotzen (1957, p. 199) in situ from the *Beneckeia* beds, which on their surface also yielded *Hybodus* and reptilian bones preliminarily identified as those of nothosaurs and possibly *Tanystropheus,* is interesting as it is diachronic with the later occurrence of abundant cyamodontoid and nothosaur material. Following the latest stratigraphic correlation proposed by Parnes (1986), the occurrence of *?P. mosis* in Israel (upper Pelsonian) corresponds in time to the occurrence of *Cyamodus tarnowitzensis* Gürich, 1884, in the Karchowice beds of the lower Muschelkalk of Upper Silesia (Szulc, 1991; see also Parnes, 1975, Table 3). By contrast, the bulk of the sau-

←

FIG. 1. Location of the Triassic outcrops at Makhtesh Ramon, Negev, Israel (after Parnes, 1986).

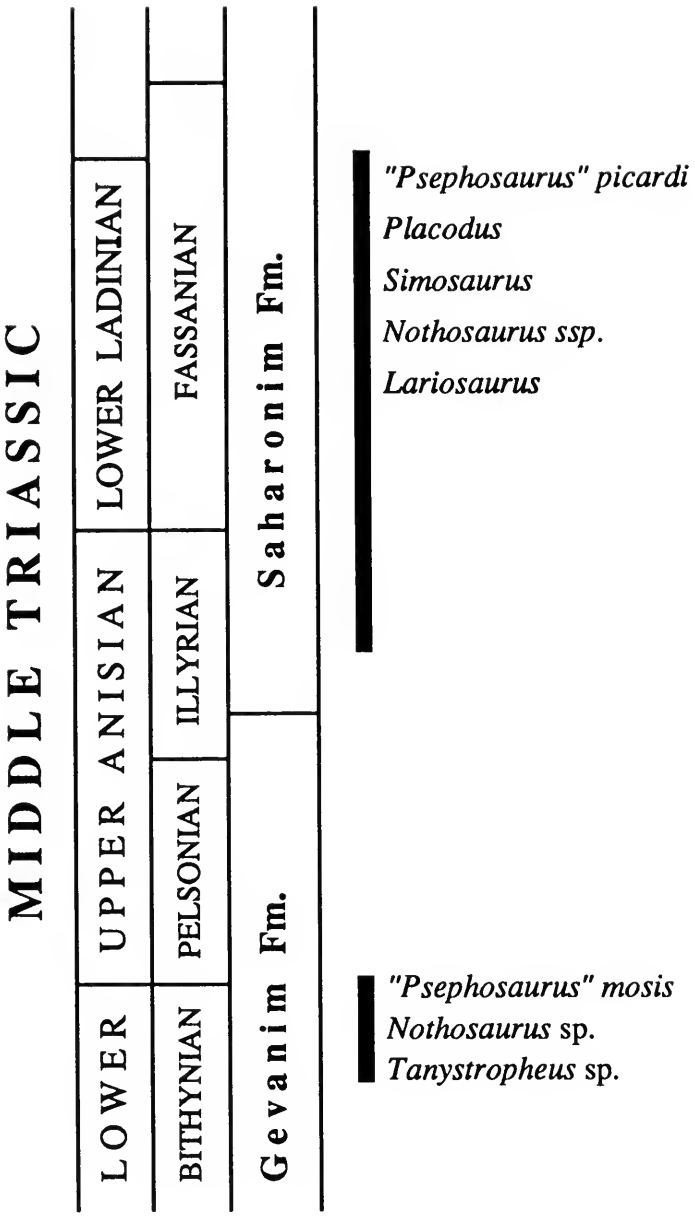

FIG. 2. Stratigraphy of the Triassic at Makhtesh Ramon, Negev, Israel (after Parnes, 1986, and Druckman, 1974).

ropterygian material, from the Fossiliferous Limestone Member of the Saharonim Formation, compares in time to the upper Muschelkalk of the Germanic Triassic, straddling the Anisian–Ladinian boundary. The significance of this stratigraphic distribution is further investigated under PALEOBIOGEOGRAPHIC HISTORY (p. 73 *ff.*).

Systematic Paleontology

Sauropterygia Owen, 1860
Placodontia Zittel, 1887–1890 (also Seeley, 1889)
Cyamodontoidea Peyer and Kuhn-Schnyder, 1955

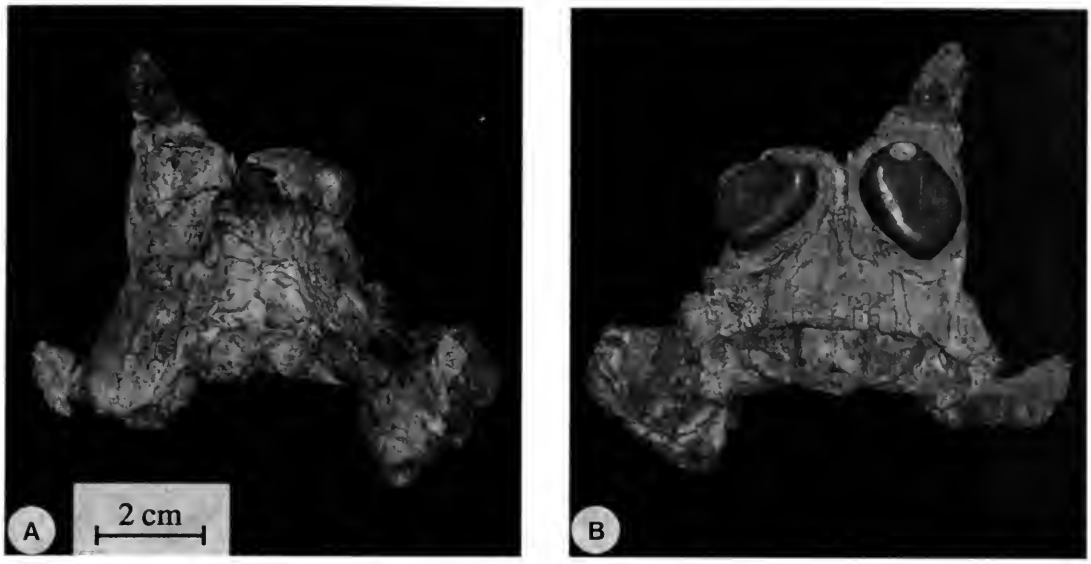

FIG. 3. Holotype of ?*Psephosaurus mosis* Brotzen, 1957 (partial skull, HUJ-Pal. 250). **A,** dorsal view. **B,** ventral view.

GENUS—*Psephosaurus* E. Fraas, 1896

TYPE SPECIES—*Psephosaurus suevicus* E. Fraas, 1896

?*Psephosaurus mosis* Brotzen, 1957

Synonymy for this material:

1955 *Psephosaurus,* Brotzen, p. 404.
1957 *Psephosaurus mosis,* Brotzen, p. 210, text figs. 3–5.
1959 *Psephosaurus mosis,* Haas, p. 15.
1962 *Psephosaurus mosis,* Parnes, p. 8.
1965 *Psephosaurus mosis,* Lehman, p. 175.
1975 *Psephosaurus mosis,* Parnes, Table 1.
1975 *Psephosaurus mosis,* Haas, p. 455, Table 1, Fig. 1.
1981 *Psephosaurus* spp., Haas, p. 33.
1985 *Psephosaurus mosis,* Parnes et al., Table 1.

HOLOTYPE—Hebrew University of Jerusalem, HUJ-Pal. 250: partial skull (Fig. 3).

REFERRED MATERIAL—HUJ-Pal. 220: partial skull (Fig. 4); HUJ-Pal 222: lower jaw fragment (Fig. 5).

STRATUM AND LOCUS TYPICUS—Middle Member of the Gevanim Formation, upper Pelsonian, upper lower Anisian, Middle Triassic, Makhtesh Ramon, Negev, Israel.

COMMENTS—*Psephosaurus* is a monotypic genus based on *P. suevicus* E. Fraas, 1896, represented by isolated osteoderms and carapace fragments from the lower Keuper of the Germanic Triassic. The osteoderms of *Psephosaurus* are of an irregular, mostly hexagonal shape, subequal in size, and meet each other along slightly interdigitating sutures (Westphal, 1975; Westphal & Westphal, 1967; and Rieppel, personal observation).

Numerous carapaces or carapace fragments from the Muschelkalk of Makhtesh Ramon (Negev) and Sinai were referred to the genus *Psephosaurus* by Brotzen (1957; *P. mosis, P. picardi*) and Haas (1959, 1969; *P. sinaiticus* and *P. rhombifer*). Of these, only *P. mosis* is from the *Beneckeia* beds; all the other cyamodontoid armor is from the younger *Ceratites* beds. Haas (1959, 1969) continuously expressed concerns about the identification of the Middle Eastern cyamodontoid material as ?*Psephosaurus* (see also Kuhn, 1969). Cyamodontoid carapace fragments from the Negev and Sinai constitute a significant variation of osteoderm shape and configuration (Westphal, 1975) and represent several taxa (Rieppel, work in progress), but none matches the carapace of *Psephosaurus* from the Germanic Triassic. Peyer (1955) found the Israeli material to also differ from the cyamodontoid genus *Psephoderma,* as carapace fragments from the Middle East lack the longitudinal ridges present in *Psephoderma* (Pinna & Nosotti, 1989). Brotzen (1957) noted similarities which the skull of ?*P. mosis* shares with

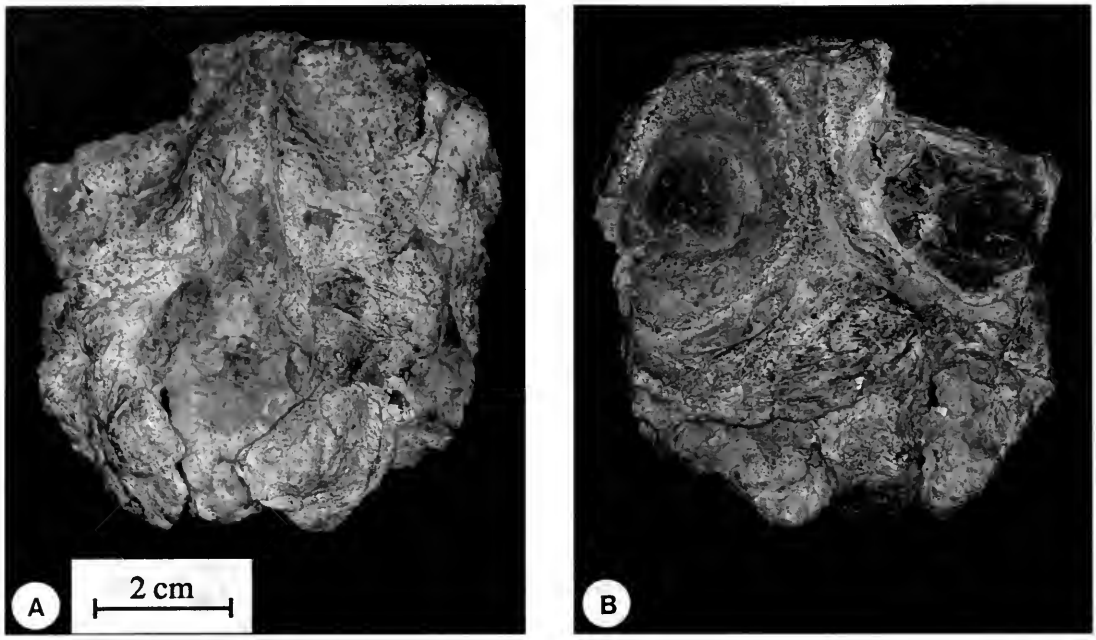

FIG. 4. An incomplete skull of ?*Psephosaurus mosis* Brotzen, 1957 (HUJ-Pal. 220). **A,** dorsal view. **B,** ventral view.

Cyamodus. However, a plastron is present in the cyamodontoids from the Middle East, but absent in *Cyamodus* (based on *C. hildegardis*). If, on the other hand, *C. hildegardis* is to be included in a different (new) genus, as advocated by Kuhn-Schnyder (1960), the genus *Cyamodus* is left to include cranial material from the Germanic Muschelkalk, from which only three fragments of cyamodontoid dermal armor have so far become known (Nosotti & Pinna, 1996, Fig. 14), which again differ from the Negev and Sinai material.

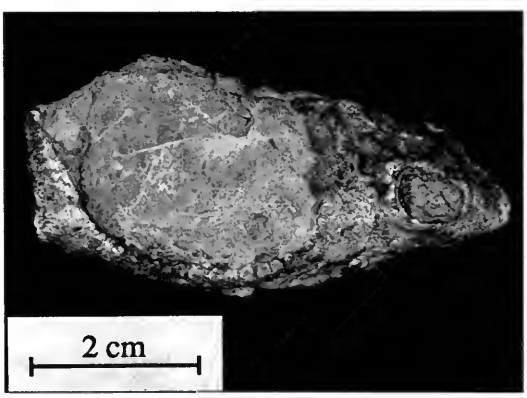

FIG. 5. A lower jaw fragment of ?*Psephosaurus mosis* Brotzen, 1957 (HUJ-Pal. 222), dorsal view.

At the bottom line, the carapace associated with the holotype (skull) of ?*P. mosis* by Brotzen (1957) in particular differs strikingly from that of *Psephosaurus* Fraas, 1896, and most probably represents a different genus, as Haas suspected (1959, 1969; see also Kuhn, 1969). A proper resolution of this problem requires review and revision of all cyamodontoid dermal armor and its potential use in taxonomy, a project that is beyond the scope of this paper.

The only skull ever referred to the genus *Psephosaurus* is that of ?*P. mosis* Brotzen, 1957, from the *Beneckeia* beds of Makhtesh Ramon. These deposits are equivalent in age to the Karchowice beds of the lower Muschelkalk of Upper Silesia, which have yielded *C. tarnowitzensis* Gürich, 1884. The holotype of ?*P. mosis* lacks the rostrum, but is rather similar to *Cyamodus* (Brotzen, 1957, p. 212). The holotype of *C. tarnowitzensis* can no longer be located today. The genotypical species is *C. rostratus* (Münster, 1839), and although the latter shows autapomorphic characters (Rieppel, work in progress), these cannot be compared to the holotype of ?*P. mosis* because the latter is too incomplete. One difference, however, is that the palatal exposure of the pterygoid behind the posterior palatine tooth plate is very short compared to the length of the palatine

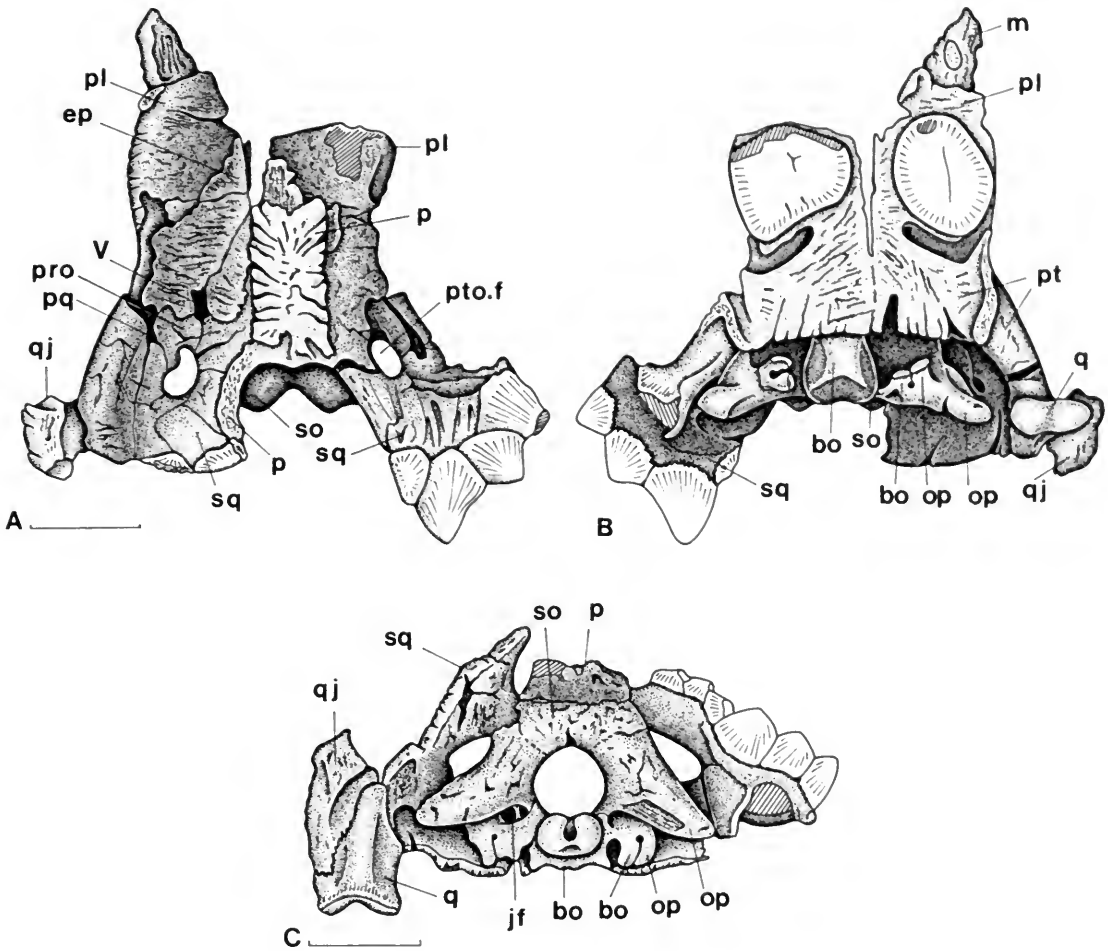

FIG. 6. Holotype of ?*Psephosaurus mosis* Brotzen, 1957 (partial skull, HUJ-Pal. 250). **A**, dorsal view. **B**, ventral view. **C**, occipital view. Scale bar = 20 mm. Abbreviations: bo, basioccipital; ep, epipterygoid; jf, jugular (vagus) foramen; m, maxilla; op, opisthotic; p, parietal; pl, palatine; pq, recess for palatoquadrate cartilage; pro, prootic; pt, pterygoid; pto.f, pteroccipital foramen; q, quadrate; qj, quadratojugal; so, supraoccipital; sq, squamosal; V, trigeminal recess for the exit of the trigeminal nerve (maxillary and mandibular branches).

in *C. rostratus* (left side of skull; Kuhn-Schnyder, 1965), but relatively much longer in the holotype of ?*P. mosis*.

At this time and in this study, the name ?*P. mosis* is retained with the provisions noted above; i.e., that the global revision of the Cyamodontoidea most likely will result in the erection of a new genus to include the material from the Middle East.

MORPHOLOGICAL DESCRIPTION—The holotype of ?*P. mosis* consists of the posterior part of the skull, including the posterior part of the parietal skull table (broken behind the pineal foramen), the posterior part of the dermal palate with the posterior palatine tooth plates preserved as well as a fragment of the left maxilla, and a well-preserved braincase (Fig. 6). The skull is compressed dorsoventrally. As preserved, the total length of the partial skull is 107.5 mm; its maximum width is 100.5 mm.

The parietals are fully fused, and their dorsal surface is ornamented with an irregular pattern of deep grooves and ridges. The posterolateral processes of the parietals meet the squamosals along the posterior margins of the upper temporal fossae. The posterolateral wing of the squamosal carries large dermal tubercles, beautifully preserved on the right side of the skull. The temporal arches are not preserved except for a fragment of the left quadratojugal attached to the quadrate. The pter-

occipital foramen (Nosotti & Pinna, 1993a), from which exits the stapedial artery supplying the temporal jaw adductor muscles, is distinct on both sides of the skull. Sutures delineating separate elements surrounding the pteroccipital foramen are difficult to identify because of extensive breakage of the bone surface, but the contact of the squamosal (posteriorly) with the prootic (anteriorly) is distinct along the ventral (lateral) edge of the pteroccipital foramen. The dorsal margin of the pteroccipital foramen is formed by the opisthotic and squamosal in other, better preserved cyamodontoid specimens (Rieppel, personal observation).

The prootic is well exposed on the left side of the skull, intercalated between the pteroccipital foramen (posteriorly) and the trigeminal recess (anteriorly). Below the trigeminal foramen, the prootic meets the epipterygoid in a well-defined suture. Dorsoventral compression of the skull deformed the cleft between the pterygoid and quadrate, which in life housed the palatoquadrate cartilage, to a narrow trough.

The epipterygoid is a large, wing-shaped element with a broad base extending far forward on the dorsal surface of the palatine and a broad dorsal contact with the laterally descending flange of the parietal. The posterior margin of the epipterygoid defines the dorsal, anterior, and ventral margins of the trigeminal foramen. Anteriorly, the epipterygoid tapers to a blunt tip.

In ventral view, the skull shows a fragment of the left maxilla attached to the left palatine and bearing a broken posterior maxillary tooth. The large posterior palatine tooth plates are both preserved, and both palatines show the dental lamina foramen located posterior to the palatine tooth plates in a distinct, transversely oriented groove, as is characteristic of cyamodontoids in general (Nosotti & Pinna, 1993a). The transverse diameter of the palatine tooth plates is 21 mm (right) and 20 mm (left) respectively; the longitudinal diameter of the left tooth plate is 23.6 mm. The sutures between palatine, ectopterygoid, and pterygoid remain indistinct, although the posterior margin of the palatine probably corresponds to the posterior margin of the groove housing the dental lamina foramen (as is the case in other cyamodontoids). The pterygoids appear to be fused along the ventral midline of the skull (the suture between the pterygoids shown by Brotzen [1957, Text Fig. 1], cannot be identified). The left side of the dermal palate shows a well-developed, longitudinally oriented pterygoid flange, and the quadrate ramus of the pterygoid extends backward to contact the quadrate. The suture between the pterygoid and the quadrate is obscured by a deep crack. The mandibular condyle of the quadrate is bipartite to fit the saddle-shaped articular surface on the mandible.

From above the posterior margin of the pterygoid emerge the occipital condyle and the distinct paroccipital processes. The cranioquadrate passage enters between the pterygoid and quadrate laterally and through the lateral braincase wall medially. The pteroccipital foramen is distinct in the roof of the cranioquadrate passage of the left side of the skull.

The occiput is well preserved in the holotype of ?*P. mosis,* although some sutures remain obscure owing to fusion of the bones. The supraoccipital is a broad plate of bone, meeting the fused parietal in a broad, transversely oriented suture along its dorsal margin and defining the dorsal margin of the foramen magnum ventrally. The dorsolateral contact of the supraoccipital with the squamosal is distinct, but the suture separating the supraoccipital and the exoccipital appears to be fused.

Distinct posttemporal fossae are bordered by the squamosal dorsally and by distinct paroccipital processes ventrally. The paroccipital processes are massive struts, within which the opisthotic and exoccipital appear to have completely fused. Distally, the paroccipital process abuts the posteromedial aspect of the squamosal.

The large metotic foramen is located below the paroccipital process, close by the lateral margin of the foramen magnum. A single strut of bone vertically subdivides the metotic foramen, separating the posterolateral passage of the glossopharyngeal and vagus nerves from the anteromedial passage of the hypoglossal nerve root(s). The ventral margin of the foramen magnum is formed by the basioccipital, which also forms the large occipital condyle. The posterior aspect of the occipital condyle appears distinctly notched, indicating the persistence of the notochord in the adult.

Lateral to the occipital condyle and ventral to the paroccipital process, the accessory articulation of the braincase with the dermal palate characteristic of the Cyamodontoidea can be observed (Nosotti & Pinna, 1993a). A distinct pedicel protrudes ventrally from below the paroccipital arch, composed of two closely juxtaposed components, which appear fused dorsad to a small foramen enclosed between them. Ventrally, these pedicels do not quite reach the posterior margin of the pter-

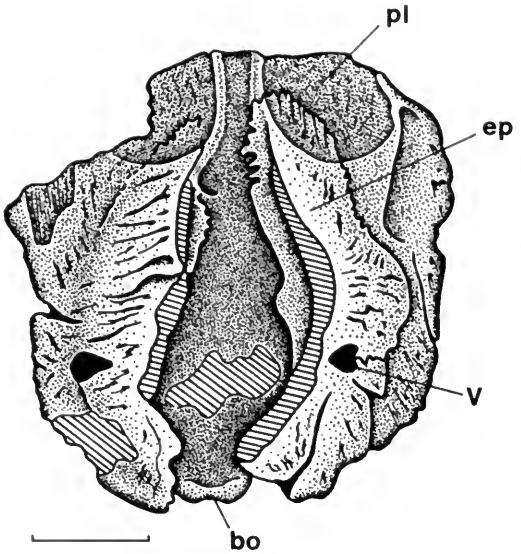

FIG. 7. Incomplete skull of ?*Psephosaurus mosis* Brotzen, 1957 (HUJ-Pal. 220), dorsal view. Scale bar = 20 mm. Abbreviations: bo, basioccipital; ep, exoccipital; pl, palatine; V, trigeminal recess for the exit of the trigeminal nerve (maxillary and mandibular branches).

ygoid, but they might have been connected to it by cartilage, as suggested by Nosotti & Pinna (1993a). The lateral component of each pedicel is formed by a ventral process of the opisthotic, but it is more difficult to assess the identity of the medial component of each pedicel, which might be exoccipital or basioccipital. An almost identical accessory articulation of the braincase with the dermal palate is well preserved in Jaekel's (1907, Pl. III) second skull of *Placechelys placodonta.* In this specimen, the two flanges forming the ventral pedicel of the braincase on either side of the occipital condyle remain separated by a distinct fissure that extends ventrally from the vagus foramen and leaves its ventral margin incomplete (Rieppel, 1995a, Fig. 47). Again, the lateral component is easily identified as a ventral process of the opisthotic, whereas the medial component is a ventrolaterally directed basioccipital process (tuber), and the same is inferred to be the case in the holotype of ?*P. mosis.*

The second skull fragment claimed to have been collected on the talus of the *Beneckeia* beds at Makhtesh Ramon (HUJ-Pal. 220; Fig. 7) is here referred to ?*P. mosis*; it is slightly larger than the holotype of the latter species, but much less complete. As preserved, the total length of the fragment is 75.8 mm, and its maximal width is 73.5 mm. In ventral view, the specimen exhibits the replacements of the posterior palatine tooth plates (the left one incomplete) set deep in the eroded surface of the palatines, with the large dental lamina foramen located behind the (right) tooth plate (Haas, 1975, Pl. 1, Fig. 1). The braincase is represented by the basioccipital condyle and strongly eroded remnants of the occiput. The dorsal surface beautifully shows the extent of the base of the broad epipterygoid (both epipterygoids are incomplete dorsally) and its relation to the surface of the pterygoid and palatine. The anterior extremity of the epipterygoid turns toward the sagittal plane of the skull and overlaps (topographically) the posterior margin of the posterior palatine tooth plate.

A poorly preserved fragment of a cyamodontoid lower jaw (HUJ-Pal. 222; Haas, 1975, Pl. 1, Fig. 4), with no indication of its stratigraphic provenience, may likewise be referred to ?*P. mosis.* It carries a larger posterior and a much smaller anterior tooth plate. The dimensions of the posterior tooth plate are approximately 31 mm (longitudinal) by 22 mm (transverse); the smaller tooth measures 8 mm (longitudinal) by approximately 5.5 mm (transverse).

DISCUSSION—The presence of cyamodontoid placodonts in the Muschelkalk of Makhtesh Ramon, ranging from the *Beneckeia* beds up well into the *Ceratites* beds, is abundantly documented by complete carapaces and numerous fragments of dermal armor as well as by cranial material, most notably the holotype of ?*P. mosis* Brotzen, 1957. Current knowledge of cyamodontoid taxonomy does not allow assessment of the generic identity of this material, but a global revision of the Cyamodontoidea will most probably result in the erection of a new genus. But whereas cyamodontoids (*Cyamodus*) coexist with *Placodus* in the lower and upper Muschelkalk of the Germanic Triassic, no diagnostic fossil indicating the existence of *Placodus* has been reported to date from the Muschelkalk of Makhtesh Ramon. Pieces referred to the latter genus by Haas (1975), in particular vertebrae of a distinctive morphology (Haas, 1975, Pl. 1, Figs. 6, 7), will be dealt with in more detail below.

Eosauropterygia Rieppel, 1994a
Pachypleurosauroidea Nopcsa, 1928
Pachypleurosauridae Nopcsa, 1928

Pachypleurosauridae Indeterminate

MORPHOLOGICAL DESCRIPTION—The humerus HUJ-Pal. 2644 (Figs. 8A–B; total length: 32.0 mm;

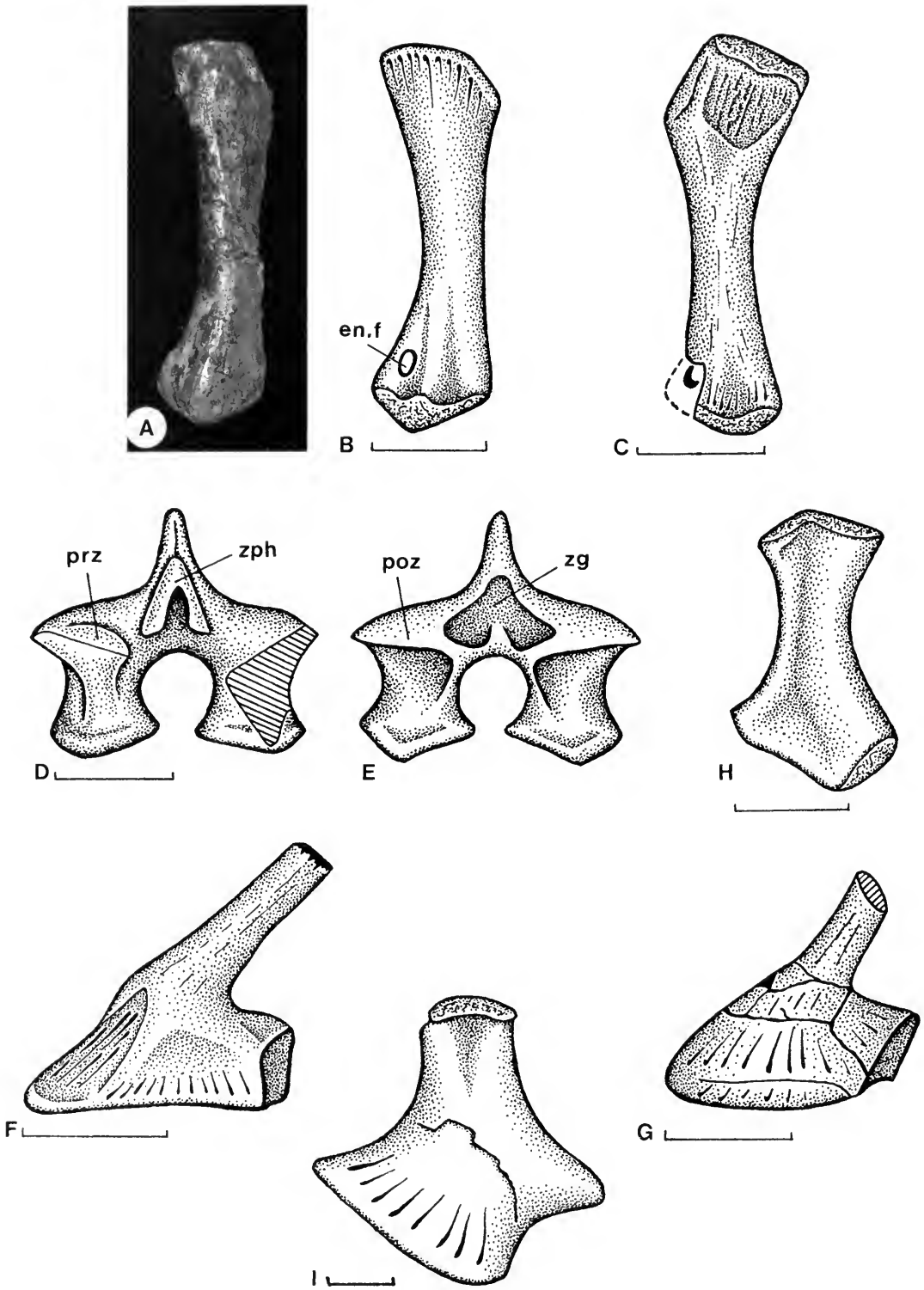

FIG. 8. Isolated sauropterygian postcranial remains probably referable to pachypleurosaurs (Eosauropterygia, Pachypleurosauria indeterminate). **A, B,** humerus (HUJ-Pal. 2644); scale bar = 10 mm. **C,** humerus (HUJ-Pal. 2054);

proximal width: 8.0 mm; minimum width: 5.0 mm; distal width: 9.1 mm) resembles pachypleurosaurs of the genus *Neusticosaurus* in its relative size and relatively poor morphological differentiation. The deltopectoral crest is weakly angulated, the preaxial margin is more strongly concave than the postaxial margin, and the differentiation of the ectepicondyle and entepicondyle is distinctly less pronounced than in *Dactylosaurus* (Rieppel & Lin, 1995). Again, the deltopectoral crest is less differentiated, and the surface of the humerus lacks the distinct striation characteristic of *Anarosaurus*. A second humerus of similar size (HUJ-Pal. 2054, Fig. 8C; total length: 32.2 mm; proximal width: 8.8 mm; minimum width: 5.0 mm; distal width: unknown due to breakage of the entepicondyle) shows a more distinctly developed deltopectoral crest, a feature that is subject to sexual dimorphism in the genus *Neusticosaurus* (Rieppel, 1989; Sander, 1989) as well as in *Dactylosaurus* (Rieppel, 1993a).

An isolated neural arch (HUJ-Pal. 572, Figs. 8D–E) of small size (total height: 10.2 mm; width across postzygapophyses: 8.0 mm) can be identified as sauropterygian on the basis of the bipartite zygosphene and the expanded sutural surface on the pedicels. It resembles pachypleurosaurs in its small size, low neural spine, the indistinct transverse processes on the neural arch, and the "domed" (pachyostotic) zygapophyses. Very similar neural arches were reported from the Middle Triassic (Muschelkalk) of the Lorraine (France) by Bardet and Cuny (1993, Pl. I, Figs. B 3–6). However, isolated neural arches of the same morphology but of larger size are also known, such as HUJ-Pal. 326 (total height: 11.2 mm; width across postzygapophyses: 17.2 mm), HUJ-Pal. 2012 (total height: 15.2 mm; width as preserved: 20.1 mm), and HUJ-Pal. 2007 (total height: 19 mm; width across postzygapophyses: 18 mm). A series of small, weakly amphicoelous or platycoelous centra might also be referred to pachypleurosaurs based on their small size (HUJ-Pal. 1059a, dorsal centrum, horizontal diameter: 8.7 mm; HUJ-Pal. 1397, dorsal centrum, horizontal diameter: 9 mm; HUJ-Pal. 2469, dorsal centrum, horizontal diameter: 8.8 mm; HUJ-Pal. 1059b, caudal centrum, horizontal diameter: 4.8 mm).

Small size is again the reason to possibly refer two isolated scapulae, both of standard sauropterygian morphology but both with a broken posterodorsal process, to pachypleurosaurs (HUJ-Pal. 2451 [Fig. 8F], length of ventral glenoid portion: 19.4 mm; HUJ-Pal. 1993 [Fig. 8G], length of ventral glenoid portion: 20.3 mm). A small coracoid (HUJ-Pal. 1131 [Fig. 8H], total length: 21.8 mm; proximal width: 9.5 mm; minimum width: 6.0 mm; distal width: 8.3 mm) shows a deeply concave anterior and posterior margin and hence a distinctly waisted structure that resembles the coracoid of the Ladinian *Neusticosaurus* (Sander, 1989) more closely than the coracoid of the Anisian genera *Dactylosaurus* and *Anarosaurus* (Rieppel & Lin, 1995), although the pectoral girdle of these latter two genera remains poorly known.

An isolated ischium (HUJ-Pal. 2749 [Fig. 8I], maximum length: 43.5 mm; maximum width: 41 mm) is noteworthy for an unusual differentiation of its posterior margin, which is drawn out into a distinct tapering projection separating a posteroventral from a posterodorsal concavity. A similar morphology of the ischium can be observed in small species of the pachypleurosaur *Neusticosaurus* (Sander, 1989).

DISCUSSION—A number of isolated postcranial elements from the *Ceratites* beds of Makhtesh Ramon may be referred to pachypleurosaurs simply on the basis of their small size. Unequivocally diagnostic elements of pachypleurosaurs have so far not been recognized. It is conceivable, however, that pachypleurosaurs were present, although relatively rare compared to nothosaurs, in the Muschelkalk of Makhtesh Ramon.

Nothosauria Seeley, 1882
Simosauridae Huene, 1948

GENUS—*Simosaurus* H. v. Meyer, 1842

TYPE SPECIES—*Simosaurus gaillardoti*, H. v. Meyer, 1842

←

scale bar = 10 mm. **D, E,** dorsal vertebra (HUJ-Pal. 572; **D,** anterior view; **E,** posterior view); scale bar = 5 mm. **F,** right scapula (HUJ-Pal. 2451, medial view); scale bar = 10 mm. **G,** left scapula (HUJ-Pal. 1993, lateral view); scale bar = 10 mm. **H,** coracoid (HUJ-Pal. 1131); scale bar = 10 mm. **I,** ischium (HUJ-Pal. 2749); scale bar = 10 mm. Abbreviations: en.f, entepicondylar foramen; poz, postzygapophysis; prz, prezygapophysis; zg, zygantrum; zph, zygosphene.

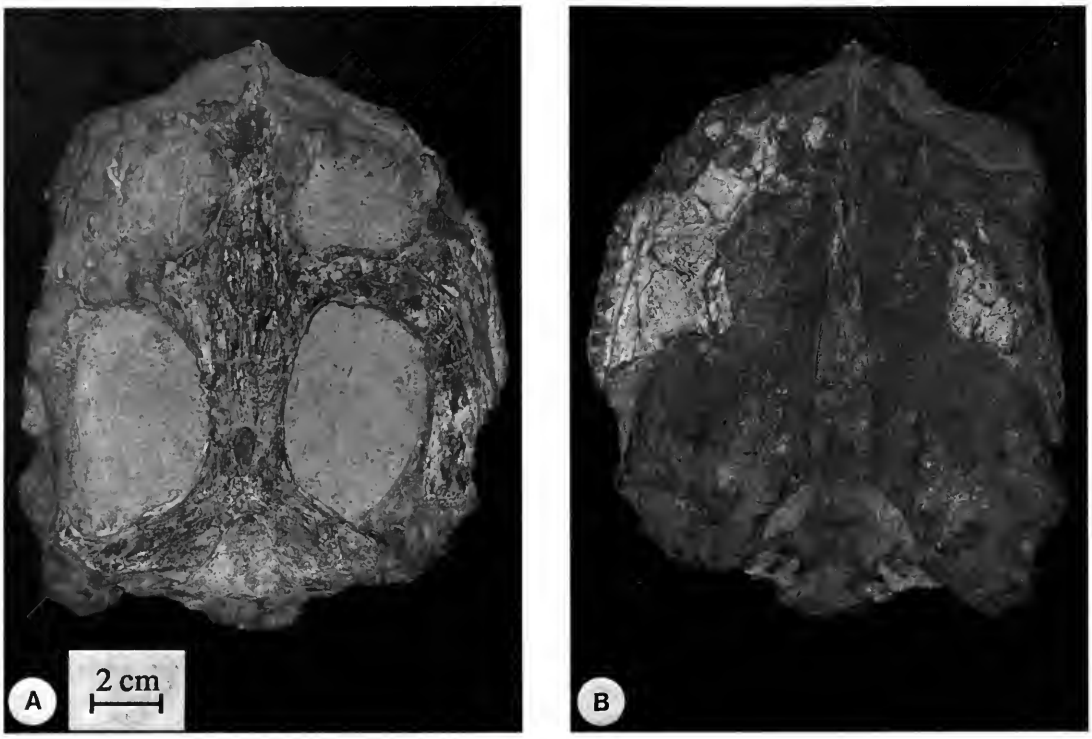

FIG. 9. A partial skull of *Simosaurus* sp. (HUJ-Pal. 2086). **A,** dorsal view. **B,** ventral view.

***Simosaurus* sp.**

COMMENTS—The genus *Simosaurus,* primarily known from the Germanic Triassic, has been the subject of a recent monographic review (Rieppel, 1994a), which recognized a single species, *S. gaillardoti* H. v. Meyer, 1842. Only two occurrences of *Simosaurus* are known outside the Germanic Triassic: postcranial remains in the Ladinian of the northern Alps (Vorarlberg, Austria; Rieppel, 1996), and a fragmentary skull in the Muschelkalk of Makhtesh Ramon (Haas, 1981). Haas (1970) also described an interclavicle from that locality, which he referred to *Tanystropheus* at a time when the interclavicle of *Tanystropheus* had not yet been described. Now that the pectoral girdle of *Tanystropheus* is known in detail (Wild, 1973), it is possible to identify the interclavicle described by Haas (1970) as that of *Simosaurus.* Other material of *Simosaurus* from the *Ceratites* beds of Makhtesh Ramon, which has not yet been described, includes a partial pectoral girdle and a possible sacral rib.

MORPHOLOGICAL DESCRIPTION—The skull (HUJ-Pal. 2086, Figs. 9–10) from the Muschelkalk of Makhtesh Ramon is rather incomplete and the bone surface is poorly preserved, obscuring much of the anatomical detail. The total length of the skull fragment is 173.5 mm; its total width is 143.5 mm.

The frontal and parietal are almost complete, but the frontoparietal suture remains indistinct. Both bones appear to be unpaired (i.e., fused), and the pineal foramen is only slightly shifted backward, characteristic for the genus. Posteriorly, the supraoccipital is seen in a horizontal exposure, overlapped laterally by the occipital flanges of the parietal, and carrying a low sagittal crest. The right postfrontal and postorbital can be identified in the right postorbital arch. As in *S. gaillardoti* (Rieppel, 1994a), the dorsal (medial) process of the postorbital tapers to a blunt tip, embraced by the two-pronged ventral (lateral) process of the postfrontal. Three elements can be discerned in the (preserved) anterior part of the right upper temporal arch: the medial postorbital, the intercalated jugal, and the right maxilla, which extends backward to a point well behind the level of the anterior margin of the upper temporal fossa. The mandibular condyle of the left quadrate is distinct in dorsal view, whereas the occipital condyle is represented only by a natural mold.

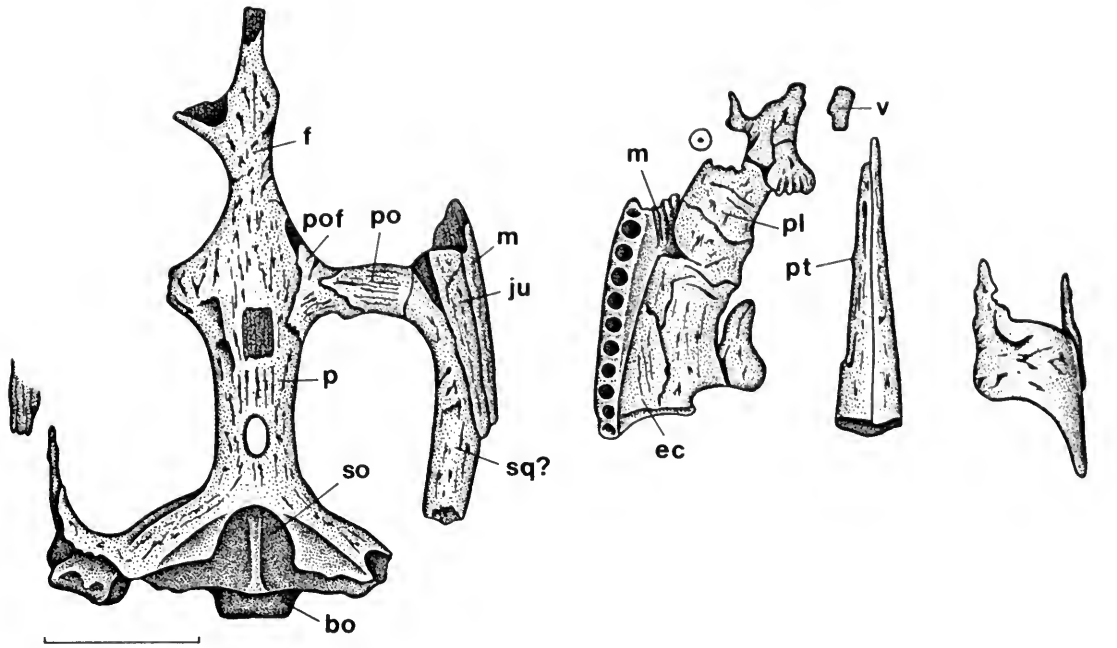

FIG. 10. A partial skull of *Simosaurus* sp. (HUJ-Pal. 2086). **A,** dorsal view. **B,** ventral view. Scale bar = 50 mm. Abbreviations: bo, basioccipital; ec, ectopterygoid; f, frontal; ju, jugal; m, maxilla; p, parietal; pl, palatine; pof, postfrontal; po, postorbital; pt, pterygoid; so, supraoccipital; sq, squamosal; v, vomer.

The ventral view of the skull (Figs. 9B, 10B) displays equally incomplete preservation of the dermal palate. Part of the right maxilla is distinct, lateral to the suture between the anterior end of the ectopterygoid and the posterior end of the palatine. The anterior end of the (broken) palatine is notched, possibly indicating the posterior margin of the internal naris. The curvature of the posterior end of the ectopterygoid appears to mark the anterior margin of the subtemporal fossa. The vomer is represented by only a bone fragment, whereas the pterygoid is represented by the anterior part of its palatal ramus.

The right half of the pectoral girdle (HUJ-Pal. 3875, Fig. 11) consists of a well-preserved clavicle, a fragment of the right lateral process of the interclavicle articulating with a facet on the ventromedial surface of the clavicle, and the broken and poorly preserved right scapula. As preserved, the total maximum length of the specimen is 185 mm; its total maximum width is 223 mm. The clavicle is typically nothosaurian, with an expanded anterolateral corner (Storrs, 1991) and a posterolateral process that is applied against the anterior and medial aspect of the scapula. The clavicle carries a small process on its anterior margin, which is autapomorphic for *Simosaurus* (Rieppel, 1994a).

The interclavicle (HUJ-Pal. 23, Fig. 12; upper *Ceratites* beds of Brotzen, 1957), first described by Haas (1970), is T-shaped, with an incompletely preserved anterior margin and unfinished bone at the tip of the lateral processes. The posterior tip of the posterior process is broken, but even as preserved, the posterior stem is relatively longer than is characteristic of *S. gaillardoti* (Rieppel, 1994a). As preserved, the interclavicle from Makhtesh Ramon has a total length of 111.7 mm and a total width of 123.3 mm, resulting in a length-to-width ratio of 0.905. A complete interclavicle of *S. gaillardoti* from the upper Muschelkalk of Crailsheim (Rieppel, 1994a, Fig. 25B) has a length-to-width ratio of 0.57. Huene (1952, Fig. 62) figured an interclavicle of *Simosaurus* from the Grenzbonebed (between Muschelkalk and Keuper) of Crailsheim with an unusually long posterior stem. In this specimen, however, the posterior stem of the interclavicle widens at its posterior end, whereas the posterior stem of the interclavicle from Makhtesh Ramon gradually tapers posteriorly up to the fracture plane.

HUJ-Pal. 2052 (Fig. 13), finally, is an element

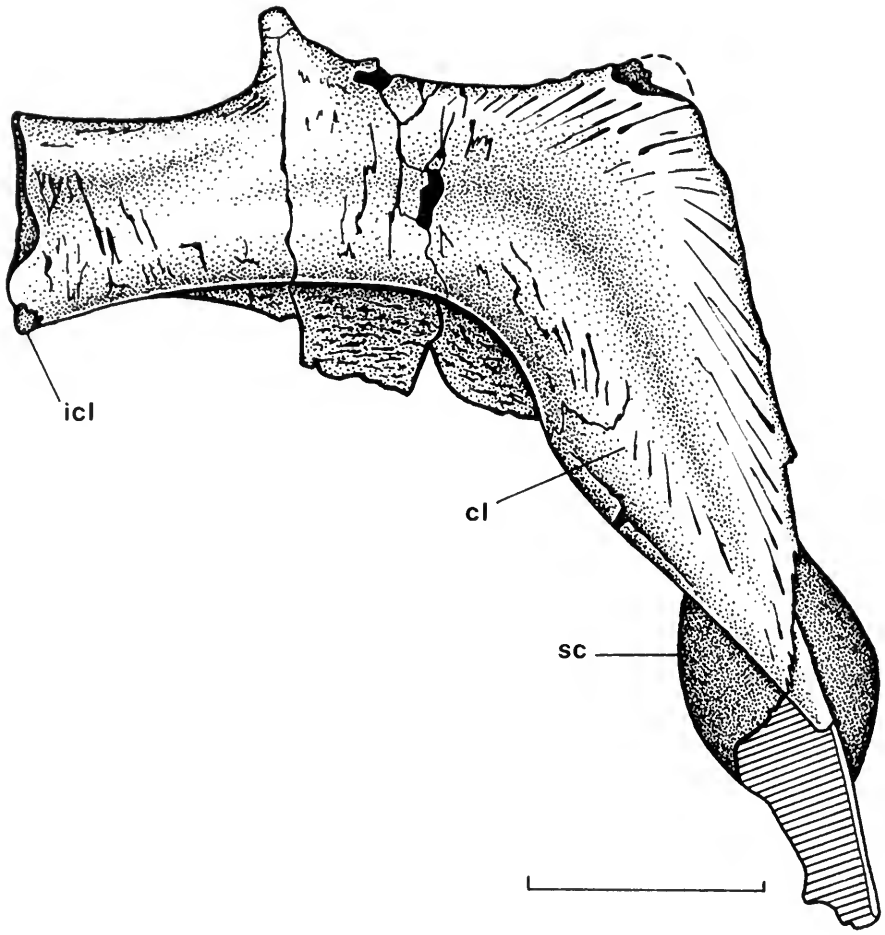

FIG. 11. Right pectoral girdle of *Simosaurus* sp. (HUJ-Pal. 3875), dorsal view. Scale bar = 50 mm. Abbreviations: cl, clavicle; icl, interclavicle; sc, scapula.

that closely resembles the principal sacral rib of *Simosaurus* (Rieppel, 1994a, Fig. 21A). Its total length is 74.5 mm; proximal width, 27 mm; minimum width, 10.9 mm; and distal width, 25.0 mm.

DISCUSSION—The fragmentary skull of *Simosaurus* from Makhtesh Ramon (Haas, 1981) is too incomplete to allow its identification at the species level, i.e., to assess whether it belongs to *S. gaillardoti* H. v. Meyer or to a separate species. The interclavicle from Makhtesh Ramon shows a posterior stem that is more strongly developed and relatively longer than is typical for *S. gaillardoti* from the upper Muschelkalk of the Germanic Triassic (Rieppel, 1994a, Fig. 25). Unfortunately, the interclavicle is not known in *S. guilielmi* (a subjective junior synonym of *S. gaillardoti*; Rieppel, 1994a) from the middle Keuper of southwestern Germany (Huene, 1959), but Huene (1952, Fig. 62) figured an interclavicle with an unusually long posterior stem from the Grenzbonebed (between Muschelkalk and Keuper) of Crailsheim, southwestern Germany. In dealing with disarticulated postcranial material, it is difficult to tell whether differences in relative length of the posterior interclavicular stem reflect individual or taxic variation. Given the incompleteness of the Makhtesh Ramon material, the simosaur from this locality is here referred to as *Simosaurus* sp.

Nothosauridae Baur, 1889
Nothosaurinae Baur, 1889

GENUS—*Nothosaurus* Münster, 1834

TYPE SPECIES—*Nothosaurus mirabilis* Münster, 1834

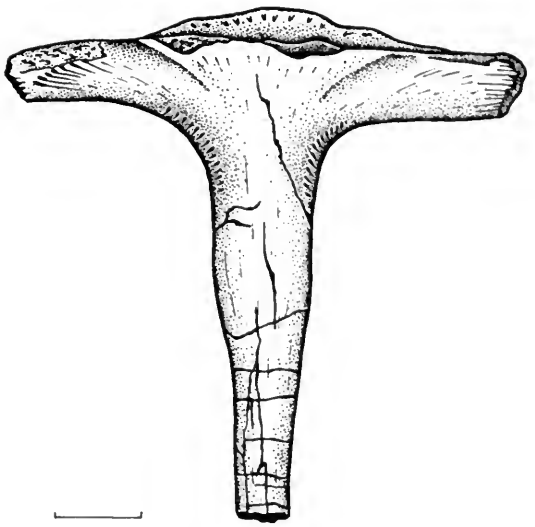

FIG. 12. An isolated interclavicula of *Simosaurus* sp. (HUJ-Pal. 23), dorsal view. Scale bar = 20 mm.

FIG. 13. A possible sacral rib of *Simosaurus* sp. (HUJ-Pal. 2052). Scale bar = 20 mm.

Nothosaurus cf. *N. giganteus* Münster, 1834

COMMENTS—*Nothosaurus giganteus*, first described by Münster (1834) on the basis of a fragmentary skull from the upper Muschelkalk (mo_1) of Bayreuth, Germany, was recently comprehensively revised by Rieppel and Wild (1996). A full list of synonymy is given by Rieppel and Wild (1996), who also showed that *Paranothosaurus* Peyer, 1939, from the Alpine Triassic is a subjective junior synonym of *Nothosaurus*. *Nothosaurus* (*Paranothosaurus*) *amsleri* Peyer, 1939, from the Alpine Triassic is most probably conspecific with *N. giganteus* Münster, 1834, but unequivocal assessment of synonymy of these two species requires further study of the Alpine material. Nevertheless, *N.* (*Paranothosaurus*) *amsleri* shows a vertebral structure that is highly characteristic (autapomorphic) and that corresponds to the structure of large vertebrae from the Germanic Triassic, referred to *N. giganteus* by Rieppel & Wild (1996). The sauropterygian material from the Muschelkalk of Makhtesh Ramon consists of a partially preserved neural arch (HUJ-Pal. 2014) identical to those of *N.* (*Paranothosaurus*) *giganteus*, which suggests reference of other large sauropterygian remains to this or a very closely related species. This material also comprises the posterior end of a left mandibular ramus, a large vertebral centrum, large girdle elements, and large proximal limb bones or fragments thereof.

MORPHOLOGICAL DESCRIPTION—A left mandibular ramus is represented by its posterior end (HUJ-Pal. 2112) with a well-preserved articular facet and a badly eroded retroarticular process (Fig. 14). As preserved, the total length of the specimen is 137.5 mm; the total width at the mandibular articulation is 42.5 mm. The longitudinal diameter of the mandibular joint surface is 42 mm, and its transverse diameter is 39 mm. The articular surface is saddle-shaped and is formed by the surangular laterally and by the articular medially (as is characteristic of *Nothosaurus* in general: Rieppel, 1994a, Fig. 12). The foramen for the chorda tympani is located at the posterior margin of the articular facet on the suture separating the surangular from the articular. The articular facet on the right (surangular) part of the joint surface is rather shallow. The articular, on the other hand, forms a high-rising flange along the posteromedial margin of the medial articular facet and is deeply excavated at the anterior and anteromedial margin of the joint. The structure of the mandibular joint effectively locks the lower jaw against the mandibular condyle of the quadrate to counteract the protractive and retractive forces generated by the dual jaw adductor muscle system characteristic of nothosaurians (Rieppel, 1994a). To judge from the size of the skull, *N. giganteus* must have possessed huge jaw adductor muscle masses (Rieppel & Wild, 1996). In front of the mandibular joint, the surangular forms a horizontal shelf for the in-

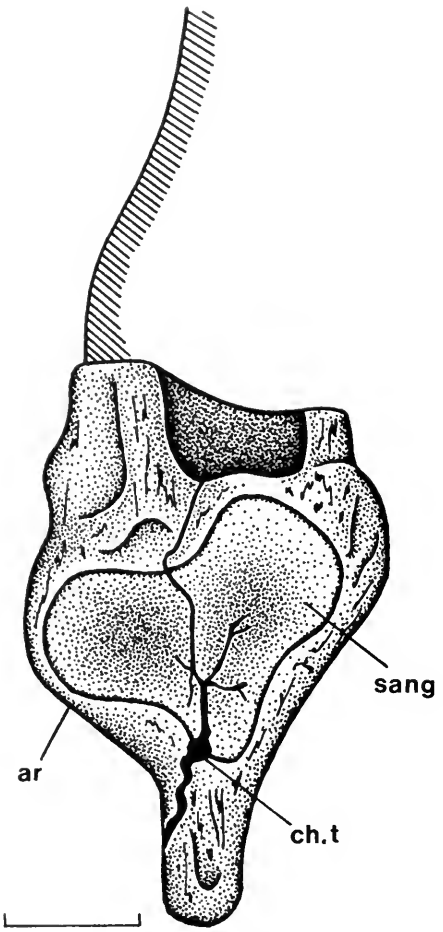

FIG. 14. The posterior part of the left mandible of *Nothosaurus* cf. *N. giganteus* (HUJ-Pal. 2112), dorsal view. Scale bar = 20 mm. Abbreviations: ar, articular; ch.t, chorda tympani foramen; sang, surangular.

sertion of superficial fibers of the external adductor, typical for nothosaurs in general.

An isolated neural arch (HUJ-Pal. 2014, Fig. 15) is only incompletely preserved and crudely prepared, but nevertheless is diagnostic for *N. giganteus* or a closely related species (Rieppel & Wild, 1996, Figs. 17, 18). The neural arch has a massive appearance with large, "swollen" (pachyostotic) and "domed" postzygapophyses rising up to a level well above the prezygapophyses. In dorsal view, pre- and postzygapophyses are separated only by a shallow embayment. The neural spine is massive but low. The orientation of the articular surfaces of the well-preserved prezygapophysis is close to horizontal, inclined by about 13°. The zygosphene is well developed and bipartite, and is located between the prezygapophyses. As preserved, the total height of the neural arch is 103 mm, and its total width is 104 mm. A large isolated dorsal centrum (HUJ-Pal. 1729; horizontal diameter: 72.2 mm; vertical diameter: 67.8 mm) shows a distinctly constricted body and platycoelous articular surfaces.

There are two large scapulae (HUJ-Pal. 3375, 3724) that may also be referred to *Nothosaurus* cf. *N. giganteus*. HUJ-Pal. 3375 is a right scapula with the broken posterolateral tip of the clavicle still attached to its anterior and medial aspect. The total height of the element is 133.2 mm, its total length is 150 mm, and the length of the ventral glenoidal part is 107.5 mm. HUJ-Pal. 3724 is a somewhat smaller right scapula (Fig. 16) with a total height of 98.5 mm and a total length of 126.5 mm (length of ventral glenoidal portion: 89.7 mm). This scapula is remarkable for the "swollen" appearance of the posterodorsal process, the anterior margin of which is expanded into a smoothly curved flange.

HUJ-Pal. 109 is a large ilium with a total height of 56.8 mm. The dorsal (supra-acetabular) portion carries no preacetabular process and only a weakly developed posterodorsal wing. HUJ-Pal. 3876 represents the proximal (dorsal) head of a large pubis (Fig. 17). The total width of the specimen is 74.2 mm (total height, as preserved: 92 mm). The fragment of the pubis shows a large, slit-like, and open obturator foramen.

Several fragments of large humeri (e.g., HUJ-Pal. 2317, 2419, 2948, and 3867) may also be referred to *Nothosaurus* cf. *N. giganteus* on the basis of their size.

DISCUSSION—The material of *Nothosaurus* cf. *N. giganteus* from the Muschelkalk of Makhtesh Ramon is very fragmentary and not diagnostic at the species level. The peculiar morphology of the neural arch (HUJ-Pal. 2014) is diagnostic, however, for *Nothosaurus* (syn. *Paranothosaurus*) species that are very close to, if not identical with, *N. giganteus*. The scapula HUJ-Pal. 3724 is almost identical in shape and size to a specimen from the lower Keuper (Lettenkeuper) of Hoheneck in southwestern Germany (FMNH UC404; Fig. 18), originally labeled as *N. chelydrops*. *Nothosaurus chelydrops* E. Fraas, 1896, is based on a strongly dorsoventrally compressed skull with peculiar proportions, and most probably is a junior synonym of *N. giganteus* (see discussion in Rieppel & Wild, 1996). *Nothosaurus giganteus* was among the top carnivores of its time, and for this reason may be expected to have had a wide geographic distribution. It is conceivable that all the

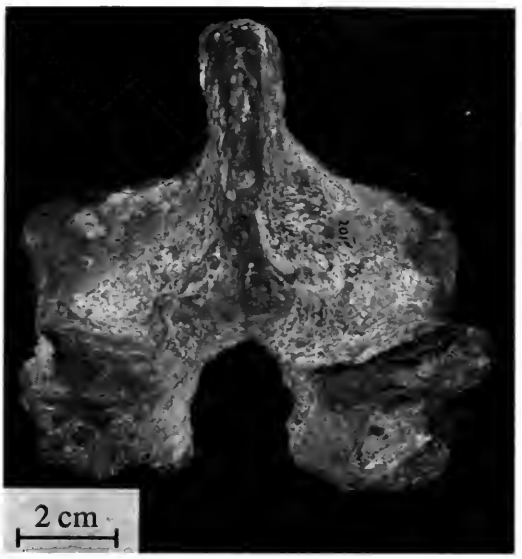

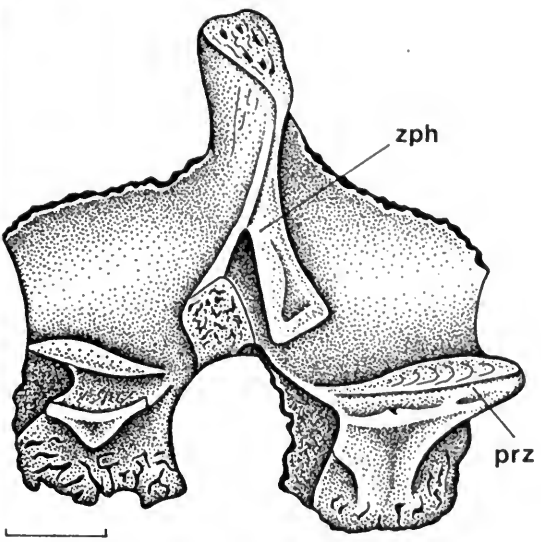

FIG. 15. A dorsal neural arch of *Nothosaurus* cf. *N. giganteus* (HUJ-Pal. 2014), anterior view. Scale bar = 20 mm. Abbreviations: prz, prezygapophysis; zph, zygosphene.

material of a very large nothosaur sharing the characteristic vertebral structure (including "*Paranothosaurus*" *amsleri* Peyer, 1939, from the Alpine Triassic) represents a single species, *N. giganteus.*

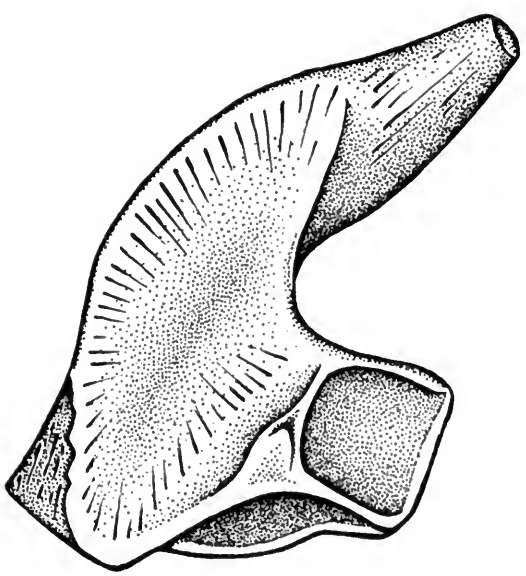

FIG. 16. The right scapula of *Nothosaurus* cf. *N. giganteus* (HUJ-Pal. 3724), medial view. Scale bar = 50 mm.

Nothosaurus haasi Rieppel, Mazin, & Tchernov, 1997

1997 *Nothosaurus haasi,* Rieppel et al., p. 992, Fig. 1.

HOLOTYPE—Hebrew University of Jerusalem, HUJ-Pal. 2250: almost complete skull (Fig. 19).

DIAGNOSIS—A small species of *Nothosaurus* (condylobasal length of skull: 123.5 mm) with a relatively long and slender rostrum, relatively long and slender external nares, posterior (nasal) process of premaxilla meeting frontal at level of anterior margin of orbit, nasal without anterior process lining the entire medial margin of external naris, postorbital with anteroventral process lining the posteroventral margin of the orbit, prefrontal absent or fused to frontal, jugal absent, upper temporal fossae relatively small, vomers fused and extending far anteriorly into rostrum, and low maxillary tooth count (13).

REFERRED MATERIAL—HUJ-Pal. 3723, partial skull (Fig. 20). For postcranial elements tentatively referred to this species, see morphological description below.

STRATUM AND LOCUS TYPICUS—Lower Member of the Saharonim Formation of late Anisian (middle and late Illyrian) or early Ladinian (Fassanian) age, Middle Triassic, Makhtesh Ramon, Negev, Israel.

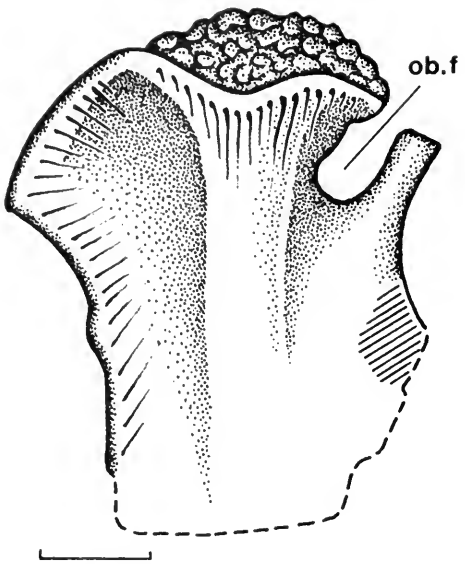

FIG. 17. The proximal part of the left pubis of *Nothosaurus* cf. *N. giganteus* (HUJ-Pal. 3876), lateral (ventral) view. Scale bar = 20 mm. Abbreviation: ob.f, obturator foramen.

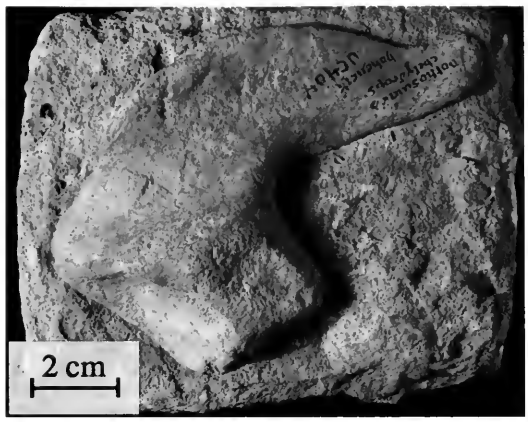

FIG. 18. The left scapula of *Nothosaurus giganteus* (FMNH UC404), lateral view, from the lower Keuper of Hoheneck (Ladinian), southern Germany (FMNH neg. no. GEO86053).

ETYMOLOGY—Named after the late Professor Dr. Georg Haas, who initiated the study of vertebrate fossils from the Muschelkalk of Makhtesh Ramon.

MEASUREMENTS—The following measurements for the holotype of *N. haasi* are all in millimeters. Values in parentheses are for the right side of the skull.

Tip of the snout to occipital condyle: 123.5
Tip of the snout to posterior margin of supraoccipital: 116
Tip of the snout to posterior margin of parietal skull table: 111
Tip of the snout to anterior margin of upper temporal fossa: 79.5
Tip of the snout to anterior margin of the orbit: 59.5
Tip of the snout to anterior margin of external naris: 38.8
Tip of the snout to the anterior margin of internal naris: 38.2
Width of skull across posterior end of squamosals: 34.5
Width of skull across postorbital arches: 35
Width of skull at anterior margin of orbits: 25.9
Width of skull at roots of maxillary fangs: 25.5
Width of skull at rostral constriction: 14.8
Maximum width of premaxillary rostrum: 16.2
Longitudinal diameter of external naris: 12 (11.6)
Transverse diameter of external naris: 4.5 (4.6)
Longitudinal diameter of orbit: 14.6 (14.7)
Transverse diameter of orbit: 10.3 (10.5)
Longitudinal diameter of upper temporal fossa:— (30.7)
Transverse diameter of upper temporal fossa:— (12.2)
Longitudinal diameter of internal naris: 14.6 (14.9)
Transverse diameter of internal naris: 3.5 (3.4)
Distance from posterior margin of external naris to anterior margin of orbit: 9.9 (10.2)
Distance from posterior margin of orbit to anterior margin of upper temporal fossa: 4.4 (4.5)
Middorsal bridge between external nares: 3.8
Middorsal bridge between orbits (minimum width): 4.0
Middorsal bridge between upper temporal fossae (behind the pineal foramen): 5.2

MORPHOLOGICAL DESCRIPTION—*Nothosaurus haasi* is represented by a skull of small size, but with a relatively elongate and slender appearance (Fig. 21). The right half of the premaxillary rostrum is the only part missing. The rostrum is relatively long and slender, with almost parallel lateral edges. The external nares are elongate. Dividing the distance from the tip of the snout to the anterior margin of the external naris by the width of the skull at the rostral constriction yields a value of 2.62 (1.5–2.5 for *N. mirabilis*). Dividing the distance from the tip of the snout to the anterior margin of the orbit by the distance from

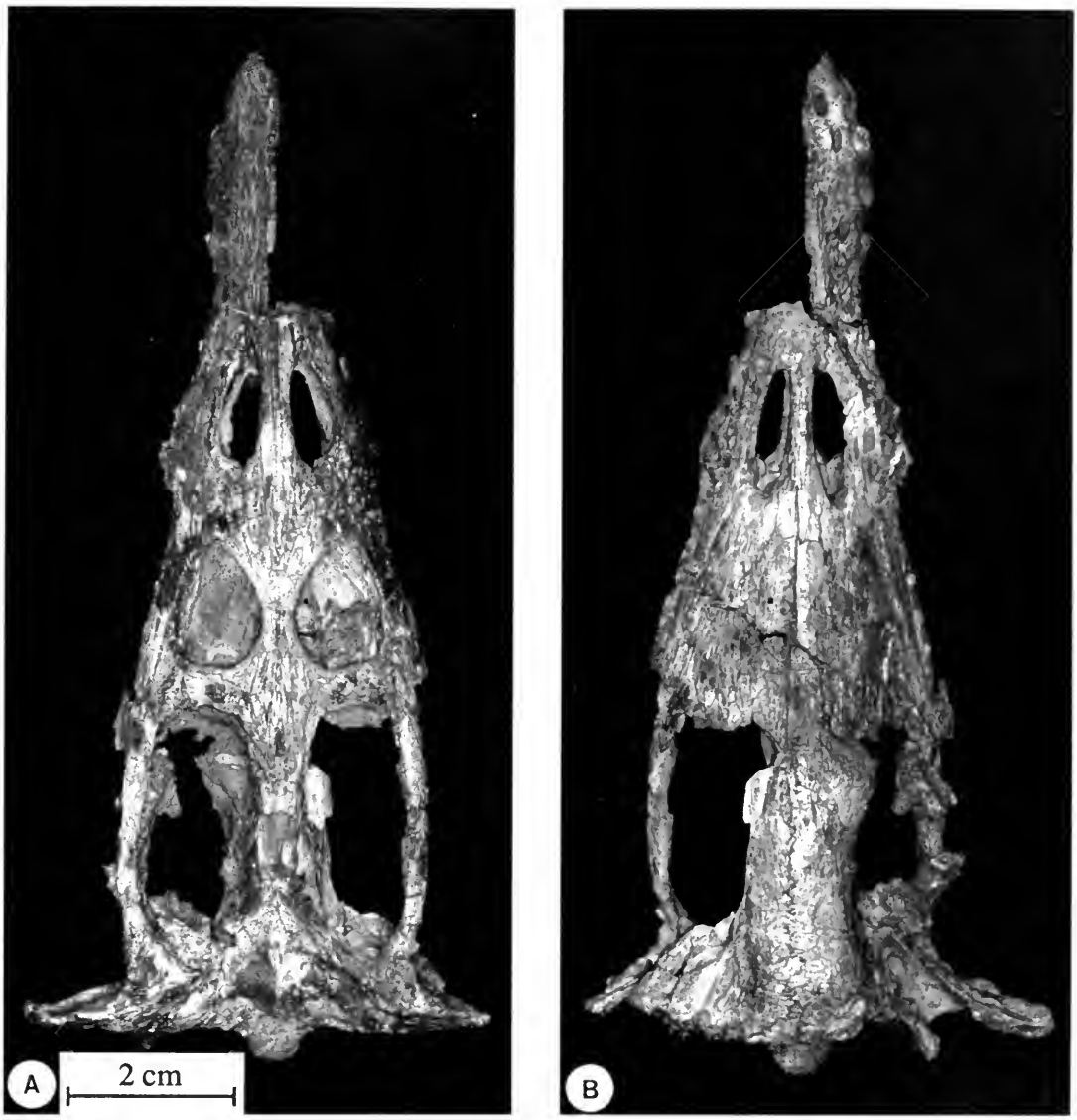

FIG. 19. Holotype of *Nothosaurus haasi* Rieppel, Mazin, and Tchernov (skull, HUJ-Pal. 2250). **A**, dorsal view. **B**, ventral view.

the tip of the snout to the anterior margin of the external naris results in an index of 1.5 (1.5–1.7 for *N. mirabilis*). Dividing the distance from the tip of the snout to the anterior margin of the upper temporal fenestra by the distance from the tip of the snout to the anterior margin of the external naris yields a ratio of 2.04 (2.2–2.7 for *N. mirabilis*). Finally, dividing the longitudinal diameter of the external naris by its transverse diameter yields a ratio of 2.59 (1.6–2.2 for *N. mirabilis*).

As can be seen in Table 1, *N. haasi* shares with *N. mirabilis* the long, slender, parallel-sided rostrum, but it differs from the latter species, as well as from all other species of *Nothosaurus*, by the proportions of its relatively large, long, and slender external nares. (*Nothosaurus edingerae* Schultze, 1970, is too incompletely known to yield comparable values for Table 1, but the longitudinal diameter of the external naris divided by its transverse diameter yields a ratio of 1.71 in SMNS 59072.)

The rostrum is formed by the paired premaxillae, carrying very long and slender posterior (nasal) processes, which extend between the elongate

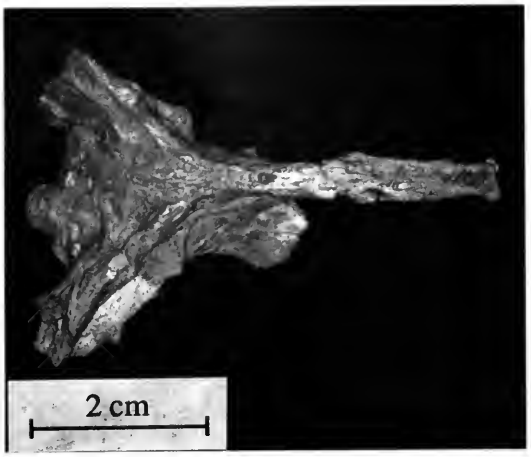

FIG. 20. A partial skull of *Nothosaurus haasi* Rieppel, Mazin, and Tchernov (HUJ-Pal. 3723), dorsal view.

nasals and meet the frontal at the level of the anterior margin of the orbit. In no other *Nothosaurus* species does the posterior (nasal) process of the premaxilla reach as far back; at most, it extends to a level midway between the posterior margin of the external naris and the anterior margin of the orbit (*N. giganteus:* Rieppel & Wild, 1996, Fig. 12; *N. mirabilis:* ibid., Fig. 60).

The nasals are unusually elongate and slender compared to other species of *Nothosaurus.* They are broadest at the posteromedial margin of the external nares and taper posteriorly to a blunt tip, which lies well behind the level of the anterior margin of the orbit. In other species of *Nothosaurus,* the nasal carries a slender anteromedial process that lines the entire medial margin of the external naris. A comparable anterior process of the nasal is absent in *N. haasi,* where the nasal remains restricted to the posterior third of the length of the external naris. Interestingly, the same configuration of the premaxillae and nasals characteristic of *N. haasi* is also observed in *Germanosaurus schafferi* Arthaber, 1924 (Rieppel, 1997a, Fig. 11).

The suture between premaxilla and maxilla is located at the anteroventral corner of the external naris, from where it extends in an anterolateral direction, curving around the base or alveolus of the anteriormost maxillary tooth. The maxilla does not have a depression with a foramen at its bottom along the lateral margin of the external naris, serving the exit of a lateral branch of the superior alveolar nerve, as is frequently observed in other species of *Nothosaurus* (Rieppel & Wild, 1996). Laterally, the maxilla shows a distinct bulge at the level of the posterior margin of the external naris, accommodating the roots of the maxillary fangs. Their position appears to be further anterior than is typical for other species of *Nothosaurus,* where the maxillary fangs are located at the level between the external naris and the orbit; the apparently more anterior position of the maxillary fangs in *N. haasi* results from the relatively larger external nares characteristic of this species. Behind the external naris, the maxilla meets the lateral margin of the nasals in a posteromedially trending suture. At the anterior margin of the orbit, the maxilla meets an anterolateral process of the frontal which enters between the nasal and the prefrontal, and the anterior margin of the prefrontal (see below for further details). Lateral to the prefrontal, the maxilla defines the anterolateral margin of the orbit. The lacrimal is absent; the lacrimal foramen lies entirely within the maxilla. Below and behind the orbit, the maxilla gradually tapers to a slender bone, carrying the maxillary toothrow backward a third of the length of the longitudinal diameter of the upper temporal fenestra.

In *Nothosaurus,* the prefrontal is usually a small element located at the anteromedial corner of the orbit. In the holotype of *N. haasi,* a deeply interdigitating suture can be observed at the anteromedial margin of the orbit, separating an anterolateral process of the frontal and what looks like the prefrontal from the maxilla. On the right side of the skull, a partial separation of the anterolateral process of the frontal from the anterior part of a prefrontal seems to be observable. More posteriorly, however, the prefrontal can no longer be separated from the frontal along the medial margin of the orbit, and a separate prefrontal is not distinct on the left side of the skull. The conclusion must be that a prefrontal is either absent or fused to the frontal. The frontal is unpaired (fused). The deeply interdigitating frontoparietal suture lies at the level of the posterior tip of the postfrontal within the anterior third of the longitudinal diameter of the upper temporal fossa.

The upper temporal fossa is relatively small in *N. haasi:* dividing the condylobasal skull length by the longitudinal diameter of the upper temporal fossa yields a ratio of 4.02 for *N. haasi,* 2.46 for *N. tchernovi* (see below), 2.6–3.0 for *N. marchicus,* and 2.3–2.5 for *N. mirabilis.*

The postfrontal is an essentially triradiate bone. Its anterior process defines the posteromedial margin of the orbit; its lateral process extends along the posterior margin of the orbit in front of the

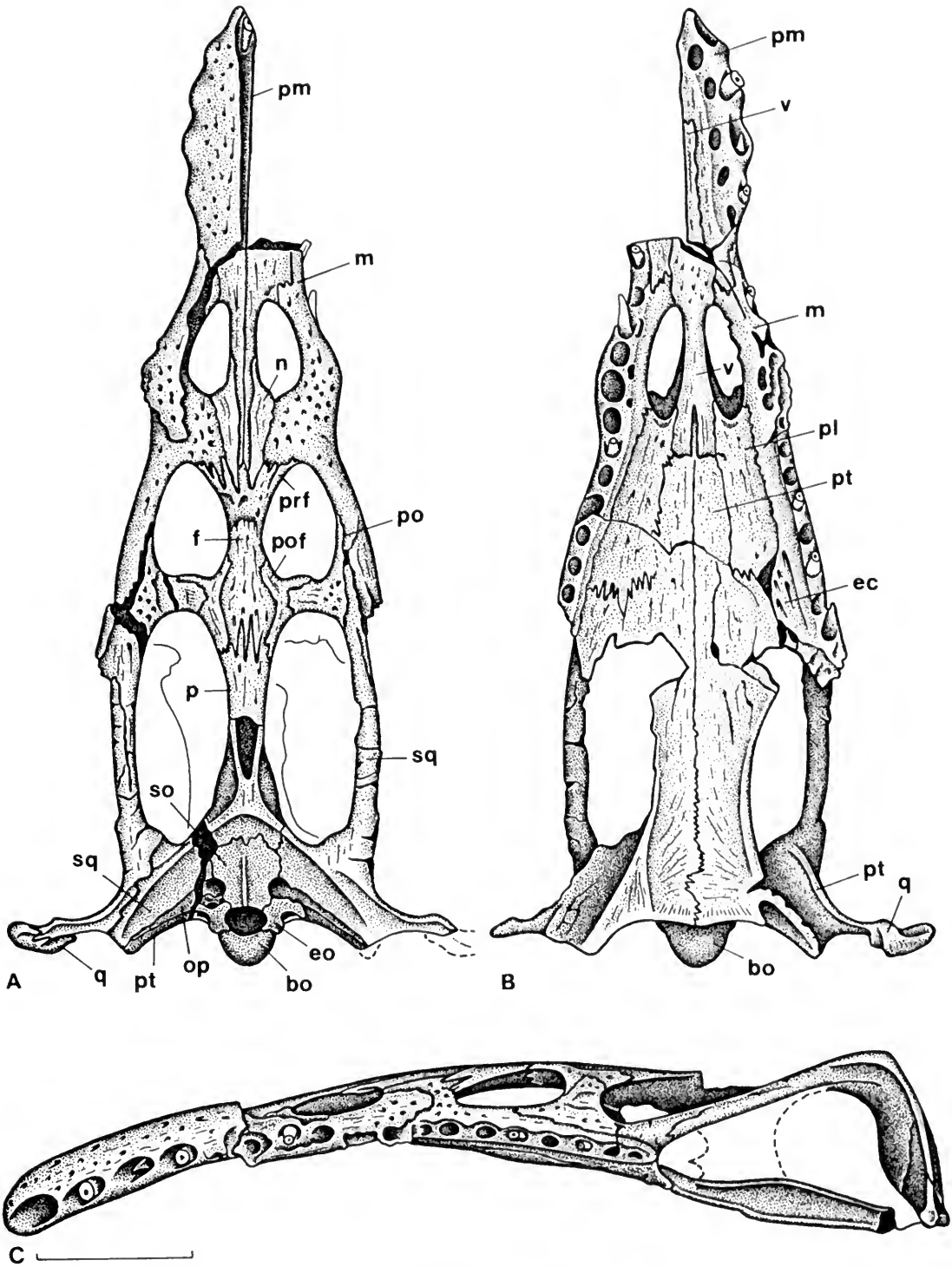

FIG. 21. Holotype of *Nothosaurus haasi* Rieppel, Mazin, and Tchernov (skull, HUJ-Pal. 2250). **A**, dorsal view. **B**, ventral view. **C**, left lateral view. Scale bar = 20 mm. Abbreviations: bo, basioccipital; ec, ectopterygoid; eo, exoccipital; f, frontal; m, maxilla; n, nasal; op, opisthotic; p, parietal; pl, palatine; pm, premaxilla; po, postorbital; pof, postfrontal; prf, prefrontal; pt, pterygoid; q, quadrate; so, supraoccipital; sq, squamosal; v, vomer.

TABLE 1. Skull proportion in *Nothosaurus*.

	Nothosaurus					
	giganteus	juvenilis	marchicus	mirabilis	haasi n.sp.	tchernovi
snout - external naris / rostral constriction	1.2 - 1.6	1.6	1.1 - 1.4	1.5 - 2.5	2.62	2.0
snout-orbit / snout - external naris	1.6 - 2.0	1.7	1.8 - 2.0	1.5 - 1.7	1.5	1.59
snout - upper temporal fossa / snout - external naris	2.6 - 3.4	2.7	2.9 - 3.4	2.2 - 2.7	2.04	2.45
longitudinal ∅ external naris / transverse ∅ external naris	juv.: 1.3 - 1.4 ad.: 1.7 - 1.85	1.36	1.0 - 1.4	1.6 - 2.2	2.59	1.56

postorbital; its posterior process defines the anteromedial margin of the upper temporal fossa. The postorbital has a broad medial process that forms most of the postorbital arch and thus defines the anterior margin of the upper temporal fossa as well as the posterolateral margin of the orbit. Anteriorly, the postorbital tapers to a slender process that extends along the lateral margin of the orbit almost to the level of its midpoint, which is unusual compared to other species of *Nothosaurus*. Posteriorly, the postorbital expands into a relatively large plate of bone sutured to the posterior end of the maxilla, separating the maxilla from the anterior process of the squamosal. More posteriorly, the postorbital tapers to a slender process lining the lateral margin of the upper temporal fossa and sutured to the anterior process of the squamosal, the two elements forming the upper temporal arch. The jugal, which in other species of *Nothosaurus* is intercalated between the posterior end of the maxilla and the postorbital, is absent in *N. haasi*.

The parietal is unpaired (fused). The posterior half of the skull table is split horizontally, exposing the matrix-filled cavity of the braincase. For this reason, the size and relative position of the pineal foramen cannot be identified. The parietal diverges posteriorly to meet the squamosals at the posterior margin of the upper temporal fossa. The occipital exposure of the parietal is limited, meeting the anterior margin of the supraoccipital in a deeply inderdigitating suture.

The squamosal defines most of the posterior margin of the upper temporal fossa. Anteriorly, it enters the upper temporal arch, tapering off alongside the lateral margin of the postorbital. Although the squamosal reaches far forward, it remains separated from the posterior end of the maxilla by the postorbital. Posteriorly, the squamosal gains a broad occipital exposure. It is sutured to the parietal and supraoccipital medially and to the opisthotic posteriorly. Laterally, the squamosal reaches far down along the lateral aspect of the quadrate. The quadratojugal is absent.

The ventral view of the skull exposes four alveoli for premaxillary fangs in the preserved left half of the rostrum. The diameters of these alveoli indicate a decreasing size of the premaxillary fangs from front to back. In a groove located medial to the functional tooth positions, five replacement pits can be identified, each located posteromedial to a functional tooth position. The count of the replacement pits indicates that the longitudinal fracture of the premaxillary rostrum passes right through the alveolus of the first, anteriormost premaxillary fang, whose replacement is exposed in dorsal but not in ventral view. The premaxilla remains excluded from the internal naris by a contact of the maxilla with the vomer at the anterior margin of the latter.

The maxilla forms the lateral margin of the internal naris and extends backward along the palatine and ectopterygoid. The suture between the maxilla and premaxilla is well exposed on the left side of the skull, and it indicates that three smaller maxillary teeth preceded the maxillary fangs. The alveoli of the maxillary fangs are crushed on the left side of the skull, but the well-preserved right maxilla evidences the presence of paired maxillary fangs, behind which the maxillary teeth decrease in size. The posterior tip of the right maxilla is incomplete, and a total of seven tooth positions can be counted posterior to the maxillary fangs. The posterior tip of the left maxilla is complete, and a total of eight tooth positions can be counted posterior to the maxillary fangs. The complete maxillary tooth count therefore is 13 (3-2-8). The structure of the vomer is different from that observed in other species of *Nothosaurus*. Between and immediately in front of the internal nares, the vomers are completely fused. More anteriorly, fusion of the vomers cannot be ascertained due to breakage of the rostrum. The vomer is unusual, however, in that it can be seen to extend far into the premaxillary rostrum for about half its total length on the preserved left side. Posterior to the internal nares, the vomers are unfused, forming two relatively broad lappets of bone that are separated from each other by a distinct cleft. The broken posterior edges of the vomers meet the pterygoids in what appears to be a transverse suture.

The palatine forms the posterior margin of the internal naris. There is no distinct choanal groove on the palatine, as is observed in *N. juvenilis* (Rieppel, 1994b). Posteriorly, the palatine is embraced by the maxilla, ectopterygoid, and pterygoid. The ectopterygoid is an unusually short element that meets the palatine in a broad, transversely oriented, deeply interdigitating suture. The pterygoid shows a weakly developed transverse process that, together with the ectopterygoid, forms a weakly pronounced ventral (ecto-)pterygoid flange. The pterygoid itself corresponds to the characteristic sauropterygian pattern. The posterior tip of the quadrate ramus is broken on both sides. This damage exposes the cranioquadrate passage in ventral view on the left side of the skull. Other species of *Nothosaurus* show a deeply interdigitating suture between the pterygoids at their posterior extremity, which is less distinct in *N. haasi*.

The occipital crest of *N. haasi* is poorly expressed due to breakage of the posterior part of the parietal skull table. The supraoccipital is a relatively broad plate that is intercalated between parietal and squamosals, more or less horizontally oriented, and that carries a distinct sagittal crest. Posterolaterally, it defines the medial margin of the rudimentary posttemporal fossa and meets the exoccipital in the dorsolateral margin of the foramen magnum.

The pedicel of the exoccipital rests on the dorsolateral aspect of the occipital condyle (basioccipital). It defines the lateral margin of the foramen magnum and in its dorsal part expands laterally, forming the ventral margin of the rudimentary posttemporal fossa along its contact with the opisthotic. Lateral to the pedicel of the exoccipital and below its dorsolateral expansion is located the large metotic (jugular) foramen, internally subdivided by a single strut of (exoccipital) bone that separates the roots of the glossopharyngeal and vagus nerves from that of the hypoglossal nerve.

The lateral margin of the rudimentary posttemporal fossa is defined by the opisthotic, which is exposed as a narrow strip of bone intercalated between the squamosal (dorsally) and pterygoid (ventrally). On the better preserved left side of the skull, the opisthotic is seen to taper off laterally, the squamosal contacting the pterygoid lateral to its distal tip. The left quadrate is well exposed. The squamosal extends far down along the lateral aspect of the quadrate, and even further on its posterior aspect, where it narrowly approaches the mandibular condyle of the quadrate.

The basioccipital tubers are distinct (5.5 mm wide) and approximately equal in diameter to the occipital condyle (6.5 mm wide). The eustachian foramen is open between the basioccipital tuber and the pterygoid on both sides of the skull. Erosion of the bone surface obscures the internal carotid foramen on the posterior aspect of the quadrate ramus of the pterygoid.

The entire otic complex is missing on both sides of the skull, but the broad epipterygoids are present on both sides of the skull, though better preserved on the right. The epipterygoid shows a broad base sutured to the pterygoid, a distinctly concave posterior margin, and a broad dorsal margin sutured to the ventrolateral edge of the parietal. The anterior margin of the epipterygoid is essentially concave, but it carries a distinct anterior spine defining a ventral recess at the anterior opening of the cavum epiptericum. A similar epipterygoid structure is observed in *Nothosaurus* cf. *N. mirabilis* (Rieppel, 1994c).

HUJ-Pal. 3723 represents the incomplete poste-

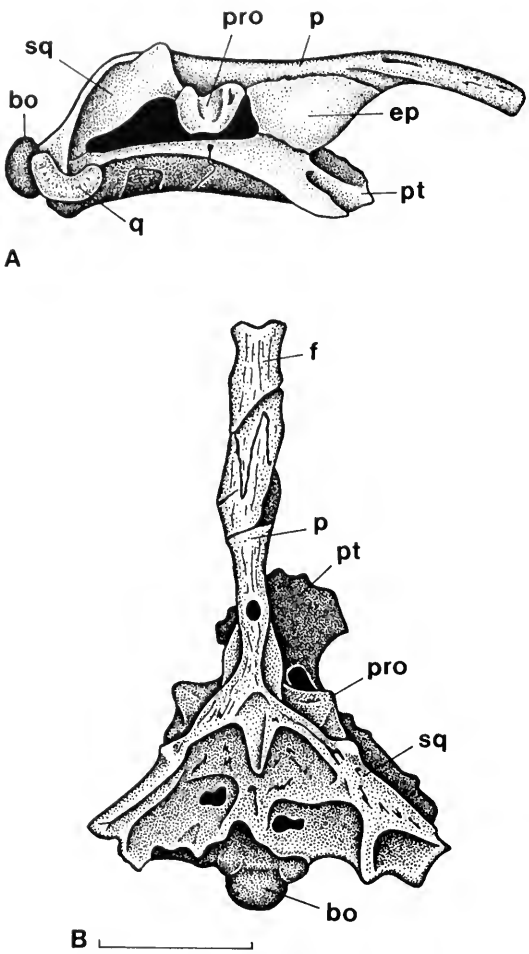

FIG. 22. A partial skull of *Nothosaurus haasi* Rieppel, Mazin, and Tchernov (HUJ-Pal. 3723). **A,** right lateral view. **B,** dorsal view. Scale bar = 15 mm. Abbreviations: bo, basioccipital; ep, epipterygoid; p, parietal; pro, prootic; pt, pterygoid; q, quadrate; sq, squamosal.

rior part of a skull of a small nothosaur referred to *N. haasi* (Fig. 22). As preserved, the total length of the fragment is 56.5 mm and its total width is 38.3 mm. The specimen is slightly smaller than the holotype of *N. haasi,* but otherwise it is closely similar and noteworthy for a well-preserved braincase. The specimen is slightly compressed and distorted; however, that did not result in a disarticulation of braincase and dermatocranial elements. Also, sutures cannot unequivocally be identified in the occiput, indicating fusion of the posterior braincase elements. Collectively, these features indicate adult age of the specimen.

Unlike the holotype, the partial skull HUJ-Pal. 3723 preserves the posterior part of the skull roof with an intact pineal foramen, located at some distance in front of the posterior margin of the skull roof but still distinctly behind the midpoint of the unpaired (i.e., fused) parietal. In posterior view, the specimen exhibits the dorsoventrally compressed foramen magnum, flanked on either side by the exoccipitals, which sit on the dorsolateral aspect of the occipital condyle. Sutures between the supraoccipital, exoccipital, opisthotic, parietal, and squamosal are indistinct, but the impressions of small (rudimentary) posttemporal fossae can be identified. Lateral to the occipital condyle (horizontal diameter: 6.5 mm), the basioccipital tubera (horizontal diameter: 4.8 mm) are distinct, as is the posterior opening of the right cranioquadrate passage between the mandibular condyle of the quadrate, the quadrate ramus of the pterygoid, and the squamosal. The posterior margins of the squamosals form an inverted V.

The lateral view of the skull fragment shows the well-developed temporal shelf of the squamosal characteristic of *Nothosaurus* (Rieppel, 1994c). The temporal shelf carries a distinct ridge, which lines up with the posterior margin of the prootic. Below the temporal shelf of the squamosal, behind the prootic, and above the quadrate ramus of the pterygoid, a large opening exposes the cranioquadrate passage laterally. The prootic itself is a spoon-shaped ossification, seemingly rather loosely set into the lateral wall of the braincase (lost in the holotype), with a convex ventral margin and a concave (indented) dorsolateral surface. In *Nothosaurus* cf. *N. mirabilis,* the prootic is essentially similar in general shape, but it carries two ventral pedicels, which rest on the dorsal surface of the pterygoid and enclosed the root of the facial nerve between them (Rieppel, 1994c). Comparable pedicels are absent in HUJ-Pal. 3723, where a narrow gap persists between the ventral margin of the prootic and the pterygoid. Between the prootic and the epipterygoid, a triangular opening represents the trigeminal recess. The comparable recess in the braincase of *Nothosaurus* cf. *N. mirabilis* is relatively larger, due to a different shape of the epipterygoid (Rieppel, 1994c). In *Nothosaurus* cf. *N. mirabilis,* the epipterygoid shows a deeply recessed anterior and posterior margin, which results in a "waisted" appearance of the bone with a broad base, a constricted body, and a broad dorsal margin. In HUJ-Pal. 3723, the anterior and posterior margins of the epipterygoid are both slightly convex; the element is sutured to a ridge on the dorsal surface of the pterygoid along its broad base and expands

dorsally to an even broader dorsal margin sutured to the ventrolateral edge of the parietal. The epipterygoid of the *N. haasi* holotype resembles that of *Nothosaurus* cf. *N. mirabilis* (Rieppel, 1994c) more closely than that of HUJ-Pal. 3723, but in view of the scarcity of the material, it is impossible to determine whether these differences indicate individual variation or taxonomic diversity.

The sauropterygian material of Makhtesh Ramon is fully disarticulated. Reference of postcranial material to specific taxa based on diagnostic skull material must therefore always remain tentative. However, the available cranial material provides a valid basis for assessing taxonomic diversity at this locality, which permits the specific identification (with some confidence) of at least some postcranial material on the basis of its relative frequency and size.

The Muschelkalk of Makhtesh Ramon has yielded a number of isolated neural arches that are referred to *N. haasi.* These neural arches are of rather gracile appearance and bear a slender but relatively high neural spine. They are represented by specimens of different absolute size, reflecting their different positions within the vertebral column. The largest specimen is HUJ-Pal. 3881 (Figs. 23A, 24A), with a well-preserved anterior surface but a badly eroded posterior surface. The total height of the neural arch is 84.1 mm, the height from the roof of the neural canal to the tip of the neural spine is 69.6 mm, and the total width across the transverse processes is 51.9 mm. The anterior aspect of the neural spine shows a rugose surface, indicating the insertion of strong muscular tendons, but the lateral surface of the neural spine is devoid of vertical striations (see description of *N. tchernovi* below).

The distinctly bipartite zygosphene is located between and above the prezygapophyses. The prezygapophyses are slightly inclined, facing dorsomedially with their articular surfaces, which enclose an angle of approximately 25° with the horizontal. The transverse processes are distinct yet relatively short and face straight laterally. They are restricted to the dorsal part of the neural arch; i.e., they do not extend ventrally all along the pedicel.

HUJ-Pal. 321 is a second neural arch of the same type (Figs. 23B, 24B), somewhat smaller but sturdier. Its total height is 49.7 mm, and the height from the roof of the neural canal to the tip of the neural spine is 39.4 mm. The total width across the transverse processes is 35 mm. HUJ-Pal. 1487 (Fig. 24C) is smaller yet, with a total height of the neural arch of 26.6 mm, a height from the roof of the neural canal to the tip of the neural spine of 16.4 mm, and a total width across the transverse processes of 22 mm. Its transverse processes are deeper, extending far down but not quite reaching the base of the neural arch pedicel. This element appears to derive from the posteriormost dorsal region. A last element of corresponding structure is HUJ-Pal. 789 (total height of neural arch: 23.8 mm; height from the roof of the neural canal to the tip of the neural spine: 15.8 mm; total width across the transverse processes: 20.7 mm).

The Muschelkalk of Makhtesh Ramon has yielded a number of humeri (Table 2) of highly distinctive morphology (Figs. 25, 26) which, again on the basis of their size and relative frequency, are referred to *N. haasi.* These humeri vary in length from 40 mm (HUJ-Pal. 2043) to 97 mm (HUJ-Pal. 2049). In an undescribed, articulated skeleton of *Nothosaurus* cf. *N. mirabilis* from the upper Muschelkalk (SMNS 56618), the ratio of condylobasal skull length (183 mm) to humerus length (142 mm) is 1.29. With the humeri here discussed referred to *N. haasi,* the ratio of condylobasal skull length (of the holotype) to humerus length is 1.27 for HUJ-Pal. 2049 (Figs. 25A, 26A). The whole humerus appears to be twisted, with the oblong terminal articular heads oriented at 90° relative to each other. Along the postaxial margin of the bone, adjacent to the proximal articular head, a distinct deltopectoral crest projects ventrally for about one-third of the length of the humerus. On the dorsal surface of the humerus, a distinct crest for the insertion of the m. latissimus dorsi extends from the preaxial margin close to the proximal articular head in a posterolateral direction. Along its preaxial margin, the humerus is expanded into a distinct horizontal flange with an evenly convex anterior margin. The posterior margin is evenly concave, which results in a broad and distinctly curved appearance of the humerus. In cross section, the dorsal surface of the humerus is flat, the ventral surface evenly concave. The ectepicondylar ridge is indistinct on all humeri and is not notched distally. An entepicondylar foramen is present in HUJ-Pal. 2060 (Fig. 26C) but absent in all other specimens. (An entepicondylar foramen is usually present in other species of *Nothosaurus.*) Among the sample of humeri possibly referable to *N. haasi* is one very small specimen (HUJ-Pal. 2043, Figs. 25C, 26E; total length: 39.8 mm) that may represent a juvenile. It differs from larger humeri of the same type in its less expanded diaphyseal region. This

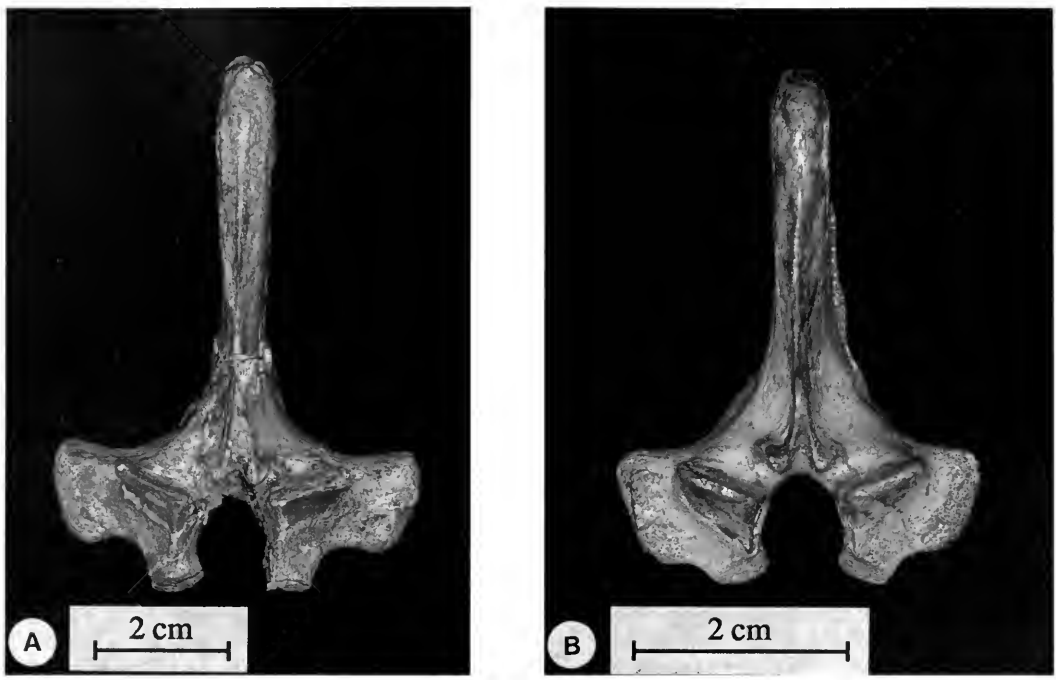

FIG. 23. Isolated neural arches of *Nothosaurus haasi* Rieppel, Mazin, and Tchernov. **A,** HUJ-Pal. 3881, anterior view. **B,** HUJ-Pal. 321, anterior view.

indicates that broadening of the diaphysis by developing an anterior flange increased with the size of the humerus.

The Muschelkalk of Makhtesh Ramon has yielded a number of lightly built femora (Fig. 27) which, again on the basis of their size, may be referred to *N. haasi.* Among the specimens in question (Table 3), one well-preserved femur (HUJ-Pal. 2173, Fig. 28) was prepared with acid. It is a slender and slightly curved element with a distinct internal trochanter that is not separated from the proximal articular head by a distinct intertrochanteric fossa.

DISCUSSION—*Nothosaurus haasi* is a relatively small species, most closely comparable to *N. juvenilis,* with a condylobasal skull length of 137.2 mm (Rieppel, 1994b). The two species share a number of other characters, such as a relatively narrow postorbital arch, the relative position of the pineal foramen, and three smaller teeth preceding the paired maxillary fangs. However, a number of characters separate the two species. *Nothosaurus juvenilis* shows a relatively shorter rostrum (see Table 1), relatively smaller external nares, relatively larger orbits, broad nasals separating the premaxillae from the frontal, distinct prefrontals, a larger postfrontal, a lesser extent of postorbital along the ventral margin of the orbit, presence of a jugal, paired vomers that do not extend as far anteriorly as in *N. haasi,* and deep choanal grooves on the palatine.

A second small species of nothosaur is *N. edingerae,* known from two specimens with a skull length of approximately 129 and 138 mm, respectively (Schultze, 1970; Rieppel & Wild, 1994). Again, the two species differ in several characters. *Nothosaurus edingerae* shows what appears to be a relatively shorter rostrum (the distance from the tip of the snout to the anterior margin of the external naris divided by the width of the snout at the rostral constriction yields a ratio of 1.01 [right] and 1.05 [left] for the holotype of *N. edingerae* [Schultze, 1970] and 2.62 for the holotype of *N. haasi*), relatively shorter and broader external nares, distinct prefrontals, a lesser extent of the postorbital along the ventral margin of the orbit, and paired vomers that extend a shorter distance anteriorly into the premaxillary rostrum. *Nothosaurus edingerae* is diagnosed by a posterior sagittal crest on the parietal (Rieppel & Wild, 1994) which, if present, would be broken

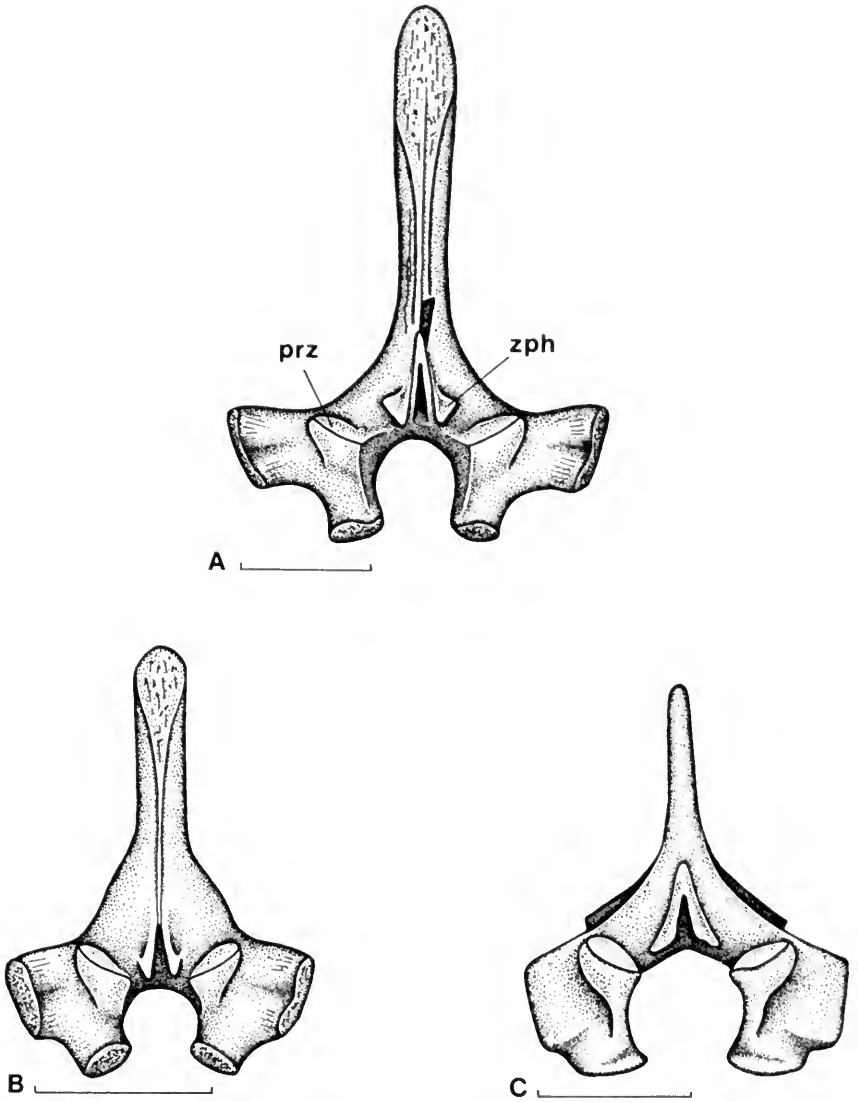

FIG. 24. Isolated neural arches of *Nothosaurus haasi* Rieppel, Mazin, and Tchernov. **A,** HUJ-Pal. 3881, anterior view; scale bar = 20 mm. **B,** HUJ-Pal. 321, anterior view; scale bar = 20 mm. **C,** HUJ-Pal. 1487, anterior view; scale bar = 10 mm. Abbreviations: prz, prezygapophysis; zph, zygosphene.

in the holotype of *N. haasi*; a sagittal crest is absent in HUJ-Pal. 3723.

Nothosaurus haasi is unique among diagnostic material of *Nothosaurus* in showing an unpaired (fused) vomer. Fusion of the vomers has so far been recorded in a single *Nothosaurus* skull fragment, from the Muschelkalk of Djebel Rehach in southern Tunisia (Gorce, 1960). However, this latter specimen is much larger than *N. haasi* and too incomplete to be diagnostic at the species level (referred to *Nothosaurus* cf. *N. giganteus* by Rieppel, 1997b).

Nothosaurus tchernovi Haas, 1980

Synonymy for this material

1955 *Nothosaurus* sp. (partim), Brotzen, p. 404.
1955 *Nothosaurus* sp., Peyer, p. 487, Fig. 1.
1957 *Nothosaurus* sp. (partim), Brotzen, p. 202.
1959 *Nothosaurus* sp. (partim), Haas, p. 3.
1962 *Nothosaurus* sp. (partim), Parnes, p. 10.

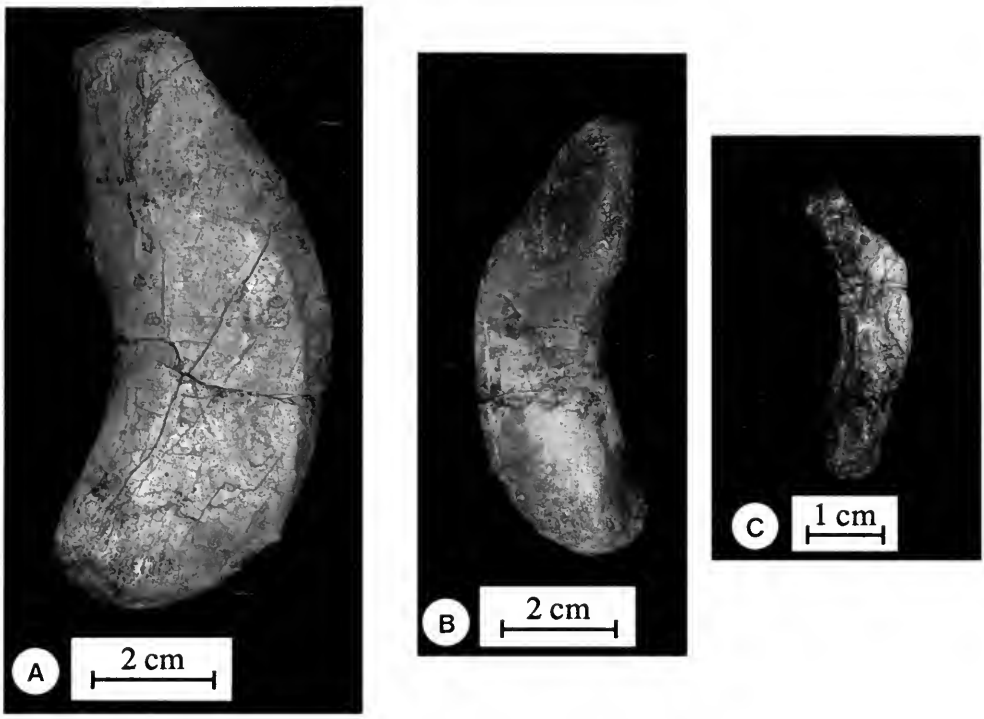

FIG. 25. Isolated humeri of *Nothosaurus haasi* Rieppel, Mazin, and Tchernov. **A,** HUJ-Pal. 2049, dorsal view. **B,** HUJ-Pal. 2060, ventral view. **C,** HUJ-Pal. 2043, ventral view.

1965 *Nothosaurus* sp. (partim), Lehman, p. 175.
1967 *Nothosaurus* sp. (partim), Haas, p. 330.
1980 *Nothosaurus tchernovi,* Haas, p. 119, Pls. 1–5.
1981 *Nothosaurus tchernovi,* Haas, p. 33.

HOLOTYPE—Hebrew University of Jerusalem, HUJ-Pal. 3665 (Figs. 29, 30), almost complete skull with articulated mandible.

DIAGNOSIS—A species of *Nothosaurus* closely similar to *N. mirabilis* with a relatively long, slender, and parallel-edged rostrum and an elongated postorbital region of the skull with long and narrow upper temporal fossae, but differing from *N. mirabilis* by the absence of a jugal, a contact of

TABLE 2. Measurements (in millimeters) for humeri referred to *Nothosaurus haasi.*

	total length	proximal width	maximal width	distal width
HUJ-Pal. 2049	96.8	24.3	36.5	27.5
HUJ-Pal. 2060	75.5	--	23.7	21.9
HUJ-Pal. 2174	63.8	17.8	22.8	19
HUJ-Pal. 2043	39.8	--	10	10

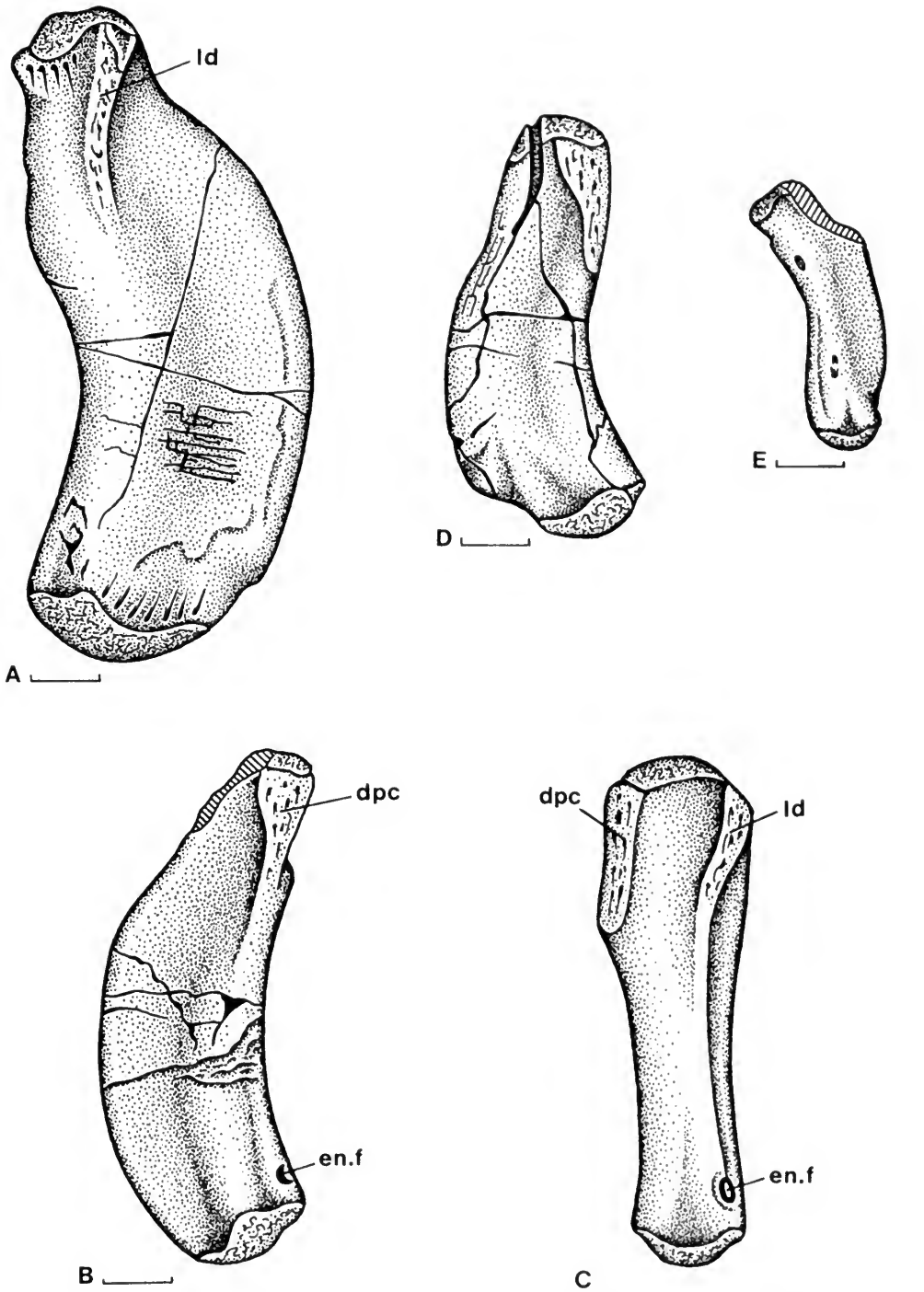

FIG. 26. Isolated humeri of *Nothosaurus haasi* Rieppel, Mazin, and Tchernov. **A,** HUJ-Pal. 2049, right humerus, dorsal view. **B,** HUJ-Pal. 2060, right humerus, ventral view. **C,** HUJ-Pal. 2060, right humerus, posterior view. **D,** HUJ-Pal. 2174, right humerus, ventral view. **E,** HUJ-Pal. 2043, left humerus, ventral view. Scale bar = 10 mm. Abbreviations: dpc, deltopectoral crest; en.f, entepicondylar foramen; ld, m. latissimus dorsi insertion.

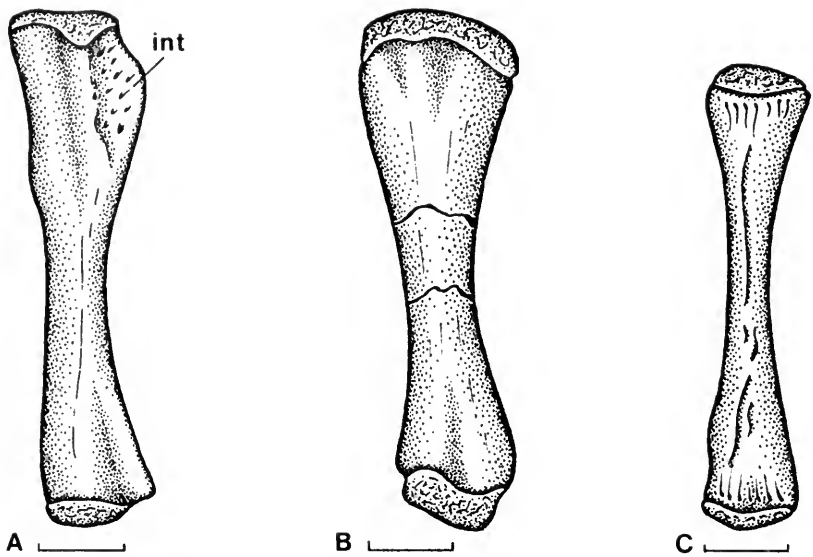

FIG. 27. Isolated femora of *Nothosaurus haasi* Rieppel, Mazin, and Tchernov. **A,** HUJ-Pal. 38B, left femur, dorsal view. **B,** HUJ-Pal. 3798, left femur, dorsal view. **C,** HUJ-Pal. 2045, femur. Scale bar = 10 mm. Abbreviation: int, internal trochanter.

the anterior end of the squamosal with the posterior end of the maxilla, and a deeply concave surface of the dermal palate at the posterior end of the pterygoids.

REFERRED MATERIAL—HUJ-uncatalogued, partial skull (mentioned by Haas, 1980: p. 123); HUJ-Pal. 3859, posterior part of skull, unprepared; HUJ-Pal. 2884, isolated basioccipital; HUJ-Pal. 1994, posterior end of lower jaw; HUJ-Pal. 759 (Fig. 31A), skull fragment; HUJ-Pal. 757 (Fig. 31B), skull fragment (original of Peyer, 1955, Fig. 1). For postcranial elements associated with this species, see morphological description below.

STRATUM AND LOCUS TYPICUS—Lower Member of the Saharonim Formation of late Anisian (middle and late Illyrian) or early Ladinian (Fassanian) age, Middle Triassic, Makhtesh Ramon, Negev, Israel.

COMMENTS—Nothosaur remains are frequent in the *Ceratites* beds of the Muschelkalk of Makhtesh Ramon and have repeatedly been reported ever since Brotzen's (1955) and Peyer's (1955) first announcements of vertebrate fossils at that locality. It was not until 1980 that a skull, collected in 1978 by one of us (E.T.), was formally described as a new taxon by Haas (1980). *Notho-*

TABLE 3. Measurements (in millimeters) for femora referred to *Nothosaurus haasi.*

	total length	proximal width	minimal width	distal width
HUJ-Pal. 3813	59.8	14.6	6.2	12.3
HUJ-Pal. 3798	59.5	16.5	7.5	13
HUJ-Pal. 2173	57.3	12.6	4.7	10.8
HUJ-Pal. 2045	53.5	12.5	5.5	11

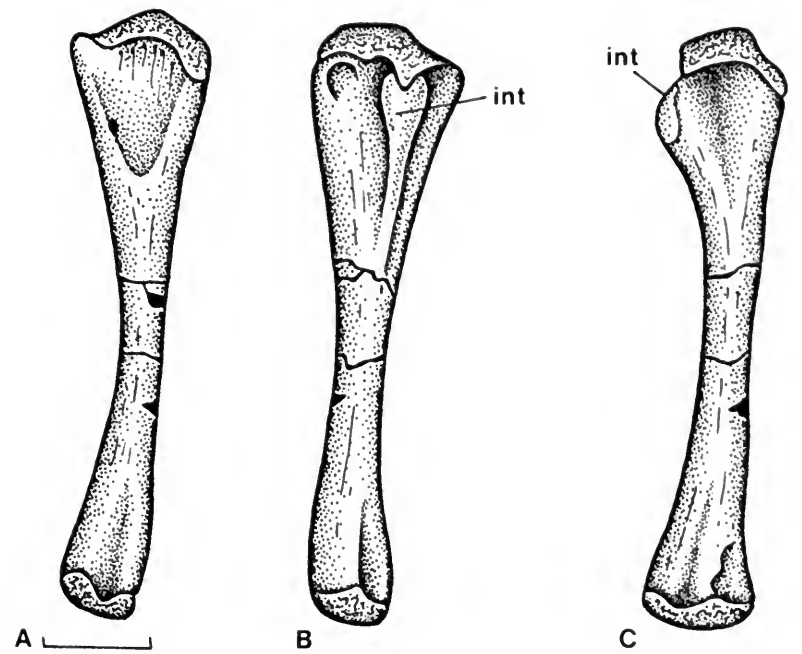

FIG. 28. Isolated right femur of *Nothosaurus haasi* Rieppel, Mazin, and Tchernov (HUJ-Pal. 2173). **A,** dorsal view. **B,** ventral view. **C,** posterior view. Scale bar = 10 mm. Abbreviation: int, internal trochanter.

saurus tchernovi is distinctly larger than *N. haasi* but smaller than *N. giganteus,* and appears to be the most frequently found nothosaur at Makhtesh Ramon.

MEASUREMENTS—The following measurements for the holotype of *N. tchernovi* are all in millimeters. Values in parentheses are for the right side of the skull.

Tip of the snout to occipital condyle: 310
Tip of the snout to anterior margin of upper temporal fossa: approximately 169 (173)
Tip of the snout to anterior margin of the orbit: 111.5 (114)
Tip of the snout to anterior margin of external naris: 70 (71)
Tip of the snout to the anterior margin of internal nares: 77.5
Width of skull across mandibular condyles of quadrate: approximately 128
Width of skull across posterior end of squamosals: approximately 118
Width of skull across postorbital arches: 85.5
Width of skull at roots of maxillary fangs: 66.3
Width of skull at rostral constriction: 35.1
Maximum width of premaxillary rostrum: 36.2
Longitudinal diameter of external naris: 23 (23)
Transverse diameter of external naris: 14.5 (15)
Longitudinal diameter of orbit: 42 (41)
Transverse diameter of orbit: 32 (35)
Longitudinal diameter of upper temporal fossa: — (126)
Transverse diameter of upper temporal fossa: — (approximately 36)
Longitudinal diameter of internal naris: 28
Transverse diameter of internal naris: 9.8
Distance from posterior margin of external naris to anterior margin of orbit: 18.1 (18.6)
Distance from posterior margin of orbit to anterior margin of upper temporal fossa: (19.9)
Middorsal bridge between external nares: 9.2
Middorsal bridge between orbits (minimum width): approximately 17.5

MORPHOLOGICAL DESCRIPTION—The holotype of *N. tchernovi* is represented by an almost complete, mechanically prepared skull (Fig. 30), with the mandible in articulation. The left postorbital region of the skull is missing, as is the parietal, which is partially preserved as a natural mold. The endocranial and middle-ear cavities are likewise preserved as natural molds, described in detail by Haas (1980).

Dividing the distance from the tip of the snout to the anterior margin of the external naris by the width of the skull at the rostral constriction yields

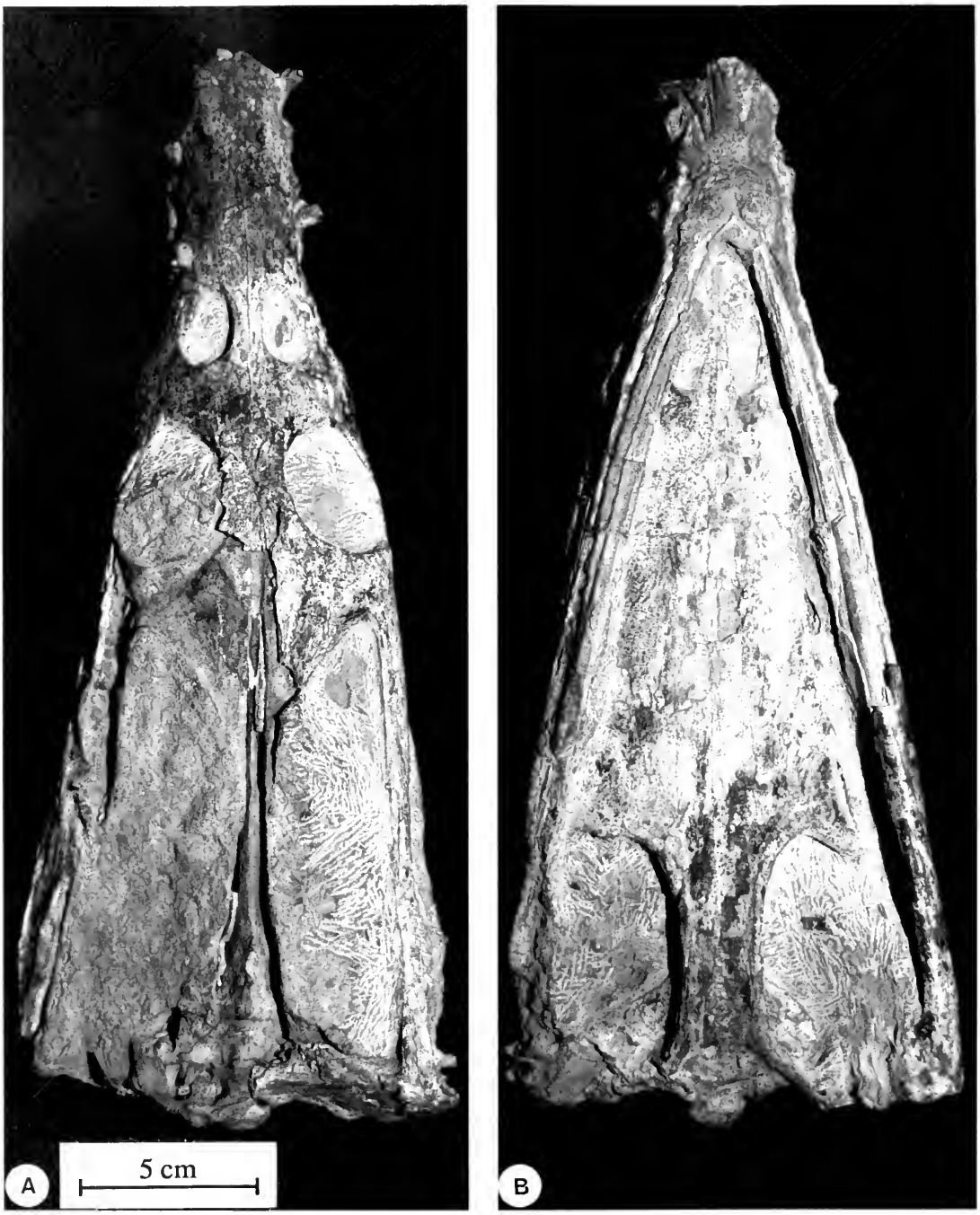

FIG. 29. Holotype of *Nothosaurus tchernovi* Haas (skull, HUJ-Pal. 3665). **A.** dorsal view. **B.** ventral view.

a value of 2.0 (1.5–2.5 for *N. mirabilis*; 2.62 for *N. haasi*). Dividing the distance from the tip of the snout to the anterior margin of the orbit by the distance from the tip of the snout to the anterior margin of the external naris results in an index of 1.59 (1.5–1.7 for *N. mirabilis*; 1.5 for *N. haasi*). Dividing the distance from the tip of the snout to the anterior margin of the upper temporal fenestra by the distance from the tip of the snout to the anterior margin of the external naris yields

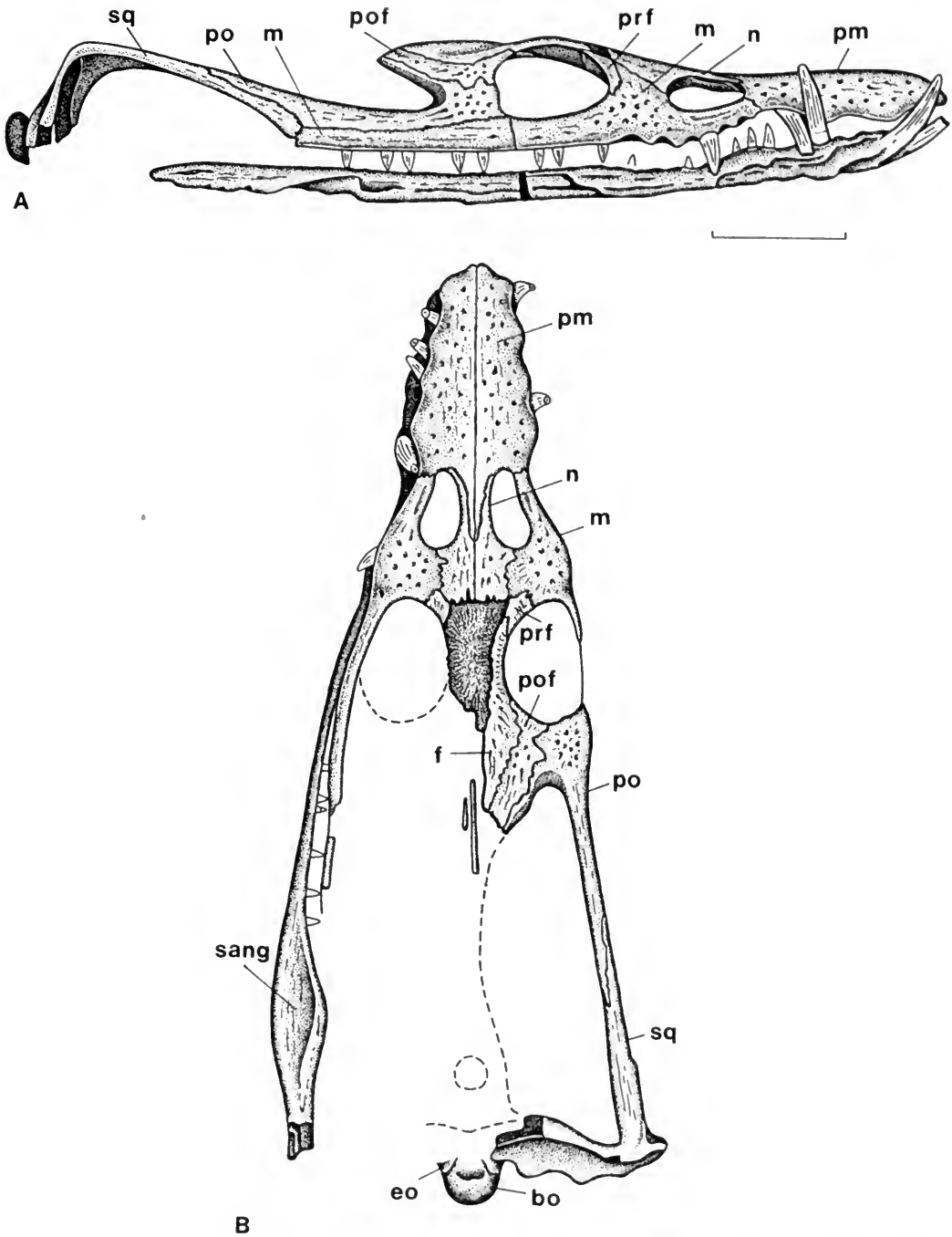

FIG. 30. Holotype of *Nothosaurus tchernovi* Haas (skull, HUJ-Pal. 3665). **A**, right lateral view. **B**, dorsal view. Scale bar = 25 mm. Abbreviations: bo, basioccipital; eo, exoccipital; f, frontal; m, maxilla; n, nasal; pm, premaxilla; po, postorbital; pof, postfrontal; prf, prefrontal; sang, surangular; sq, squamosal.

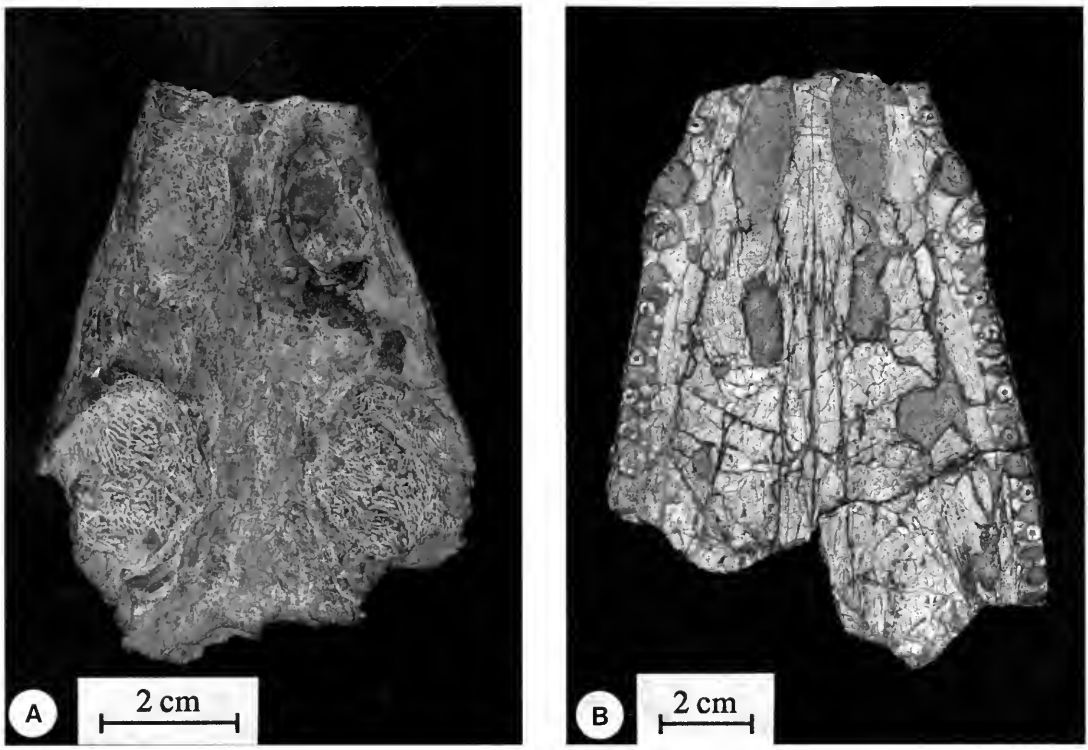

FIG. 31. Incomplete skull remains referred to *Nothosaurus tchernovi* Haas. **A,** HUJ-Pal. 759, anterior part of skull, dorsal view. **B,** HUJ-Pal. 757, anterior part of skull, ventral view.

a ratio of 2.45 (2.2–2.7 for *N. mirabilis*; 2.04 for *N. haasi*). Finally, dividing the longitudinal diameter of the external naris by its transverse diameter yields a ratio of 1.56 (1.6–2.2 for *N. mirabilis*; 2.59 for *N. haasi*). As can be seen from Table 1, *N. tchernovi* shares with *N. haasi* and *N. mirabilis* the elongate, slender, and parallel-edged rostrum, but the shape and proportions of the external nares are more similar to *N. mirabilis* than to *N. haasi.*

The rostrum is formed by the paired premaxillae. The posterior (nasal) processes of the premaxillae extend backward to a level slightly in front of the posterior margins of the external nares, and they remain separated from the frontal by the nasals. The ventral surface of the premaxillary rostrum is obscured by the symphysis of the articulated mandible. Haas (1980) counted four premaxillary fangs, but there are actually five in each element, the anteriormost one (missed by Haas, 1980) situated adjacent to the midline of the rostrum and pointing straight forward.

The transversely oriented suture between the premaxilla and maxilla is located at the anterolateral corner of the external naris. The nasals are relatively broad elements, meeting each other along an extended medial suture. Each nasal carries a slender anterolateral process that extends along the entire medial margin of the external naris. Unfortunately, the bone surface is badly damaged in the area of contact between nasals and frontal, so that no details of the sutural contact between these elements can be identified. On the left side of the skull, the nasal contacts the prefrontal, thus separating the frontal from the maxilla. A comparable contact of nasal and prefrontal is less distinct on the right side of the skull, and may indeed be absent. A similar bilateral asymmetry of the nasal–prefrontal relations is also observed in *N. mirabilis* (Rieppel, 1993b) as well as in *S. gaillardoti* (Rieppel, 1994a). The frontal is unpaired (fused) and forms most of the dorsal margin of the orbits. The reduced prefrontal, distinct from the frontal, is located at the anteromedial corner of the orbit. A lacrimal is absent.

The maxilla forms all of the lateral and posterolateral margin of the external naris. Lateral to the external naris, a shallow depression can be identified on the maxilla; however, it lacks a foramen at its bottom, in contrast to most specimens

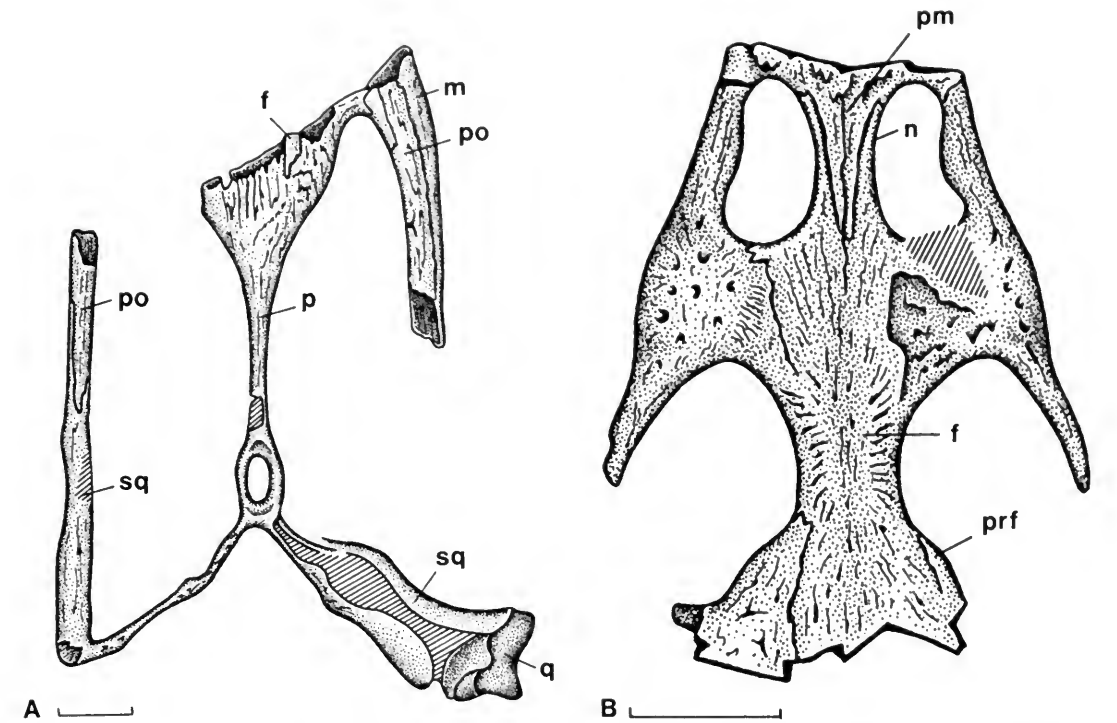

FIG. 32. Partial skulls of *Nothosaurus tchernovi* Haas. **A,** HUJ-Pal. uncatalogued, dorsal view. **B,** HUJ-Pal. 759, dorsal view. Scale bar = 20 mm. Abbreviations: f, frontal; m, maxilla; n, nasal; p, parietal; pm, premaxilla; po, postorbital; prf, prefrontal; sq, squamosal; q, quadrate.

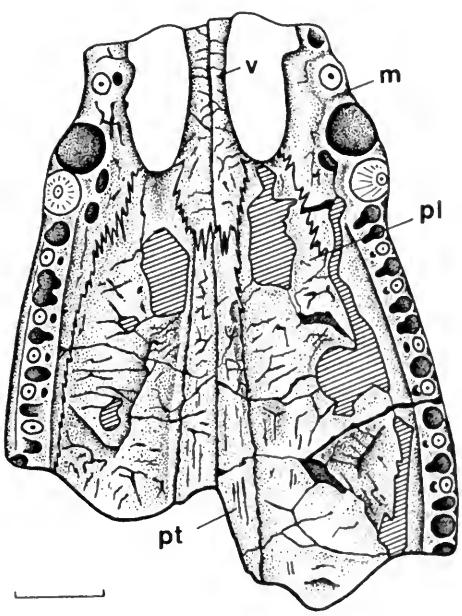

FIG. 33. A partial skull of *Nothosaurus tchernovi* Haas (HUJ-Pal. 757), ventral view. Scale bar = 20 mm. Abbreviations: m, maxilla; pl, palatine; pt, pterygoid; v, vomer.

of *N. mirabilis.* A distinct lateral expansion at the level between the external naris and the orbit indicates the position of the paired maxillary fangs. The lateral view of the skull shows that the maxilla extends back to a level slightly beyond the first third of the longitudinal diameter of the upper temporal fossa. The longitudinal diameter of the upper temporal fossa is 126 mm; the posterior ramus of the maxilla entering the upper temporal arch measures 47 mm. Due to the articulated mandible, it is difficult to describe the maxillary dentition in detail. The lateral and ventrolateral view of the (complete right) maxilla allows the identification of four smaller teeth preceding the paired maxillary fangs. Eight maxillary teeth are preserved behind the paired maxillary fangs, obviously an incomplete number. A minimum of 18 teeth must be assumed to have followed the paired maxillary fangs, bringing the total number of maxillary teeth up to a minimum of 24 (26 in *N. mirabilis:* Rieppel & Wild, 1996).

The postfrontal is a relatively broad element, defining the posteromedial margin of the orbit. It shows the characteristic postorbital constriction,

which also is observed in *N. mirabilis* (as well as other species: Rieppel & Wild, 1996). Posteriorly, the postfrontal continues as a relatively broad element with parallel lateral margins, much as it does in *N. mirabilis,* closely approaching but not entering the anteromedial margin of the upper temporal fossa. The posterior margin of the postfrontal is broken, rendering it impossible to assess whether the bone remains excluded from the upper temporal fossa for its entire length, or whether it entered the medial margin of the latter more posteriorly (a variable character in *N. mirabilis*).

The broad postorbital forms most of the postorbital arch, defining the posterolateral margin of the orbit as well as the anterior margin of the upper temporal fossa. The postorbital does not extend anteriorly along the lateral margin of the orbit, as is the case in *N. haasi.* Posteriorly, it extends as a relatively broad element along the dorsal margin of the maxilla and into the upper temporal arch along the medial edge of the latter. A jugal, intercalated between maxilla and postorbital in other species of *Nothosaurus,* is missing in *N. tchernovi.* The squamosal completes the posterior half of the upper temporal arch, defines the posterolateral and posterior margin of the upper temporal fossa, gains a broad occipital exposure, and extends ventrally lateral to the quadrate. Unfortunately, the right suspensorium is badly broken, and the left one is not preserved at all. A diagnostic character of *N. tchernovi* is the broad contact between the anterior tip of the squamosal and the posterior tip of the maxilla, which meet in a well-defined, interdigitating suture.

Due to the articulated mandible, the ventral surface of the skull is only partially exposed. The exposed surface of the dermal palate is furthermore badly eroded and/or damaged by preparation, which renders the identification of details difficult. The vomers are paired elements. The epipterygoid–pterygoid suture can be identified on the right side of the palate, continuing anteriorly into the epipterygoid–palatine suture. The sutural pattern indicates a weakly developed transverse process of the pterygoid, comparable to that of *N. haasi* or *N. mirabilis.* More posteriorly, however, at the posterior ends of the pterygoids underlying the basioccipital and basisphenoid, the ventral surface of the dermal palate is deeply concave, more so than is typical for other species of *Nothosaurus.* This characteristic was also emphasized by Haas (1980).

The occiput is difficult to analyze in detail because of dorsoventral compression as well as incomplete preservation and/or preparation. Nevertheless, the exoccipitals are distinct, forming pillar-like structures on the dorsolateral aspect of the occipital condyle and defining the lateral margin of the large foramen magnum. The laterally oriented basioccipital tubera (horizontal diameter: 16.2 mm) are almost equal in size to the occipital condyle (horizontal diameter: 18 mm). The eustachian foramen is either fully closed or reduced to a narrow, slit-like aperture.

The lower jaw is very poorly preserved. In particular, the ventral surface of the symphysis is deeply eroded, obscuring symphyseal proportions and exposing the roots of the anterior dentary fangs. The posterior end of the left mandibular ramus has a rather distinct horizontal shelf formed by the surangular for the insertion of superficial jaw adductor muscle fibers. As noted by Haas (1980), the holotype of *N. tchernovi,* with the mandible articulated to the skull, rather nicely displays details of dental occlusion. As preserved, the anteriormost right dentary fang is positioned posterolateral to the alveolus of the anteriormost premaxillary fang, which itself is located adjacent to the midline of the rostrum, pointing anteriorly. This means that in a complete skull, the two anteriormost fangs of both premaxillae are both located between the two anteriormost fangs of the two dentaries. The succeeding dentary fangs continue to be located behind the corresponding premaxillary fang, leaving the posteriormost (fifth) symphyseal fang (not preserved) to be located within the rostral constriction at jaw closure. The presence of five symphyseal fangs is inferred from a lateral bulging of the lateral margin of the mandible behind the (preserved) fourth symphyseal fang; Haas (1980) counted four symphyseal fangs in the holotype of *N. tchernovi.*

Haas (1980, p. 123; Fig. 32A) mentions a second, less well-preserved skull (HUJ-Pal. uncatalogued) of similar size as the holotype of *N. tchernovi,* which shares with that species the deep concavity of the dermal palate at the posterior end of the pterygoids. The specimen is incompletely prepared, but the parietal skull table, the partially preserved right suspensorium, the posterior part of the left upper temporal arch, and the anterior part of the right temporal arch are exposed. As preserved, the total length of the skull fragment is 176.5 mm and its maximal width is 132 mm. Due to extensive erosion of the exposed bone surface, little anatomical detail can be seen. The right posterior tip of the frontal is distinct, somewhat behind the level of the anterior margin of the right

upper temporal fossa. The anterior corner of the upper temporal fossa is constricted by a distinct lateral convexity of the parietal. Most important, perhaps, the anterior part of the right temporal arch shows the maxilla sutured to the postorbital, confirming the absence of a jugal in *N. tchernovi.* The pineal foramen is rather large (longitudinal diameter: 12.2 mm; transverse diameter: 6.2 mm) and shifted to a position immediately in front of the posterior margin of the parietal skull table, as in *N. mirabilis* (Rieppel & Wild, 1996, Figs. 58, 59).

HUJ-Pal. 759 is another, rather poorly prepared, middle section of a nothosaur skull (Fig. 32B), broken transversely at the level of the anterior margin of the external naris and of the posterior margin of the orbits. The total length of the fragment is 82.5 mm, its width at the rostral constriction is 34 mm, and its width across the maxillary fangs (located at a level between the external nares and the orbits) is 50.7 mm. Dividing the longitudinal diameter of the left external naris (25 mm) by its transverse diameter (12.2 mm) yields a quotient of 2.05, which is distinctly higher than the corresponding ratio in the skull of the *N. tchernovi* holotype but which fits into the range of variability of *N. mirabilis* (see Table 1). The overall size of the specimen is somewhat smaller than the holotype of *N. tchernovi,* but the specimen differs from *N. haasi* by the relatively shorter external nares, the presence of an anteromedial process of the nasal lining the medial margin of the external naris, and the position of the posterior tip of the nasal process of the premaxilla at the level of the posterior margin of the external naris. The specimen is too large to fit the mandibular symphysis HUJ-Pal. 1904 or the partial premaxillary rostrum HUJ-Pal. 223 (both specimens are described below as *Nothosaurus* sp.), and hence is here referred to *N. tchernovi*; the specimen represents a relatively small individual of that species.

A badly eroded middle section of a nothosaur skull (HUJ-Pal. 757), exposing little more than part of the dermal palate (Fig. 33), was first described and figured by Peyer (1955) and is here referred to *N. tchernovi.* As preserved, the total length of the skull fragment is 137.5 mm; its maximal width is 98.5 mm. The specimen displays the posterior parts of the internal nares, which are separated by paired vomers. The alveoli of the paired maxillary fangs are located at the level of the posterior margins of the internal nares. The anterior end of the palatine, defining the posterior margin of the internal naris, is rather narrow, intercalated between the maxilla and the widening posterior end of the vomer. Behind the level of the vomer–pterygoid suture, the palatine widens considerably, while the palatal ramus of the pterygoid is rather narrow.

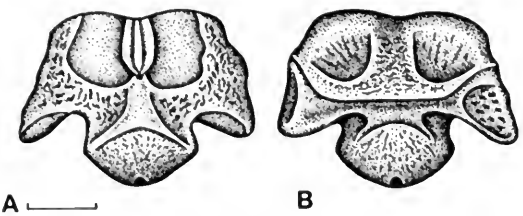

FIG. 34. An isolated basioccipital referred to *Nothosaurus tchernovi* Haas (HUJ-Pal. 2884). **A**, dorsal view. **B**, ventral view. Scale bar = 10 mm.

HUJ-Pal. 2884 represents an isolated basioccipital (Fig. 34) that is only slightly smaller than that of the holotype of *N. tchernovi,* to which this specimen is referred. Its total length is 29.3 mm; its maximum width is 35.5 mm. The dorsal surface of the basioccipital shows paired shallow depressions separated from one another by a median trough with raised edges. The structure of this basioccipital corresponds to that of *Cymatosaurus,* described by Koken (1893, p. 370) and Rieppel and Werneburg (1998), except that the trough separating the collateral depressions is more pronounced in HUJ-Pal. 2884. The collateral depressions must represent the posterior part of the sella turcica, extending backward onto the basioccipital. The ventral surface of HUJ-Pal. 2884 shows the paired facets for the articulation of the pterygoids, which have separated from the basioccipital. The posterior aspect of the basioccipital displays the occipital condyle (horizontal diameter: 15.5 mm) with the laterally oriented basioccipital tubers (horizontal diameter: 10.9 mm).

HUJ-Pal. 1994 is the posterior end of a lower jaw (Fig. 35) that neatly matches the holotype of *N. tchernovi* in size. The fragment is very incomplete; it comprises the posterior part of the surangular, the posterior part of the medial adductor fossa, the articular facet, and proximal parts of the retroarticular process. As preserved, the total length of the fragment is 130 mm, and its width across the mandibular articulation is 32.7 mm. The horizontal shelf on the lateral aspect of the surangular, serving the insertion of superficial jaw adductor muscle fibers, is distinct, as in all nothosaurs. The articular facet is saddle-shaped and, as is characteristic for *Nothosaurus* (see also the description of *Nothosaurus* cf. *N. giganteus* above),

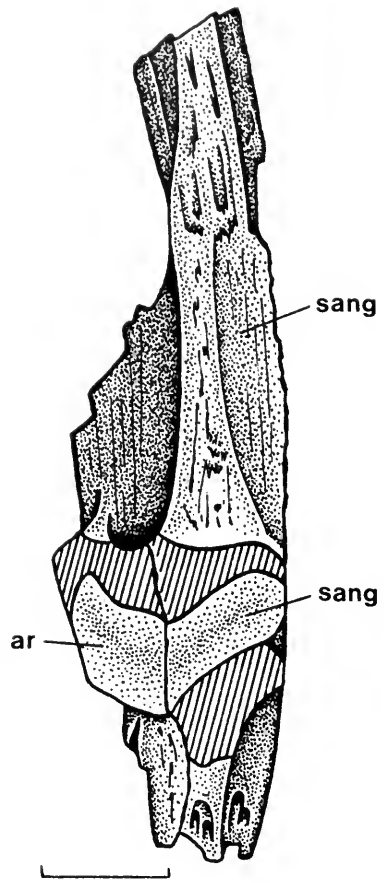

FIG. 35. The posterior part of a right lower jaw ramus referred to *Nothosaurus tchernovi* Haas (HUJ-Pal. 1994), dorsal view. Scale bar = 20 mm. Abbreviations: ar, articular; sang, surangular.

its lateral part is formed by the surangular. Unfortunately, the anterior as well as the posterolateral margins of the articular facet are badly eroded. Breakage of the retroarticular process obscures the position of the foramen for the chorda tympani.

Nothosaurus tchernovi is another nothosaur species based on cranial material. Reference of isolated postcranial material to this species is subject to the same problems as detailed in the description of *N. haasi.* Nevertheless, *N. tchernovi* is a larger species than *N. haasi* but a smaller species than *N. giganteus.* To judge from the cranial material, it is the most common nothosaur species in the Muschelkalk of Makhtesh Ramon. (The scarcity of the small *N. haasi* may be a taphonomic bias, and the scarcity of *Nothosaurus* cf. *N. giganteus* may reflect its role as top carnivore of this fauna.) It is on this basis that postcranial remains of appropriate size and abundance are here referred to *N. tchernovi.*

The *Ceratites* beds of the Muschelkalk of Makhtesh Ramon have yielded a fairly large number of vertebrae of appropriate size (Fig. 36) to be referred to *N. tchernovi,* with dorsal elements being characterized by a tall neural spine, similar to the vertebral structure characteristic of *N. mirabilis.*

HUJ-Pal. 1726 is a cervical centrum (horizontal diameter: 27.8 mm; vertical diameter: 30.5 mm) dissociated from the neural arch (Fig. 37A), but with part of the bicipital right cranial rib still attached to the parapophysis and diapophysis on the centrum. The articular surface of the centrum is slightly amphicoelous or platycoelous, and the cervical rib carries the free anterior process characteristic of all Sauropterygia. HUJ-Pal. 330 is a second cervical centrum of somewhat smaller size (horizontal diameter: 21.9 mm; vertical diameter: 20.6 mm) with the neural arch still attached to it. The neural spine is broken, but its preserved base is rather narrow, indicating a low neural spine. The zygantrum is also broken, but the zygosphene forms a deep trough on the posterior surface of the neural arch, which is subdivided by an internal vertical septum. The articular surfaces of the pre- and postzygapophyses are inclined at an angle of approximately 15° to the horizontal (facing dorsomedially). The neurocentral suture passes through the diapophysis, the neural arch contributing narrowly to its dorsal margin.

HUJ-Pal. 3882 represents a very well-preserved and well-prepared dorsal vertebra of characteristic structure (Figs. 36A–B, 37B–C). The neural arch is still attached to the centrum. The total height of the vertebra is 165 mm, the height of the neural arch is 119 mm, and the height of the neural spine (measured from the roof of the neural canal to its dorsal tip) is 97 mm. The width across the transverse processes is 83.5 mm. The horizontal diameter of the centrum is 40.9 mm, and its vertical diameter is 49.1 mm. The dorsal tip of the neural spine is formed by unfinished or eroded bone, and hence may have been slightly higher or capped by cartilage. The zygosphene (presumably bipartite, as in other specimens) is broken, but the zygantrum is represented by a deep and wide trough located between and above the postzygapophyses. From the posterior edge of the neural spine emerges a vertical septum that extends into the zygantrum from above, but with its ventral part broken. Pre- and postzygapophyses are complete but somewhat

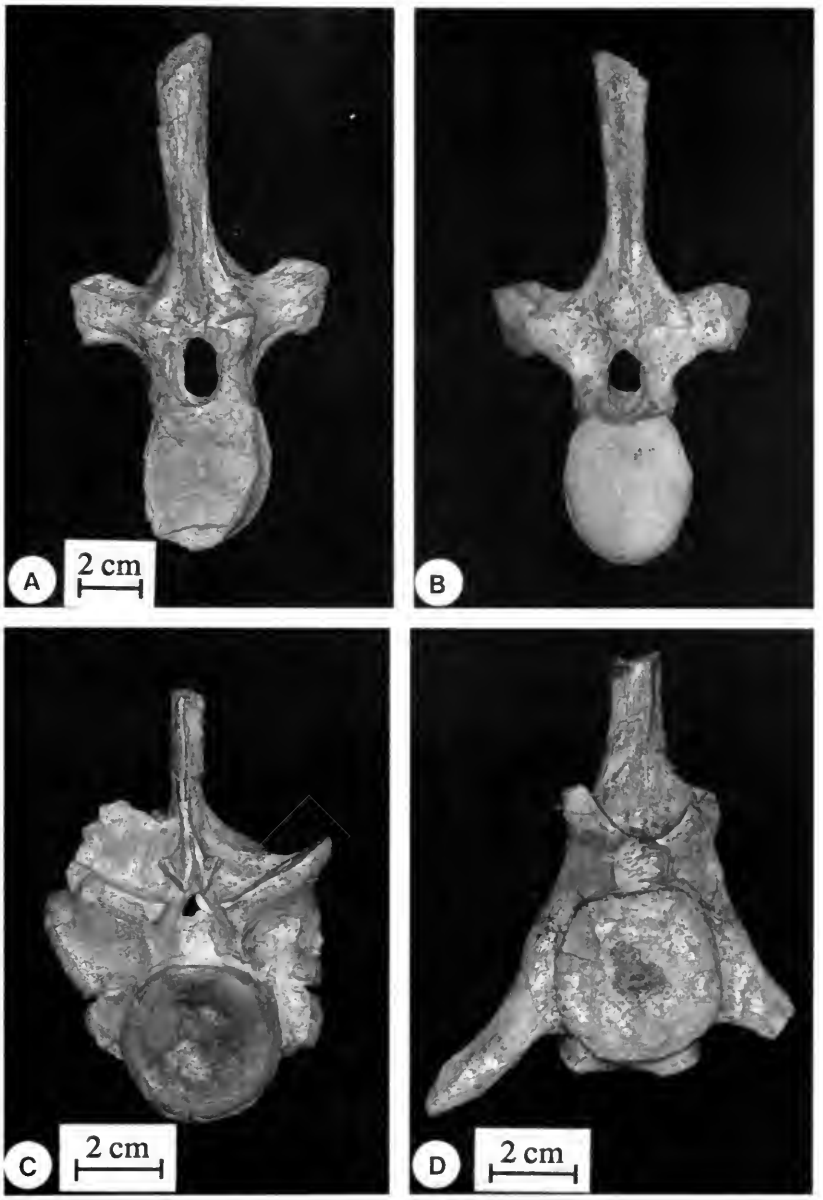

FIG. 36. Isolated vertebrae referred to *Nothosaurus tchernovi* Haas. **A,** HUJ-Pal. 3882, dorsal vertebra, anterior view. **B,** HUJ-Pal. 3882, dorsal vertebra, posterior view. **C,** HUJ-Pal. 812, posterior dorsal or sacral vertebra, anterior view. **D,** HUJ-Pal. 2001, anterior caudal vertebra, anterior view.

distorted, which renders it difficult to determine the exact orientation of their articular surfaces. The articular surface of the left prezygapophysis is inclined by approximately 12° from the horizontal facing dorsomedially, the articular surface of the left postzygapophysis by approximately 30° from the horizontal facing ventrolaterally. A distinctive character of the vertebra is the presence of broad bony flanges that protrude below the postzygapophyses from the dorsolateral margins of the neural canal, shielding the dorsal surface of the spinal cord. The transverse processes are separated from the postzygapophyses by a deep incisure. Their ventral margin lies at about the level of the roof of the neural canal, such that the transverse processes are fully separated from the

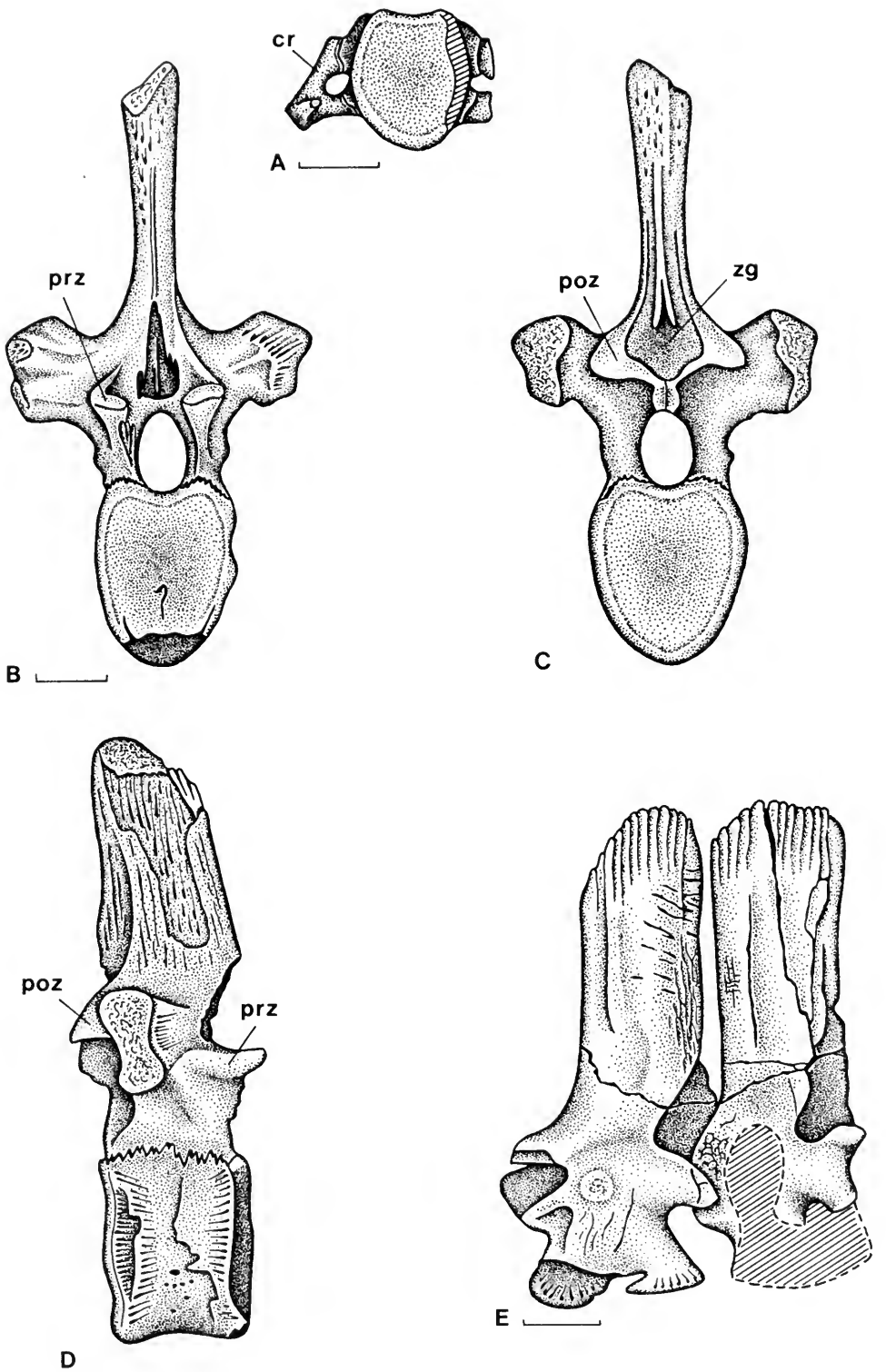

FIG. 37. Isolated vertebrae referred to *Nothosaurus tchernovi* Haas. **A,** HUJ-Pal. 1726, cervical centrum and cervical rib, anterior view. **B,** HUJ-Pal. 3882, dorsal vertebra, anterior view. **C,** HUJ-Pal. 3882, dorsal vertebra, posterior

neural arch pedicels. Trending in a posterolateral direction, the rather slender transverse processes show a slight distal expansion. Their lateral articular head is oblong. The centrum is oval in transverse section; its articular surfaces are slightly amphicoelous or platycoelous. The body of the centrum is slightly constricted. HUJ-Pal. 1509 represents a closely similar vertebra of similar size, but it is badly broken. HUJ-Pal. 3879 represents three neural arches of similar size and morphology in articulation; however, the anteriormost neural arch is incomplete (and hence omitted in Fig. 37E). Preservation in general is rather poor, the zygapophyses being partially crushed and the pedicels of the neural arch abraded to a variable degree. However, the specimen documents the close juxtaposition of the neural arches, the vertical orientation of the neural spines, and the distinct vertical striation on the lateral surface of the neural spines, which is obscured on HUJ-Pal. 3882.

HUJ-Pal. 812 represents a posterior dorsal or, more likely, sacral vertebra (Figs. 36C, 38A). Preservation is rather poor, with the posterior surface being completely eroded, the left transverse process incomplete, and the right prezygapophysis broken. The total height of the vertebra is 109 mm, the reconstructed width across the transverse processes is approximately 81 mm, and the height of the neural spine (measured from the roof of the neural canal to its tip) is 49 mm. The horizontal diameter of the centrum is 38 mm; its vertical diameter is 39.3 mm. Again, the dorsal tip of the neural spine is formed by unfinished bone, indicating that it was capped by cartilage in life. The dorsomedial inclination of the articular surface of the left prezygapophysis appears to be more pronounced than in the cervical or dorsal elements, in that it slopes at an angle of approximately 30°. The zygosphene is distinct and bipartite, its two articular projections separated by a medial cleft that accommodates the vertical septum subdividing the zygantrum. The transverse processes are short, stout, and deep, formed jointly by the neural arch and the centrum. The neurocentral suture passes through their lower part. The body of the centrum is slightly constricted, and its articular surface is platycoelous.

HUJ-Pal. 2001 represents a proximal caudal vertebra (Figs. 36D, 38B). The tip of the neural spine is broken, but relatively its preserved part is almost as high as is the complete neural spine on the sacral vertebra HUJ-Pal. 812. As preserved, the total height of the caudal vertebra is 112.5 mm, and its total width across the transverse processes is 42.1 mm. Assuming that part of the neural spine is missing, it appears that the height of the neural spines increased behind the sacral region. The postzygapophyses are set closely by the midline, leaving between them only a narrow space, which was not subdivided by a vertical septum. And although there is some broken bone between the prezygapophyses, it appears that the zygosphene is absent. Accessory vertebral articulation, therefore, does not extend into the caudal region. The inclination of the articular surfaces of the prezygapophyses (and postzygapophyses) is further increased compared to the sacral and dorsal region, as they enclose an angle of approximately 35° with the horizontal. The neural arch pedicel contributes dorsally to the broad sutural facet on the lateral aspect of the centrum receiving the proximal head of the sturdy caudal rib. The right caudal rib is broken; the left one is completely preserved, and both are in articulation with the vertebra. The body of the centrum (horizontal diameter: 40.1 mm; vertical diameter: 41.3 mm) is slightly constricted. Its articular surface is platycoelous, and from its posteroventral margin project paired facets for the articulation of the chevron bone.

Additional vertebrae with the same structure as described above (HUJ-Pal. 344, 1061, 1226, 2013, 3880, and more) remain unprepared. The prepared material described above, as well as isolated centra (HUJ-Pal. 1967 [cervical], 1884 [dorsal], 2438 [dorsal], and 656 [caudal]), all show a variable pattern of irregularly placed, small nutritive foramina on the lateroventral and ventral aspects of the centrum. Such foramina may be absent altogether (HUJ-Pal. 1967) or asymmetrically placed (e.g., HUJ-Pal. 1884: three distinct foramina on one side, none on the other side of the centrum). They may be few (e.g., HUJ-Pal. 1726: three foramina on the ventral side of the centrum) or numerous (e.g., HUJ-Pal. 2001: ten foramina of variable size on the ventral side of the centrum). Sim-

---

←

view. **D,** HUJ-Pal. 3882, dorsal vertebra, right lateral view. **E,** HUJ-Pal. 3897, two dorsal vertebrae, right lateral view. Scale bar = 20 mm. Abbreviations: cr, cervical rib; poz, postzygapophysis; prz, prezygapophysis; zg, zygantrum.

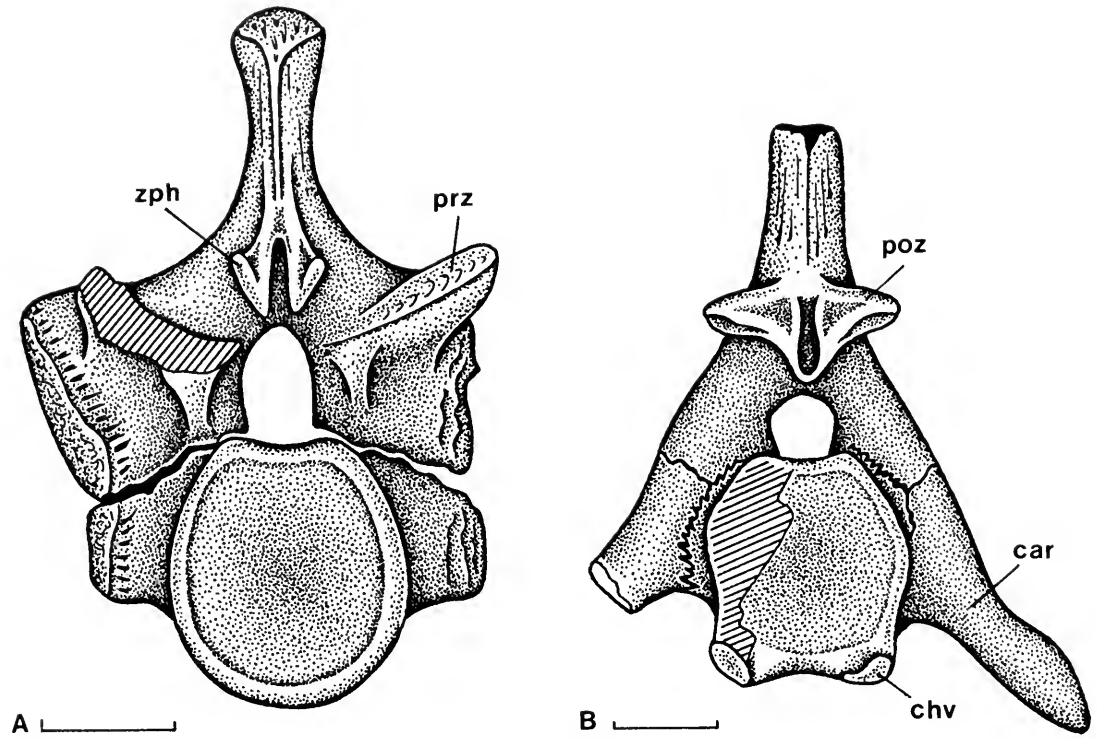

FIG. 38. Isolated vertebrae referred to *Nothosaurus tchernovi* Haas. **A,** HUJ-Pal. 812, anterior dorsal or sacral vertebra, anterior view. **B,** HUJ-Pal. 2001, proximal caudal vertebra, posterior view. Scale bar = 20 mm. Abbreviations: car, caudal rib; chv, articular facet for a chevron; poz, postzygapophysis; prz, prezygapophysis; zph, zygosphene.

ilar irregularly placed nutritive foramina may occasionally be seen on centra of *N. mirabilis* from the Germanic Triassic, but in no case has the presence of relatively large, well-defined, paired, and symmetrically placed nutritive foramina diagnostic of *Pistosaurus* (Sues, 1987) been recorded for *Nothosaurus*.

The Muschelkalk of Makhtesh Ramon has yielded a large number of humeri of the standard nothosaur type (Rieppel, 1994a), with HUJ-Pal. 2055 and HUJ-Pal. 3862 (Fig. 39) among the best preserved and acid-prepared specimens (for measurements, see Table 4). The humeri appear curved, with a distinct angulation in the proximal third of the preaxial margin representing the deltopectoral crest. The crest for the insertion of the m. latissimus dorsi forms a distinct projection into the concavity of the postaxial margin. The distal end is slightly expanded, the ectepicondylar groove is poorly developed, and the entepicondylar foramen is present.

In view of the generalized nothosaurian pattern of these humeri, it is indeed arbitrary and based solely on absolute size whether they are referred to *N. tchernovi* or to *Nothosaurus* cf. *N. giganteus*. The same is true for femora of corresponding size and equally generalized nothosaurian structure (Rieppel, 1994a), which are much rarer than humeri, and of which HUJ-Pal. 2168 (Fig. 39B) is one of the best preserved specimens (total length: 219 mm; proximal width: 56.5 mm; minimum width: 26 mm; distal width: 45 mm). Still, the bone surface is badly eroded, as is the internal trochanter.

DISCUSSION—*Nothosaurus tchernovi* is a nothosaur closely similar to *N. mirabilis* from the Germanic Triassic, if slightly larger than the average adult of the latter species. Diagnostic characters of *N. tchernovi* are the absence of a jugal (a characteristic shared with *N. haasi*), the well-defined contact of the squamosal with the posterior tip of the maxilla, and the deep concavity of the ventral surface of the posterior part of the pterygoids.

GENUS—*Lariosaurus* Curioni, 1847

TYPE SPECIES—*Lariosaurus balsami* Curioni, 1847

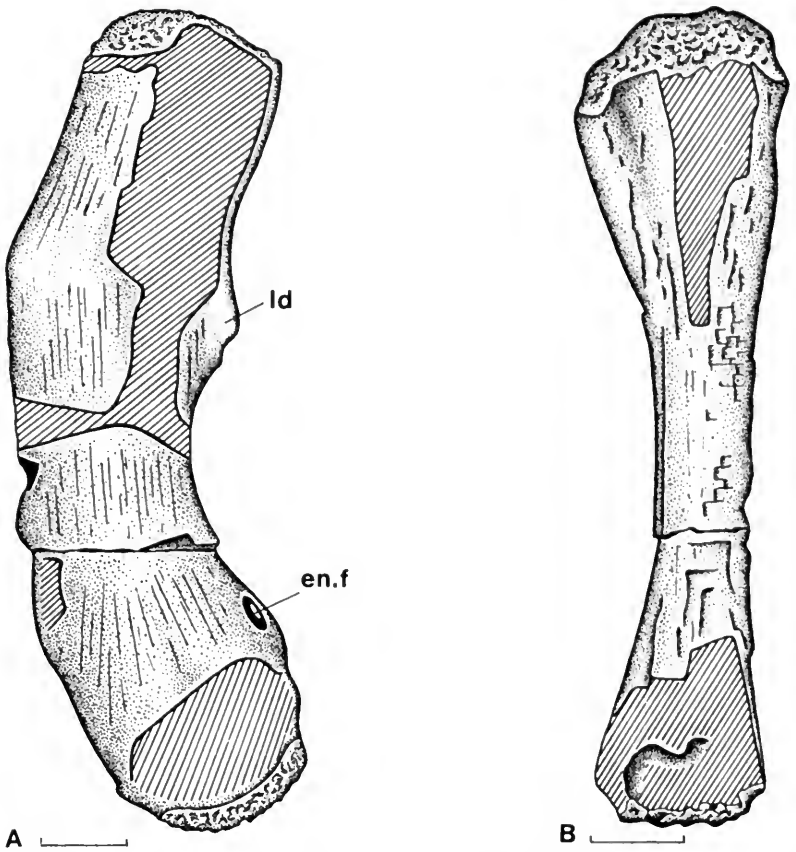

FIG. 39. Stylopodial elements referred to *Nothosaurus tchernovi* Haas. **A,** HUJ-Pal. 3862, left humerus. **B,** HUJ-Pal. 2168, right femur. Scale bar = 25 mm. Abbreviations: en.f, entepicondylar foramen; ld, m. latissimus dorsi insertion.

***Lariosaurus stensioei* (Haas, 1963)**

Synonymy for this material:

1963	*Micronothosaurus stensiöi,* Haas, p. 161, Fig. 1, Pl. 11.
1970	*Micronothosaurus stensioei,* Schultze, p. 231.
1981	*Micronothosaurus stensioei,* Haas, p. 34.
1987	*Micronothosaurus,* Sues, p. 129.
1991	*Micronothosaurus,* Storrs, p. 136.
1997a	*Micronothosaurus stensioei,* Rieppel, p. 2.

HOLOTYPE—Hebrew University of Jerusalem, HUJ-Pal. 756 (Fig. 40), posterior part of skull.

DIAGNOSIS—A small species of *Lariosaurus* with a parietal of elongate triangular shape; pineal foramen located close to midpoint of parietal; upper temporal fossa relatively broad and equal in size to or slightly smaller than the orbit; prominent, knob-like process or crest on supraoccipital.

STRATUM AND LOCUS TYPICUS—Lower Member of the Saharonim Formation of late Anisian (middle and late Illyrian) or early Ladinian (Fassanian) age, Middle Triassic, Makhtesh Ramon, Negev, Israel.

COMMENTS—The holotype of "*M.*" *stensioei* was stated by Haas to have been found by surface collecting on Brotzen's (1957) layer D2 (*Ceratites* beds). The taxon is represented by the posterior part of a skull, which is significantly smaller than that of any species of *Nothosaurus* (or *Cymatosaurus*) at adult size. Schultze (1970) proposed that "*Micronothosaurus*" may in fact represent *Cymatosaurus,* based on the forward position of the pineal foramen, the shape and size of the upper temporal fenestrae, the slender postorbital arch, the relative size and position of the orbits,

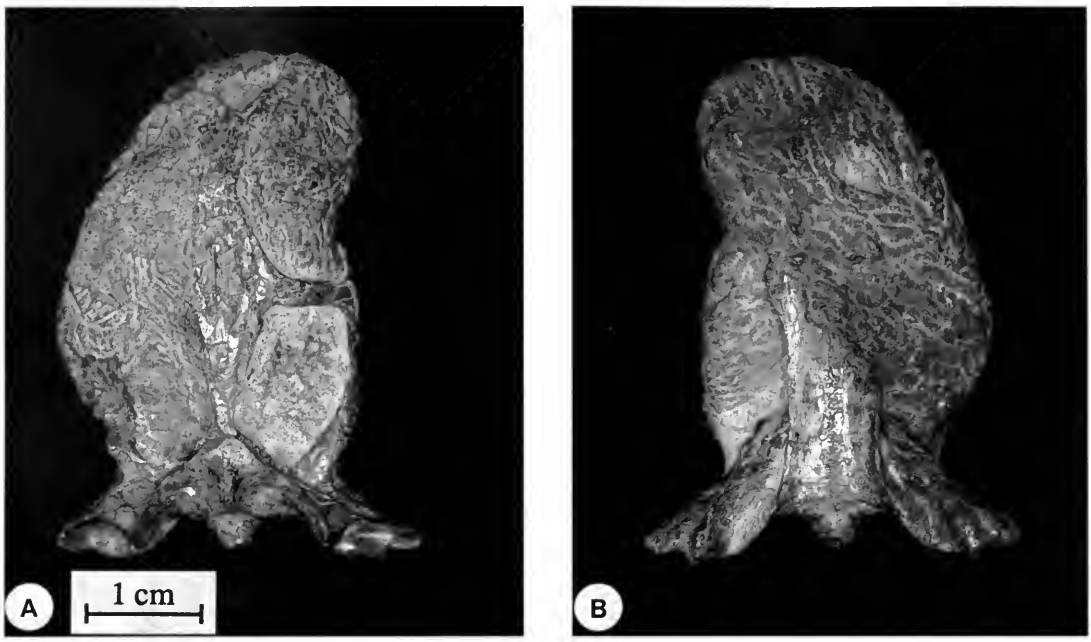

FIG. 40. Holotype of *Lariosaurus stensioei* (Haas) (posterior part of skull, HUJ-Pal. 756). **A,** dorsal view. **B,** ventral view.

and the orientation of the suspensorium. Schultze's (1970) assessment of the taxonomic status of "*Micronothosaurus*" was accepted by Sues (1987) and Storrs (1991). Rieppel (1997a) noted that *Cymatosaurus* is otherwise restricted to the lower Muschelkalk in the Germanic Triassic, and that its occurrence in the *Ceratites* beds of Makhtesh Ramon would considerably extend the geological range of occurrence of *Cymatosaurus,* indicating that this genus persisted much longer in the Negev Muschelkalk than in the Germanic Muschelkalk. Synonymy of "*Micronothosaurus*" with *Cymatosaurus* furthermore implies that the latter genus would coexist with *Nothosaurus* in the Muschelkalk of Makhtesh Ramon, whereas the two genera tend to exclude each other in their spatial and temporal occurrence in the Germanic Muschelkalk (Rieppel & Werneburg, 1998). Indeed, a recent revision of the genus *Cymatosaurus* (Rieppel, 1997a; Rieppel & Werneburg, 1998) indicates that the genus "*Micronothosaurus*" cannot be considered a junior synonym of *Cymatosaurus.* In particular, *Cymatosaurus* retains an "open" occiput, with well-defined paroccipital processes forming the lower margin of a distinct posttemporal fossa and articulating in a notch at the lower margin of the occipital exposure of the squamosal. By contrast, "*Micronothosaurus*" shows the "closed" and platelike occiput characteristic of nothosaurs, with a more or less horizontal supraoccipital firmly sutured to the neighboring dermatocranial elements (parietal, squa-

TABLE 4. Measurements (in millimeters) for humeri referred to *Nothosaurus tchernovi.*

	total length	proximal width	minimal width	distal width
HUJ-Pal. 2055	252	73	54	73.5
HUJ-Pal. 3862	245	61	50	65

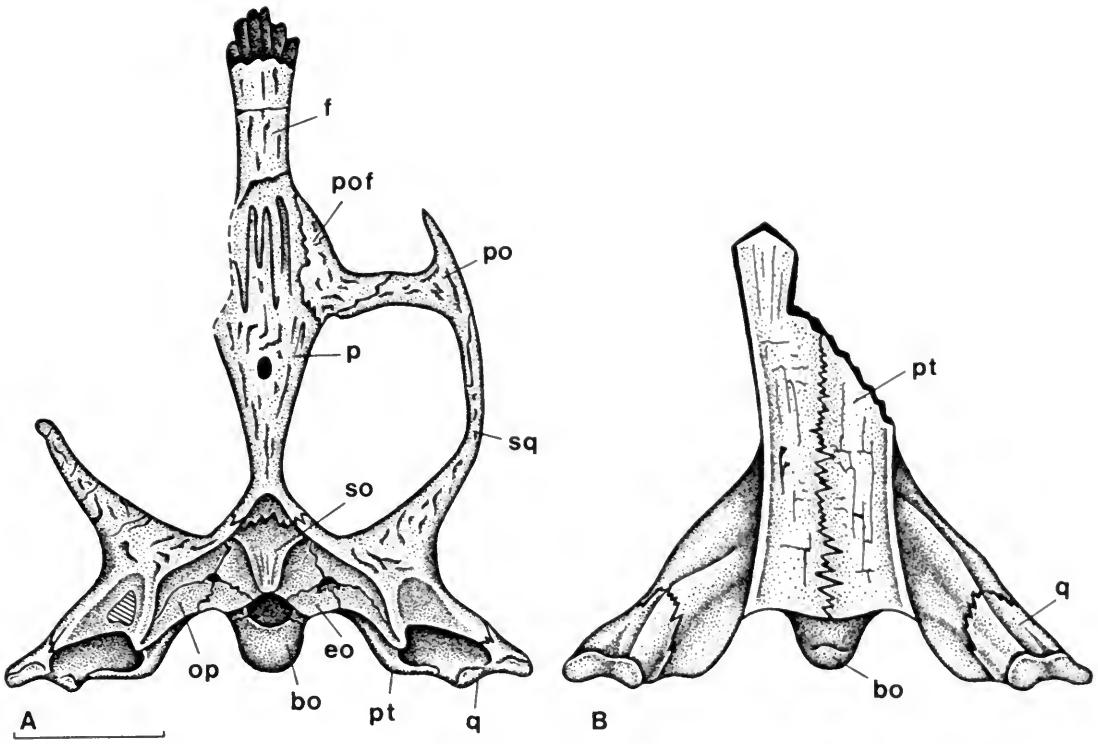

FIG. 41. Holotype of *Lariosaurus stensioei* (Haas) (HUJ-Pal. 756). **A,** dorsal view. **B,** ventral view. Scale bar = 10 mm. Abbreviations: bo, basioccipital; eo, exoccipital; f, frontal; op, opisthotic; p, parietal; po, postorbital; pof, postfrontal; pt, pterygoid; q, quadrate; so, supraoccipital; sq, squamosal.

mosal), no distinct paroccipital processes, and rudimentary posttemporal fossae. Among nothosaurs, the specimen is unusual, however, for its forward placement of the frontoparietal suture, the anterior position of the pineal foramen, and the proportions of the upper temporal fossae. With respect to these features, "*M.*" *stensioei* resembles some lariosaurs (*Lariosaurus buzzii* Tschanz, 1989) more closely than *Nothosaurus*.

MEASUREMENTS—The following measurements for the holotype of "*M.*" *stensioei* are all in millimeters. Values in parentheses are for the right side of the skull.

Maximum length of skull fragment: 44
Width of skull across mandibular condyles of quadrate: 34.7
Width of skull across posterior end of squamosals: 20.4
Longitudinal diameter of orbit: (>15)
Longitudinal diameter of upper temporal fossa: (14.6)
Transverse diameter of upper temporal fossa: (9.1)
Distance from posterior margin of orbit to anterior margin of upper temporal fossa: (2.3)
Middorsal bridge between orbits: approximately 4.0
Middorsal bridge between anterior parts of upper temporal fossae: approximately 8
Middorsal bridge between posterior parts of upper temporal fossae: 1.8

MORPHOLOGICAL DESCRIPTION—The holotype of "*M.*" *stensioei* is represented by a small skull fragment comprising the interobital and postorbital parts of the skull roof, the right postorbital and upper temporal arches, the occiput, the posterior part of the dermal palate, and the lateral wall of the braincase (Fig. 41).

The frontal and parietal are both unpaired, i.e., fully fused, indicating adult status of the specimen. The anterior relations of the frontal to the prefrontal, nasal, maxilla, and premaxilla are not preserved. The frontal broadly enters the dorsal margin of the orbit, separating the prefrontal from

the postfrontal. The concave curvature of the lateral margin of the frontal allows the inference that the longitudinal diameter of the orbit cannot have been less than 15 mm, indicating that it may have been equal to or even somewhat larger than the longitudinal diameter of the upper temporal fossa. The frontoparietal suture is partly obscured by breakage of the bone surface, but on the left side of the skull a long and slender posterolateral process of the frontal can be identified, forming a deeply interdigitating suture with an anteromedial process of the parietal at the level of the postorbital arch.

The parietal is relatively broad at the level of the anterior margin of the upper temporal fossa but gradually and steadily narrows toward the posterior margin of the skull table. The pineal foramen is located approximately at the midpoint of the parietal, but, because of the anterior position of the frontoparietal suture, the pineal foramen lies at a level between the anterior parts of the upper temporal fossae. The distance from the posterior margin of the pineal foramen to the posterior margin of the parietal skull table is 7.3 mm.

The postfrontal broadly defines the posteromedial margin of the orbit, but only very narrowly enters the anteromedial margin of the upper temporal fossa between the parietal and the postorbital. The postfrontal carries a distinct lateral process, lining the posterior margin of the orbit and broadly overlapping a medial process of the postorbital in the formation of the postorbital arch.

The postorbital is a distinctly triradiate element, with a tapering anterior process lining the posterolateral margin of the orbit, a medial process entering the postorbital arch, and a posterior process forming the anterior part of the upper temporal arch. The right maxilla is not preserved, and nothing can be said concerning the presence or absence of a jugal.

The squamosal meets the parietal at the posteromedial corner of the upper temporal fossa and broadly overlaps the postorbital within the anterior third of the upper temporal arch. The squamosal reaches far anteriorly within the upper temporal arch, its anterior tip lying at the level of the anterior margin of the upper temporal fossa lateral to the postorbital. Again, nothing can be said about its relation to the posterior part of the maxilla because the latter is not preserved. The shape and proportions of the upper temporal fossa of "*M.*" *stensioei* are unusual among Eosauropterygia. More or less equal in size to the orbit, the upper temporal fossa is relatively short and broad. Somewhat similar proportions of the upper temporal fossa are known in only two other Eosauropterygia: *L. buzzii* from the Grenzbitumen horizon (Anisian–Ladinian boundary) of the southern Alps (Tschanz, 1989) and *Corosaurus alcovensis* from the Alcova Limestone (uppermost Lower Triassic or basal Middle Triassic) of Wyoming (Storrs, 1991).

Laterally, the squamosal descends along the lateral aspect of the quadrate down to a level shortly above the mandibular condyle of the latter. A quadratojugal is absent. In ventral view, the skull fragment shows nothing more than the posterior parts of the pterygoids, with the well-preserved quadrate ramus articulating with the quadrate on both sides. As is typical for *Nothosaurus* (Rieppel, 1994c), the quadrate ramus of the pterygoid carries well-developed lateral and medial flanges for the attachment of the deep and superficial layers of the pterygoideus muscle, which reach backward to the mandibular condyle of the quadrate. Medially, the two pterygoids meet in an interdigitating suture.

The occipital exposure of the squamosal meets the supraoccipital medially, enters the margin of the posttemporal fossa medioventrally, forms a broad suture with the opisthotic ventrally, and forms the dorsal margin for the posterior opening of the cranioquadrate passage laterally.

The supraoccipital is oriented almost horizontally and is firmly sutured to the neighboring dermatocranial elements (parietal and squamosal). Posterolaterally, the supraoccipital enters the margin of the posttemporal fossa. The supraoccipital bears a very prominent, knob-like process or crest on its dorsal surface.

The rudimentary posttemporal fossa is located between the supraoccipital, exoccipital, opisthotic, and squamosal. The opisthotic extends laterally and separates the squamosal from the pterygoid as it enters the medial margin of the posterior opening of the cranioquadrate passage. The exoccipital sits on the dorsolateral aspect of the occipital condyle, defining the lateral margin of the foramen magnum medially and forming the medial margin of the metotic foramen laterally. Mechanical preparation does not allow identification of an internal subdivision of the metotic foramen that would separate a vagus foramen from the passage of hypoglossal nerve roots. Haas (1963, Pl. 11, Fig. 1) shows the exoccipital as meeting the opisthotic ventral to the metotic foramen. We are unable to either corroborate or refute this observation, as the exoccipital–opisthotic suture (if

present) remains indistinct ventral to the metotic foramen. Lateral to the occipital condyle (horizontal diameter: 3.7 mm), distinct basioccipital tubers (horizontal diameter: 2.5 mm) extend laterally. As indicated by Haas (1963), the eustachian foramen is open, seemingly somewhat wider on the right side than on the left side of the skull.

The horizontal diameter of the foramen magnum is 5.2 mm, and its vertical diameter is 4.3 mm. The posterior opening of the cranioquadrate passage is distinct, bordered dorsally and laterally by the occipital exposure of the squamosal, medioventrally by the quadrate ramus of the pterygoid, and ventrolaterally by the quadrate.

As noted by Haas (1963), the lateral braincase wall is fully ossified, as is indicated by the presence of the prootic and epipterygoid. The epipterygoid has a typically nothosaurian structure, with a broad base attached to the pterygoid, a broad dorsal contact with the parietal, a concave posterior margin, and a concave anterior margin with an anteroventral incisure marking the anterior opening of the cavum epiptericum (see discussion of *N. haasi* above and Haas, 1963, Pl. 11, Fig. 4).

Discussion—Haas (1963, Fig. 1) reconstructed the skull of "*M.*" *stensioei* with a relatively short premaxillary rostrum, using the cranial proportions of *N. juvenilis* as a basis of comparison. Should the isolated lower jaw (HUJ-Pal. uncatalogued), discussed in detail below under the heading Sauropterygia Incertae Sedis (p. 55), indeed represent "*M.*" *stensioei,* its proportions would corroborate the presence of a short premaxillary rostrum in the latter species. The most striking features of "*M.*" *stensioei* are the anterior position of the frontoparietal suture, the anterior position of the pineal foramen, and the relative size of the upper temporal fossa, which is similar in size to, or even somewhat smaller than, the orbit. Dividing the longitudinal diameter of the upper temporal fossa by the longitudinal diameter of the orbit yields a ratio ranging from 2.1 (*N. marchicus*) to 3.9 (*N. mirabilis*) within the genus *Nothosaurus,* and from 1.0 (*L. buzzii*) to 1.8 within the genus *Lariosaurus.* It is also in the genus *Lariosaurus* that the pineal foramen may be located close to the midpoint of the parietal (Tschanz, 1989; Renesto, 1993) and the frontoparietal suture may bridge the level of the postorbital arch. However, "*M.*" *stensioei* differs from all species of *Lariosaurus* in the shape of the parietal, which is broad anteriorly but gradually narrows posteriorly, resulting in an elongate triangular shape. Dividing the longitudinal diameter of the upper temporal fossa by its transverse diameter yields a ratio that ranges from 1.71 (*L. buzzii*) to 3.21 within the genus *Lariosaurus,* with one exception: the (poorly preserved) "Maxberg specimen" (Sanz, 1983a, Pl. 5, Fig. A), which has a ratio of 1.33. The corresponding ratio is 1.6 in "*M.*" *stensioei,* indicating relatively broad upper temporal fenestrae in the latter taxon.

In spite of its incomplete preservation, "*M.*" *stensioei* was entered into the data matrix used to test the interrelationships of the *Lariosaurus* species (Rieppel, 1998), including a total of 28 terminal taxa and 122 characters. The character definitions are given in Appendix 1 (p. 83 *ff.*) the data matrix in Table 5. "*Micronothosaurus*" *stensioei* could be coded for 29 characters, or 23.7% of the total number of characters. All multistate characters were treated as unordered, except character 27 (for a discussion of this character, see Rieppel, 1994a). A heuristic search, rooted on an all-0 ancestor (search settings employed random stepwise addition [20 replications] and branch swapping on minimal trees only) yielded ten equally most parsimonious trees (MPTs) with a tree length (TL) of 483 steps, a consistency index (CI) of 0.625, and a retention index (RI) of 0.761. Lack of resolution was restricted to lariosaur interrelationships and archosauromorph taxa. All sauropterygian interrelationships as specified by Rieppel (1997a) were shown to be stable. The result of the analysis shows "*M.*" *stensioei* to be nested within the monophyletic genus *Lariosaurus.* Interestingly, addition of the poorly known "*M.*" *stensioei* did not increase the number of MPTs obtained for that data set.

The strict consensus tree for the ten MPTs shows "*M.*" *stensioei* to be the sister taxon of *L. buzzii,* the two taxa falling into an unresolved trichotomy with *L. calcagnii* and *L. valceresii.* These four taxa form a monophyletic clade, which in turn falls into an unresolved trichotomy with *L. balsami* and *L. curionii* (Fig. 42A). Six out of the ten MPTs show fully resolved lariosaur interrelationships, the 50% majority rule consensus tree therefore reading ((*L. balsami, curionii*) (*L. calcagnii* (*valceresii* (*buzzi, stensioei*)))) (Fig. 42B).

Synapomorphies that "*M.*" *stensioei* shares with *L. buzzi* are the relatively small upper temporal fossa (13[1]) and the postfrontal with a distinct lateral process entering the postorbital arch (26[1]). Both of these characters are reversals within the genus *Lariosaurus,* although the implemented DELTRAN character optimization tech-

TABLE 5. Data matrix for the analysis of the phylogenetic relationships of *Lariosaurus* ("*Micronothosaurus*") *stensioei*.

Micronothosaurus 1		1	2	3	4	5	6	7	8	9	10
1	Ancestor	0	0	0	0	0	0	0	0	0	0
2	Captorhinidae	0	0	0	0	0	0	0	0	0	0
3	Testudines	0	0	0	0	0	0	0	0	1	0&1
4	Araeoscelidia	0	0	0	0	0	0	0	0	0	0
5	Younginiformes	0	0	0	0	0	0	0	0	1	0
6	Kuehneosauridae	0	0	0	0	0	0	0	0	1	0
7	Rhynchocephalia	0	0	0	0	0	0	0	0	1&2	0
8	Squamata	0	0	0	0	0	0	0	0	1&2	0&1
9	Rhynchosauria	1	1	0	0	0	0	0	0	1	0
10	Prolacertiformes	1	1	0	0	1	0	0	0	1	0
11	Trilophosaurus	1	?	0	0	0	0	0	0	?	1
12	Choristodera	1	1	0	0	1	0	0	0	1	0
13	Archosauriformes	1	1	0	0	1	0	0	0	1	0
14	Claudiosaurus	0	0	0	0	0	0	0	0	1	0
15	Dactylosaurus	1	0	0	0	0	0	0	0	2	0
16	Serpiano-Neustico	1	0	0	0	0	0	0	0&1	2	0
17	Simosaurus	1	0	0	0	0	1	0	1	2	0
18	Nothosaurus	1	0	1	1	0	0	0	0&1	2	0
19	Ceresiosaurus	1	0	1	1	0	0	0	0	2	0
20	L. balsami	1	0	1	1	0	0	0	1	2	0
21	L. curionii	1	0	0	1	0	0	0	1	2	0
22	L. valceresii	1	0	1	1	0	0	0	0	2	0
23	Silvestrosaurus	1	0	1	1	0	0	0	0	2	0
24	Corosaurus	1	0	0	0	0	0	0	0	2	0
25	Cymatosaurus	1	0	1	0	0	2	0&1	1	2	0&1
26	Germanosaurus	1	0	1	1	0	1	0	1	2	0
27	Pistosaurus	1	0	0	0	0	2	1	1	2	0
28	Placodus	1	0	1	0	1	0	0	0	2	1
29	Micronothosaurus	?	?	?	1	?	?	?	?	0	?

nique favors convergence over reversals. The other characters that diagnose the hierarchy of the species of *Lariosaurus* cannot be coded for "*M.*" *stensioei,* which is nested within the latter genus on grounds of global parsimony. It is for this reason that "*Micronothosaurus*" must be considered a junior synonym of *Lariosaurus,* in order not to render the latter genus paraphyletic.

Nothosaurus sp.

MATERIAL—HUJ-Pal. 223, Muschelkalk, Makhtesh Ramon. The original label reads: "Found on road near *Beneckeia* at entrance of amphitheater, Layers I–II." Fragmentary premaxillary rostrum of *Nothosaurus* sp.

MORPHOLOGICAL DESCRIPTION—The specimen represents the anterior tip of the premaxillary rostrum of a small nothosaur (Figs. 43A, 44). The total length of the specimen (as preserved) is 38.5 mm, and its maximum width is 30.2 mm. The specimen shows a total of seven alveoli for procumbent premaxillary fangs, with replacement pits located posteromedial to the functional tooth positions. The arrangement of the alveoli is highly unusual in that three tooth positions can be identified at the front end of the (fused) premaxillae, with a median alveolus seemingly located on the midline of the snout. This asymmetry may result from some dislocation of the alveoli, of which three would belong to the right side, four to the left side of the rostrum.

TABLE 5. *Continued.*

Micronothossurus 2		11	12	13	14	15	16	17	18	19	20
1	Ancestor	0	0	0	0	0	0	0	0	0	0
2	Captorhinidae	0	0	0	0	0	?	0	0&3	0	0
3	Testudines	0	0&2	0	0	0	?	0	4	0	1
4	Araeoscelidia	0	1	1	0	1	0	0	0	0	0
5	Younginiformes	0	1	1	0	1	0	0	0	0	0
6	Kuehneosauridae	0	0	1	0	1	0	0	3	0	1
7	Rhynchocephalia	0	0	1	0&1	0&1	0	0&1	0&3	0&2	1
8	Squamata	0	0&1&2	1	0&1	0	0	0&1	0&3&4	0&2	1
9	Rhynchosauria	0	0	1	0	0	0	1	4	3	1
10	Prolacertiformes	0	1	1	0	0&1	0	0&1	3&4	0	1
11	Trilophosaurus	0	1	1	0	0	1	0	4	3	1
12	Choristodera	0	2	1	0	0	0	0	4	1	1
13	Archosauriformes	0	0&1	1	0&1	0&1	0&1&2	0&1	0&4	0&2	1
14	Claudiosaurus	0	1	1	0	1	0	0	0	0	1
15	Dactylosaurus	0	1	3	0	1	0	0	0	0	1
16	Serpiano-Neustico	0	1	3	0	1	0	0	0	0	1
17	Simosaurus	0	2	2	1	0	0	2	1	1	1
18	Nothosaurus	1	2	2	1	1	0	2	1&2	2&3	1
19	Ceresiosaurus	1	2	2	1	1	0	2	2	2	1
20	L. balsami	1	2	2	1	1	0	2	1&2	1&2	1
21	L. curionii	1	2	2	1	1	0	2	1	2	1
22	L. valceresii	1	2	2	1	1	0	2	1&2	1&2	1
23	Silvestrosaurus	1	2	1	1	1	0	2	1	0	1
24	Corosaurus	0	0	1	0	1	1	0	0	1	1
25	Cymatosaurus	0	2	2	0	1	1&2	1&2	0	2&3	1
26	Germanosaurus	1	2	2	0	1	1	1	1	1	1
27	Pistosaurus	0	1	2	0	1	2	1	3	3	1
28	Placodus	0	0	2	0&1	1	0	0&2	3	0	1
29	Micronothosaurus	?	?	1	1	1	0	2	0	2	1

HUJ-Pal. 223 was originally identified by Haas (1975, p. 452, Pl. I, Figs. 3A–C) as either a mandibular symphysis or a premaxillary rostrum of an unknown placodont. However, the nothosaurian identity of the specimen is beyond doubt. The rostrum is too large and robust to represent a second specimen of *N. haasi*. On the other hand, the specimen is smaller than the tip of the snout of the holotype of *N. tchernovi*.

Nothosaurus sp.

MATERIAL—HUJ-Pal. 1904, Muschelkalk, Makhtesh Ramon. Mandibular symphysis of a small *Nothosaurus* sp.

MORPHOLOGICAL DESCRIPTION—A partially preserved mandibular symphysis of a small species of *Nothosaurus* with an unusually low length-to-width ratio (Figs. 43B, 45). The total length of the fragment (as preserved) is 25.5 mm, the total length of the symphysis is 11.7 mm, the maximum width of the symphysis is 21.5 mm, and the length-to-width ratio is 0.54. This is lower than is typical for *N. marchicus* from the Germanic Muschelkalk, which, with a length-to-width ratio of at least 0.7, has the shortest mandibular symphysis among all the nothosaur species from the Germanic Muschelkalk (Rieppel & Wild, 1994). A similarly short mandibular symphysis (with a length-to-width ratio of 0.59) is characteristic of a much smaller lower jaw fragment from the Muschelkalk, described in more detail below.

TABLE 5. *Continued.*

Micronothosaurus 3		21	22	23	24	25	26	27	28	29	30
1	Ancestor	0	0	0	0	0	0	0	0	0	0
2	Captorhinidae	1	0	0	0	0	0	0	0	0	0
3	Testudines	1	0&1	0	0	0	?	0	1	0	0
4	Araeoscelidia	0	0	0	0	0	1	0&1	0	0	0
5	Younginiformes	0&1	0	0	0	0	1	1	0	0	0
6	Kuehneosauridae	1	1	0	0	0	1	2	1	1	1
7	Rhynchocephalia	1	0&1	0&1	1	0	1	1&2	0	0	1
8	Squamata	1	0&1	0&1	0	0	1	2	1	1	?
9	Rhynchosauria	1	1	0	1	0	1	1	1	0	0
10	Prolacertiformes	1	0&1	0	0&1	0	1	2	1	0&1	1
11	Trilophosaurus	1	?	0	?	0	1	0	?	0	?
12	Choristodera	1	1	0	0	0	1	1	1	0&1	0
13	Archosauriformes	1	0&1	0	1	0	1	1	1	0	0
14	Claudiosaurus	1	1	0	0	0	1	2	0	0	1
15	Dactylosaurus	1	1	?	0	0	2	2	0	0	1
16	Serpiano-Neustico	1	1	0	0	0	2	2	0	0	1
17	Simosaurus	1	1	0	0	1	1	2	0	0	1
18	Nothosaurus	1	1	1&2	0	1	1&2	2	0	0&1	1
19	Ceresiosaurus	1	1	1&2	0	1	2	2	0	?	?
20	L. balsami	1	1	?	0	1	2	2	0	?	?
21	L. curionii	1	1	?	?	?	2	2	0	?	?
22	L. valceresii	1	1	?	0	1	2	2	0	?	?
23	Silvestrosaurus	1	1	?	0	1	1	2	0	?	?
24	Corosaurus	1	1	?	0	0	1	2	0	?	?
25	Cymatosaurus	1	1	1	0	0	1	2	0	1	?
26	Germanosaurus	1	1	2	0	1	1	2	0	?	?
27	Pistosaurus	1	1	?	0	1	1	2	0	1	?
28	Placodus	1	1	0	0	1	1	2	0	0	0
29	Micronothosaurus	1	1	?	?	?	1	2	0	1	?

HUJ-Pal. 1904 shows alveoli for three procumbent symphyseal fangs within the symphyseal area. Two more enlarged alveoli for anterior dentary fangs are located entirely behind the level of the posterior margin of the symphysis. In lower jaw fragments with a relatively short symphysis from the lower Muschelkalk of the Germanic Triassic, it is usually only the fifth dentary fang that lies entirely behind the level of the posterior margin of the symphysis. The angle defined by the symphysis of HUJ-Pal. 1904 is too large to fit the narrow and almost parallel-sided rostrum of *N. haasi*. It is therefore concluded that the specimen HUJ-Pal. 1904 is not diagnostic at the species level.

***Nothosaurus* sp.**

MATERIAL—A series of distinctive neural arches from the Muschelkalk of Makhtesh Ramon (Table 6).

MORPHOLOGICAL DESCRIPTION—The neural arches are characterized by a relatively low and slender neural spine without striations on the dorsal part of the lateral surface (Fig. 46). The zygosphene, located above and between the prezygapophyses, is bipartite, the two articular tips being separated by a deep and rather wide cleft. The zygantrum, located between and above the postzygapophyses, is subdivided by a vertical septum. The pre- and postzygapophyses are slightly in-

TABLE 5. *Continued.*

Micronothosaurus 4		31	32	33	34	35	36	37	38	39	40
1	Ancestor	0	0	0	0	0	0	0	0	0	0
2	Captorhinidae	0	0	0	?	0	0	0	0	0	0
3	Testudines	0	0	0&2	0	0	0	1	1	0	0
4	Araeoscelidia	0	0	0	1	0	0	0	0	?	0
5	Younginiformes	0	0	0	1	0	0	1	1	?	0
6	Kuehneosauridae	0	0	0	1	0	1	1	1	?	1
7	Rhynchocephalia	0&1	0	0	1	0	0&1	1	1	1	0&1
8	Squamata	0	0	0&1&2	0&1	0&1	0&1	1	1	1	1
9	Rhynchosauria	1	0	0	0	0	0	1	1	1	0
10	Prolacertiformes	1	0	0	1	0	0	1	1	?	0
11	Trilophosaurus	1	0	2	?	0	?	1	1	0	0
12	Choristodera	1	0	1	1	0	1	1	1	?	0
13	Archosauriformes	0&1	0	0&1&2	1	0	0&1	1	1	?	0
14	Claudiosaurus	0	0	0	?	0	0	0	0	?	0
15	Dactylosaurus	2	0	0	?	1	0	1	1	1	0
16	Serpiano-Neustico	2	0	0	?	1	0	1	1	1	0
17	Simosaurus	2	0	1	1	0	0	0	1	0	0
18	Nothosaurus	2	0	0&1	1	1	1	0	1	0	0
19	Ceresiosaurus	2	0	0	1	1	1	0	1	0	0
20	L. balsami	2	0	0	1	1	1	0	1	?	0
21	L. curionii	2	0	0	1	1	1	0	1	?	0
22	L. valceresii	2	0	0	1	1	1	0	1	?	0
23	Silvestrosaurus	2	0	0	1	1	1	0	1	?	0
24	Corosaurus	1	1	1	1	0	1	0	1	1	0
25	Cymatosaurus	1	1	1	?	0	0&1	0	1	?	0
26	Germanosaurus	?	?	?	?	?	0	0	1	?	0
27	Pistosaurus	1	?	1	?	0	1	0	1	1	0
28	Placodus	1	0	0	1	0	0	1	1	1	0
29	Micronothosaurus	2	0	0	?	1	?	1	1	0	0

clined, the articular surfaces facing dorsomedially or ventrolaterally, respectively. The pre- and postzygapophyses are located rather low on the neural arch, at the level of or even slightly below the roof of the neural canal. The transverse processes are very prominent. They are relatively deep, narrowly approaching the base of the pedicels, and show a slight expansion toward their distal ends.

The bipartite zygosphene and internally subdivided zygantrum allow the identification of these neural arches as those of *Nothosaurus*. Although the neural spine is relatively low compared to the middorsal vertebrae of *N. haasi* or *N. tchernovi*, it is still about twice as high and more slender (in anterior view) than the low neural spines of *N. marchicus* from the Germanic Muschelkalk (Rieppel & Wild, 1996). In fact, comparable neural arches are currently not known from the Germanic Muschelkalk (Wild, in litt., 6 November 1996), and may thus represent a *Nothosaurus* endemic for the Makhtesh Ramon Muschelkalk. The very prominent transverse processes and the relatively low neural spine might indicate that these neural arches represent posterior dorsal elements, perhaps referable to *N. haasi*.

***Nothosaurus* sp.**

MATERIAL—A series of scapulae (HUJ-Pal. 1111, 1993, 2041, 2063, 2451, 3375, 3724, 3818) from the Muschelkalk of Makhtesh Ramon, of different sizes, ranging from a very small size per-

TABLE 5. *Continued.*

Micronothosaurus 5		41	42	43	44	45	46	47	48	49	50
1	Ancestor	0	0	0	0	0	0	0	0	0	0
2	Captorhinidae	0	0	0	0	0	1	0	0	0	0
3	Testudines	0&1	0	1	0	0&1	1	0	0&1	0	0
4	Araeoscelidia	0	0	1	0	0	0	0	0	0	0
5	Younginiformes	0	0	1	0	0	0	0	1	1	0
6	Kuehneosauridae	0	0	1	0	?	?	0	1	0	0
7	Rhynchocephalia	0	0	1	0	0	0	0	1	1	0
8	Squamata	0	0	1	0	0&1	0	0	1	1	0
9	Rhynchosauria	0	0	1	0	1	0	0	1	1	0
10	Prolacertiformes	0	0	1	0	0	0	0	1	0&1	0
11	Trilophosaurus	0	0	1	0	0	0	0	1	1	0
12	Choristodera	?	0	1	0	1	0	0	1	0	0
13	Archosauriformes	0&1	0	1	0	0&1	0&1	0	1	0&1	0
14	Claudiosaurus	0	0	1	1	0	0	0	0	0	?
15	Dactylosaurus	1	?	0	1	0	1	?	1	0	0
16	Serpiano-Neustico	1	?	0	1	0	1	?	1	0	0
17	Simosaurus	1	2	0	1	0	0	1	1	0	1
18	Nothosaurus	1	2	0	0&1	1	0	1	1	0	1
19	Ceresiosaurus	1	2	0	1	1	0	?	1	0	1
20	L. balsami	1	2	0	1	1	0	?	1	0	1
21	L. curionii	1	2	0	1	1	0	?	1	0	1
22	L. valceresii	1	2	0	1	1	0	?	1	0	1
23	Silvestrosaurus	1	2	0	1	1	0	?	1	0	1
24	Corosaurus	1	?	0	0	?	0	?	1	1	1
25	Cymatosaurus	1	?	0	0	1	0	1	?	0	?
26	Germanosaurus	1	?	?	?	?	?	?	?	?	?
27	Pistosaurus	1	?	0	0	?	0	?	?	?	?
28	Placodus	1	1	0	0	1	0	0	1	1	0
29	Micronothosaurus	1	2	0	1	?	?	?	?	?	?

haps characteristic of pachypleurosaurs (HUJ-Pal. 1993, 2451; see description above) up to the size characteristic of *Nothosaurus* cf. *N. giganteus* (HUJ-Pal. 3375, 3724; see description above).

MORPHOLOGICAL DESCRIPTION—All of these scapulae correspond to the basic sauropterygian pattern (Fig. 47). A ventral glenoidal portion can be distinguished from a more or less slender posterodorsal wing or process. The clavicular facet is located on the anterior and anteromedial aspect of the ventral body of the scapula. Within the series of scapulae of increasing size, an interesting change can be observed in the contours of the posterodorsal wing. Slender in the small specimens, the posterodorsal wing is more pronounced in larger specimens and in fact expanded into an anteriorly protruding flange with a distinctly convex anterior margin. The anteriorly expanded posterodorsal wing is best exemplified by HUJ-Pal. 3724 (Fig. 16; total height: 98.5 mm; length of ventral glenoid portion: 89.7 mm; total length including posterodorsal process: 126.5 mm), which in both size and shape is virtually identical to a scapula from the lower Keuper (Lettenkeuper) of southwestern Germany, originally labeled *N. chelydrops* (FMNH UC 404). *Nothosaurus chelydrops* Fraas, 1896, is a taxon based on a nothosaur skull from the lower Keuper with peculiar proportions (Schultze, 1970). In view of the possibility that the aberrant proportions could be the result of extreme dorsoventral compression of this rather large skull, Rieppel & Wild (1996) suggested

TABLE 5. *Continued.*

Micronothosaurus 6		51	52	53	54	55	56	57	58	59	60
1	Ancestor	0	0	0	0	0	0	0	0	0	0
2	Captorhinidae	0	0	0	0	?	0	0	0	0	0
3	Testudines	0	1	?	?	?	?	?	0	0&1	0&2
4	Araeoscelidia	0	1	0	0	0	0	0	0	0	0
5	Younginiformes	0	?	0	0	0	1	0	0	0	0
6	Kuehneosauridae	0	?	0	0	0	1	0	1	1	0
7	Rhynchocephalia	0	1	1	0	0	1	0	1	0&1	0
8	Squamata	0	1	1	0	0	1	0	1	1	0&2
9	Rhynchosauria	0	0	0	?	0	1	0	1	1	0
10	Prolacertiformes	0	1	0	0	0	1	0	0&1	1	0&2
11	Trilophosaurus	0	?	0	?	0	1	0	1	1	1&2
12	Choristodera	0	1	0	0	0	1	0	0	1	1
13	Archosauriformes	0	1	0	0	0	1	0	0&1	1	0&1&2
14	Claudiosaurus	0	1	0	0	0	1	0	0	?	0
15	Dactylosaurus	0	?	0	0	0	1	0	1	1	0
16	Serpiano-Neustico	0	?	0	0	0	1	0	1	1	0
17	Simosaurus	0	1	0	1	0	1	2	1	1	1
18	Nothosaurus	2	1	0	1	1	0	2	1	1	1
19	Ceresiosaurus	2	1	0	1	1	0	2	1	1	1
20	L. balsami	2	1	0	1	1	0	2	1	1	1
21	L. curionii	2	1	0	1	1	0	2	1	1	1
22	L. valceresii	2	1	0	1	1	0	2	1	1	1
23	Silvestrosaurus	2	1	0	1	1	0	2	1	1	1
24	Corosaurus	1	?	0	1	1	0	1	1	1	0
25	Cymatosaurus	2	1	0	1	1	0	1	1	1	1
26	Germanosaurus	?	?	0	1	1	1	1	?	?	?
27	Pistosaurus	?	?	0	1	1	0	1	1	1	1
28	Placodus	2	0	0	1	0	1	0	1	0	0
29	Micronothosaurus	?	?	?	?	?	?	?	1	?	?

treating *N. chelydrops* as a junior synonym of *N. giganteus* Münster until better preserved material could corroborate the status of *N. chelydrops* as a valid separate species. Whatever the correct taxonomic conclusion, the scapula HUJ-Pal. 3724 further corroborates the presence of a nothosaur species very close to *N. giganteus,* and hence the affinities of the sauropterygian fauna from Makhtesh Ramon with that of the upper Muschelkalk and lower Keuper of the Germanic Triassic.

***Nothosaurus* sp.**

MATERIAL—A series of five coracoids from the Muschelkalk of Makhtesh Ramon (Table 7).

MORPHOLOGICAL DESCRIPTION—The coracoids all have the structure characteristic of *Nothosaurus* (Fig. 48). The smaller specimens (HUJ-Pal. 747, 1131) are incompletely ossified and do not (yet) show a distinct notch on their proximal margin, which indicates the position of the coracoid foramen (located between coracoid and scapula) in larger specimens.

The specimens HUJ-Pal. 747 and 1998 are distinguished by a deep concavity in their posterior margin (Figs. 48A,D), which is less distinct in the other specimens.

***Nothosaurus* sp.**

MATERIAL—A series of four ilia from the Muschelkalk of Makhtesh Ramon (Table 8).

TABLE 5. *Continued.*

Micronothosaurus 7		61	62	63	64	65	66	67	68	69	70
1	Ancestor	0	0	0	0	0	0	0	0	0	0
2	Captorhinidae	0	0	0	0	?	0	0	0	0	0
3	Testudines	1	0&1	1	0	0	0	0	0	0	0
4	Araeoscelidia	0	0	1	0	?	0	0	0	0	0
5	Younginiformes	0	0	1	0	0	0	0	0	0	0
6	Kuehneosauridae	1	1	1	0	?	1	0	0	0	1
7	Rhynchocephalia	0&1	0	1	1	0	0	0	0	0	0
8	Squamata	1	0	1	0&1	0	0	0	0	0	0&1
9	Rhynchosauria	0	0	1	0	?	0	0	0	0	0&1
10	Prolacertiformes	0&1	0&1	1	0	?	0	0	0	0	0
11	Trilophosaurus	0	0	1	0	?	0	?	0	0	0
12	Choristodera	1	0	1	0	1	0	0	0	0	0
13	Archosauriformes	0&1	0&1	1	0	0	1	0	0	0	0&1
14	Claudiosaurus	0	0	1	0	?	0	0	0	0	0
15	Dactylosaurus	1	1	1	1	1	0	1	0	1	0
16	Serpiano-Neustico	1	1	1	1	1	0	1	0	1	0
17	Simosaurus	1	1	1	1	1	0	0	0	0	1
18	Nothosaurus	1	1	1	1	1	0	1	0	0&1	0
19	Ceresiosaurus	1	1	1	1	1	0	1	0	1	0
20	L. balsami	1	1	1	1	1	0	1	0	1	0
21	L. curionii	1	1	1	1	1	0	1	0	1	?
22	L. valceresii	1	1	1	1	1	0	1	0	1	0
23	Silvestrosaurus	1	1	1	1	1	0	1	0	1	0
24	Corosaurus	1	1	1	0	1	0	0	1	0	1
25	Cymatosaurus	1	1	?	1	1	0	0	0	?	?
26	Germanosaurus	?	?	?	?	?	?	?	?	?	?
27	Pistosaurus	?	?	?	1	1	0	0	1	0	?
28	Placodus	1	1	1	0	0	1	0	0	0	1
29	Micronothosaurus	?	?	?	?	?	?	?	?	?	?

MORPHOLOGICAL DESCRIPTION—The ilia differ somewhat from the morphology typical for *Nothosaurus* in the Germanic Muschelkalk; they more closely resemble those of *Lariosaurus* except for their larger size (Fig. 49). All specimens show a rather indistinct constriction separating the ventral acetabular portion from the dorsal wing. The dorsal wing is rather poorly developed and, indeed, differentiated as a rather sturdy dorsal process. A preacetabular spine is present in HUJ-Pal. 85 (Fig. 49B), but absent in HUJ-Pal. 109 and 114 (Fig. 49A). The dorsal part of the ilium lacks a clearly demarcated posterior process, but rather extends into a posterior flange that never projects beyond the posterior margin of the ventral acetabular portion. The medial surface of the ilium is ornamented with radiating striations on the ventral part, and tubercles may be present on the medial surface of the dorsal process. The lateral (glenoidal) surface of the ilium usually shows a deep vertical trough, and a particularly clearly differentiated acetabular facet is evident in HUJ-Pal. 85 (Fig. 49B).

Nothosaurus sp.

MATERIAL—Two astragali from the Muschelkalk of Makhtesh Ramon.

MORPHOLOGICAL DESCRIPTION—Two isolated astragali (HUJ-Pal. 236 [Fig. 50A]; width: 30 mm; proximodistal depth: 24 mm. HUJ-Pal. 3606 [Fig.

TABLE 5. *Continued.*

Micronothosaurus 8		71	72	73	74	75	76	77	78	79	80
1	Ancestor	0	0	0	0	0	0	0	0	0	0
2	Captorhinidae	0	0	0	0	0	?	0	0	0	0
3	Testudines	0	0	0	0	0	1	0	0	0	0
4	Araeoscelidia	0	0	0	0	0	0	0	0	0	0
5	Younginiformes	0	0	0	0	0&1	0&1	1	0	0	0
6	Kuehneosauridae	?	0	0	0	1	?	?	?	?	?
7	Rhynchocephalia	0	0	0	0	1	1	1	0	0	0
8	Squamata	0	0	0	0	1	1	0&1	0	0	0
9	Rhynchosauria	0	0	0	0	0	1	1	0	0	0
10	Prolacertiformes	1	0	0	0	1	1	1	0	0	0
11	Trilophosaurus	1	0	0	0	?	1	1	0	0	0
12	Choristodera	1	0	1	0	0	1	1	1	0	0
13	Archosauriformes	1	0	0&2	0	0&1	1	1	0	0	0
14	Claudiosaurus	1	0	0	0	1	1	1	0	0	0
15	Dactylosaurus	1	0	1	1	0	1	0	1	1	1
16	Serpiano-Neustico	1	1	1	1	0	1	0	1	1	0
17	Simosaurus	1	0	1	0	0	1	0	1	1	1
18	Nothosaurus	1	0&1	1	1	0&1	1	0&1	1	1	1
19	Ceresiosaurus	1	0	2	1	0	1	1	1	0	1
20	L. balsami	1	0&1	2	1	0	1	0	1	1	1
21	L. curionii	1	1	?	?	?	1	0	1	1	1
22	L. valceresii	1	0	2	1	0	1	?	1	?	?
23	Silvestrosaurus	1	0	?	1	0	1	1	1	0	0
24	Corosaurus	1	0	1	0	1	1	1	1	0	1
25	Cymatosaurus	?	0	?	?	0	1	?	?	?	?
26	Germanosaurus	?	?	?	?	?	1	?	?	?	?
27	Pistosaurus	1	0	?	?	?	1	?	?	?	?
28	Placodus	1	0	1	0	0	1	1	1	0	0
29	Micronothosaurus	?	?	?	?	?	?	?	?	?	?

50B]; width: 36.4 mm; proximodistal depth: 29.8 mm) both display a distinct concavity on their proximal margin, indicating the course of the pedal perforating artery proximal to the astragalus, between the distal heads of the tibia and fibula (see Rieppel [1994a] for a more detailed discussion of this character).

Sauropterygia Incertae Sedis

Under this heading specimens will be discussed that cannot with any confidence be referred to any of the taxa above, which are based on diagnostic cranial or vertebral structure. Although not diagnostic at the genus or species level, these specimens are important in assessing the paleobiogeographical affinities of the sauropterygian fauna from the Muschelkalk of Makhtesh Ramon.

Lower Jaw Fragment (HUJ-Pal. Uncatalogued)

The specimen (Figs. 51, 52) comprises the anterior part of both mandibular rami in articulation at the symphysis. Both mandibular rami are broken in front of the coronoid area, and their posterior part is missing. As preserved, the total length of the fragment is 22.3 mm; its maximum width is 16.9 mm. The contours of the anterior end of the lower jaw indicate a constricted snout, and the symphysis is fortified and spoon-shaped.

TABLE 5. *Continued.*

Micronothosaurus 9		81	82	83	84	85	86	87	88	89	90
1	Ancestor	0	0	0	0	0	0	0	0	0	0
2	Captorhinidae	0	0	?	0	?	0	1	0	0	0
3	Testudines	0	1	0	0	?	?	0	0	1	0
4	Araeoscelidia	0	1	0	0	?	0	1	0	0	0
5	Younginiformes	0	0&1	0	0	?	1	0	0	0	0
6	Kuehneosauridae	?	?	?	1	?	1	0	0	0	0
7	Rhynchocephalia	0	1	0	0	?	1	0	0	0	0
8	Squamata	0	1	0&1	0	?	1	0	0	0	0
9	Rhynchosauria	0	1	0	0	?	1	0	0	0&1	0
10	Prolacertiformes	0	0	?	0	?	1	0	0	0	0
11	Trilophosaurus	0	1	0	0	?	1	0	0	0	0
12	Choristodera	0	1	0	0	?	1	0	0	0	0
13	Archosauriformes	0	1	0	0	?	1	0	0	0&1	0
14	Claudiosaurus	0	1	0	0	?	1	0	0	0	0
15	Dactylosaurus	1	?	?	1	0	1	0	2	1	1
16	Serpiano-Neustico	1	0&1	2	1	0	1	0	2	1	1
17	Simosaurus	1	1	1	1	0	1	0	2	1	1
18	Nothosaurus	1	0&1	2	1	0	1	0	2	1	1
19	Ceresiosaurus	1	0	2	1	0	1	0	2	1	1
20	L. balsami	1	0	2	1	0	1	0	2	1	1
21	L. curionii	1	0	2	1	0	1	0	2	1	1
22	L. valceresii	1	?	?	1	0	1	0	2	1	1
23	Silvestrosaurus	1	?	?	1	0	1	0	2	1	1
24	Corosaurus	1	1	1	1	1	1	0	1	1	1
25	Cymatosaurus	?	?	?	?	?	?	0	?	?	?
26	Germanosaurus	?	?	?	?	?	?	0	?	?	?
27	Pistosaurus	?	?	?	1	1	1	0	3	?	?
28	Placodus	1	1	1	0	?	1	0	0	1	1
29	Micronothosaurus	?	?	?	?	?	?	?	?	?	?

These characters exclude pachypleurosaurian affinities of this small specimen. The length of the lower jaw symphysis is 3.9 mm, and its maximum width is 6.6 mm, resulting in a length-to-width ratio of 0.59. The length-to-width ratio for the lower jaw symphysis varies from 0.7 (*N. marchicus*) to 1.7 (*N. mirabilis*) within the genus *Nothosaurus*. Few specimens of *Lariosaurus* display a well-preserved lower jaw in ventral view; the one specimen (SMF R-13) with the best preserved mandibular symphysis (Boulenger, 1898; Rieppel, 1994a, Fig. 44A) shows a length-to-width ratio very close to 1. These values indicate that although the mandibular symphysis is elongated in the lower jaw from the Muschelkalk of Makhtesh Ramon, it is relatively less so than is typical for *Nothosaurus* or *Lariosaurus*. On the other hand, the preservation of the lower jaw from Makhtesh Ramon is less than perfect, and distortion could explain the low length-to-width ratio obtained for its symphysis.

The broadened symphyseal area shows five alveoli for procumbent symphyseal fangs, decreasing in size from front to back, but all five still larger than those of the succeeding marginal dentary teeth. None of the five symphyseal fangs is preserved. The alveolus of the fourth fang lies partially, that of the fifth fang entirely, behind the broadened symphyseal area. Both mandibular rami show a total of 18 marginal dentary teeth of pointed conical shape following the five symphyseal fangs.

TABLE 5. *Continued.*

	Micronothosaurus 10	91	92	93	94	95	96	97	98	99	100
1	Ancestor	0	0	0	0	0	0	0	0	0	0
2	Captorhinidae	0	0	0	0	0	0	0	0	0	0
3	Testudines	0	0	0	0	0&1	0&2	1	0	1&2	0
4	Araeoscelidia	1	0	0	0	0	0	0	0	0	0
5	Younginiformes	1	0	0	0	0	0&2	0	0&1	0	0
6	Kuehneosauridae	1	0	0	0	0	2	1	2	0	0
7	Rhynchocephalia	1	0	0	0	0	2	0	0	0	0
8	Squamata	1	0	0	0	0	0&2	1	0	0	0
9	Rhynchosauria	1	0	0	0	0	0	1	0	0	0
10	Prolacertiformes	1	0	0	0	0	0	1	1&2	0	0
11	Trilophosaurus	1	0	0	?	0	0	1	0	0	0
12	Choristodera	1	0	0	0	0	0&2	1	2	0	0
13	Archosauriformes	1	0	0	0	0&1	0	1	0	0	0
14	Claudiosaurus	0	0	1	1	1	1	0	0	0	0
15	Dactylosaurus	0	1	0	1	0	0	0	1	3	0
16	Serpiano-Neustico	0	1	0	1	0&1	0&1	0	1&2	3	0&1
17	Simosaurus	0	1	0	1	1	1	1	2	2	1
18	Nothosaurus	0	1	0&1	0&1	1	0&1	0	2	2	1
19	Ceresiosaurus	0	1	1	1	1	1	0	?	3	1
20	L. balsami	0	1	1	1	1	1	0&1	0&2	3	0
21	L. curionii	0	1	1	1	1	1	0	0	?	?
22	L. valceresii	0	1	0	1	1	0	0	0	3	0
23	Silvestrosaurus	0	1	0	1	1	1	1	1	3	0
24	Corosaurus	0	1	1	1	1	0	0	2	1	0
25	Cymatosaurus	0	0	0	0	0	0	0	?	?	0
26	Germanosaurus	?	?	?	?	?	?	?	?	?	?
27	Pistosaurus	0	1	?	1	1	1	1	2	0	?
28	Placodus	0	1	1	1	1	0	1	2	1	0
29	Micronothosaurus	?	?	?	?	?	?	?	?	?	?

Because of a very similar type of preservation, the lower jaw fragment from the Muschelkalk of Makhtesh Ramon superficially resembles the slightly larger lower jaw fragment (with a symphyseal length-to-width ratio of approximately 0.68) from the lower Anisian of the eastern Alps, originally described as *Anarosaurus multidentatus* Huene, 1958, now referred to the genus *Cymatosaurus* (Rieppel, 1995b). However, *C. multidentatus* shows distinct heterodonty, with the much enlarged symphyseal fangs and small, triangular marginal dentary teeth, which is not observed in the lower jaw from Makhtesh Ramon. Also, the small vertebral centra associated with the holotype of *C. multidentatus* are distinctly amphicoelous (Huene, 1958; Rieppel, 1995b), whereas all adequately prepared vertebral centra of similar size known from the Muschelkalk of Makhtesh Ramon are weakly amphicoelous or platycoelous (HUJ-Pal. 2674, 2662, 2462, 1397a–c, 1059; see also description of pachypleurosaur material above).

In conclusion, the lower jaw fragment from Makhtesh Ramon is here treated as Sauropterygia incertae sedis, with the provision that it could represent *L. stensioei*, which it closely matches in size.

Vertebrae (HUJ-Pal. 28, 824, 2898)

The Muschelkalk of Makhtesh Ramon has yielded three vertebrae of distinctive structure, the

TABLE 5. *Continued.*

Micronothosaurus 11		101	102	103	104	105	106	107	108	109	110
1	Ancestor	0	0	0	0	0	0	0	0	0	0
2	Captorhinidae	0	0	0	0	0	0	0	0	0	0
3	Testudines	0	1	0	0	0	0	1	1	1	0
4	Araeoscelidia	0	0	0	0	0	0	0	0	0	0
5	Younginiformes	0	0	1	1	0	1	0	1	0	0
6	Kuehneosauridae	0	1	1	1	0	1	0	1	?	0
7	Rhynchocephalia	0	1	1	1	0	1	0	1	1	0
8	Squamata	0	1	1	1	0	1	0	1	1	0
9	Rhynchosauria	0	0	1	1	0	1	0	1	1	0
10	Prolacertiformes	0	0&1	1	1	0	1	0	1	0	0
11	Trilophosaurus	0	0	1	1	0	1	0	1	0	0
12	Choristodera	0	0	1	1	0	1	1	1	?	0
13	Archosauriformes	0	0	1	1	0	1&2	0&1	1	0	0
14	Claudiosaurus	0	0	1	1	0	1	1	1	0	0
15	Dactylosaurus	0	1	1	?	1	?	?	?	?	0
16	Serpiano-Neustico	0&1	1	1	1	1	2	1	1	1	1
17	Simosaurus	0	1	1	1	1	2	1	1	1	1
18	Nothosaurus	0	1	1	1	1	2	1	1	1	1
19	Ceresiosaurus	1	1	1	1	1	2	1	1	1	1
20	L. balsami	1	1	1	1	1	2	1	1	1	1
21	L. curionii	?	?	?	?	?	?	?	?	?	?
22	L. valceresii	?	1	1	1	1	2	1	1	1	1
23	Silvestrosaurus	1	1	1	1	1	2	1	1	1	?
24	Corosaurus	1	1	1	1	0	1	1	1	1	1
25	Cymatosaurus	1	1	1	1	0	1	1	1	?	?
26	Germanosaurus	?	?	?	?	?	?	?	?	?	?
27	Pistosaurus	?	?	?	1	1	?	?	?	?	?
28	Placodus	0	1	1	1	0	1	1	1	1	0
29	Micronothosaurus	?	?	?	?	?	?	?	?	?	?

best preserved of which is HUJ-Pal. 824 (Figs. 53, 54A–B). This vertebra was originally described by Haas (1975, p. 452, Pl. I, Figs. 6, 7) as that of a placodont resembling *Placodus* or *Paraplacodus*. The specimen shows a broken neural arch and an incomplete right transverse process. As preserved, its total height is 89.8 mm, and its total width is 108.9 mm. The complete left transverse process measures 61.7 mm from the sagittal plane of the specimen to its distal tip. The height of the neural canal is 16.6 mm; its width is 9.5 mm. The vertical diameter of the centrum is 35.1 mm, and its horizontal diameter is 32.8 mm.

The centrum has a constricted body. Its articular surface is deeply amphicoelous; due to incomplete preparation, it is impossible to determine whether a notochordal canal persists, as is characteristic of *Placodus* (Rieppel, 1995a). A most remarkable feature is the presence of a pair of distinct and well-defined subcentral foramina located on the ventrolateral aspect of the centrum. Subcentral foramina are not known from placodonts but are otherwise characteristic of pistosaurs and the Jurassic–Cretaceous crown-group Sauropterygia.

The neural canal is relatively high and narrow, located between distinct pedicels of the neural arch, as is characteristic for *Placodus* (Rieppel, 1995a) and *Paraplacodus* (Peyer, 1935). The transverse processes, however, have a very distinctive shape in the Makhtesh Ramon specimen. Located high up on the neural arch, they broaden

TABLE 5. *Continued.*

Micronothosaurus 12		111	112	113	114	115	116	117	118	119	120
1	Ancestor	0	0	0	0	0	0	0	0	0	0
2	Captorhinidae	0	0	0	0	0	0	0	0	0	0
3	Testudines	0	0	0&1	1	0	1	1	0	?	0
4	Araeoscelidia	0	1	0	0	0	0	0	1	0	0
5	Younginiformes	0	1	0	0	0	1	0	1	0	0
6	Kuehneosauridae	?	?	?	?	?	?	?	?	?	0
7	Rhynchocephalia	0	1	0&1	1	0	1	1	1	0	0
8	Squamata	0	1	1	1	0	1	1	1	?	0
9	Rhynchosauria	1	1	0	1	0	1	1	?	0	0
10	Prolacertiformes	0&1	1	0&1	1	0	1	0&1	1	0	0
11	Trilophosaurus	1	1	0	1	0	1	1	?	?	0
12	Choristodera	1	1	0	1	0	1	1	?	?	0
13	Archosauriformes	1	1	0&1	1	0	1	1	1	0	0
14	Claudiosaurus	0	1	0	0	0	0	0	?	0	0
15	Dactylosaurus	?	?	?	?	?	?	?	0	0	0
16	Serpiano-Neustico	0	0	1	1	2	0	0	0	0	0
17	Simosaurus	0	0	1	1	1	0	0	0	1	0
18	Nothosaurus	0	0	1	1	1	0	0	0	1	0
19	Ceresiosaurus	0	0	1	1	1	0	0	0	0	1
20	L. balsami	0	0	1	1	0	0	0	0	0	1
21	L. curionii	?	?	?	?	?	?	?	0	?	1
22	L. valceresii	0	0	1	1	1	0	0	0	0	1
23	Silvestrosaurus	0	0	?	?	?	?	?	0	0	1
24	Corosaurus	0	0	1	1	1	?	?	0	1	0
25	Cymatosaurus	?	?	?	?	?	?	?	0	0	0
26	Germanosaurus	?	?	?	?	?	?	?	0	?	0
27	Pistosaurus	?	?	?	?	?	?	?	0	?	0
28	Placodus	0	0	1	1	2	0	0	0	0	0
29	Micronothosaurus	?	?	?	?	?	?	?	?	?	?

distinctly as they extend laterally. The transverse processes of dorsal vertebrae of *Placodus* and *Paraplacodus* are much more slender and show no significant distal expansion. Pre- and postzygapophyses are eroded in HUJ-Pal. 824, as are accessory intervertebral articulations, if present. HUJ-28 (Fig. 54C) is a partially prepared neural arch of the same type, with the left prezygapophysis exposed. From below the prezygapophysis protrudes a distinct flange that might be considered a hypantrum, albeit of a distinctly different morphology than is characteristic for the hypantrum of *Placodus* (Rieppel, 1995a, Fig. 38A). A hyposphene–hypantrum articulation was present in *Paraplacodus*, according to Peyer (1935, Text Fig. 4), who described a distinct trough located between and below the prezygapophyses and lined laterally by a ridge of bone extending down from the prezygapophysis.

The identity of the vertebrae HUJ-Pal. 28, 824, and 2898 as those of a placodont is indicated by the deeply amphicoelous (perhaps even notochordal) vertebral centrum, the relatively high and narrow neural arch, and the distinct transverse processes. The possible presence of a hypantrum points to the *Placodus–Paraplacodus* clade of placodonts (Rieppel & Zanon, 1997), since a hyposphene–hypantrum articulation is absent in cyamodontoids. However, the specimens differ from all known placodonts by the presence of paired subcentral foramina and by the distinct distal expansion of the transverse processes.

TABLE 5. *Continued.*

Micronothosaurus 13		121	122
1	Ancestor	0	0
2	Captorhinidae	0	0
3	Testudines	0	0
4	Araeoscelidia	0	0
5	Younginiformes	0	0
6	Kuehneosauridae	0	0
7	Rhynchocephalia	0	0
8	Squamata	0	0
9	Rhynchosauria	0	0
10	Prolacertiformes	0	0
11	Trilophosaurus	0	0
12	Choristodera	0	0
13	Archosauriformes	0	0
14	Claudiosaurus	0	0
15	Dactylosaurus	0	0
16	Serpiano-Neustico	0	0
17	Simosaurus	1	0
18	Nothosaurus	1	0
19	Ceresiosaurus	0	1
20	L. balsami	1	1
21	L. curionii	1	?
22	L. valceresii	1	?
23	Silvestrosaurus	?	?
24	Corosaurus	?	?
25	Cymatosaurus	?	?
26	Germanosaurus	?	?
27	Pistosaurus	?	?
28	Placodus	?	0
29	Micronothosaurus	?	?

Phylogenetic Interrelationships within the Genus *Nothosaurus*

The sauropterygian fauna from the *Ceratites* layers of the Muschelkalk of Makhtesh Ramon shows close relationships to the fauna from the upper Muschelkalk and lower to middle Keuper of the Germanic Triassic, particularly due to the presence of *Nothosaurus* species putatively close to *N. giganteus* and *N. mirabilis* and the presence of *Lariosaurus*. These faunal affinities contrast with Hirsch's concept of a Sephardic faunal realm (1977, 1984, 1986), based on the claim that the circum-Mediterranean Muschelkalk deposits are characterized by an invertebrate fauna that differs radically from that of the Germanic Triassic (Hirsch, 1986, p. 223). The paleobiogeographical history of the fauna from the Muschelkalk of Makhtesh Ramon will be discussed in greater detail below, following the analysis of the phylogenetic interrelationships of the species of *Nothosaurus*. The problem here is that *N. haasi*, although from the *Ceratites* layers, shows an interesting mixture of characters shared with *Germanosaurus* from the lower Muschelkalk of the Germanic Triassic, on the one hand, and with *N. mirabilis* from the upper Muschelkalk on the other. Characters shared with *Germanosaurus* are the relation of the premaxillae with the frontal, the shape and relations of the nasals, and possibly the relatively small upper temporal fossa. The most notable character shared with *N. mirabilis* is the slender and elongated rostrum. The purpose of the phylogenetic analysis of nothosaur interrelationships is to test whether *N. haasi* is the sister taxon to all other species of *Nothosaurus*, which would support the hypothesis of a Sephardic faunal province, or whether *N. haasi* is nested within nothosaur species otherwise known from the upper Muschelkalk of the Germanic Triassic (Rieppel & Wild, 1996).

Based on earlier analyses of sauropterygian interrelationships, *Simosaurus* and the Pachypleurosauroidea were chosen as consecutive outgroups of the Nothosauridae (Rieppel, 1997a). Terminal taxa of the Nothosauridae are *Germanosaurus schafferi* (see Rieppel, 1997a, for the morphological description) and the species of *Nothosaurus* currently considered valid (Rieppel & Wild, 1996): *N. edingerae, giganteus, juvenilis, marchicus, mirabilis, haasi,* and *tchernovi*. Included in the data matrix is also an undescribed taxon of *Nothosaurus* from the lower Muschelkalk of Winterswijk (kept in private collections).

The cladistic analysis is based on the 25 characters listed below (the data matrix is given in Table 9):

1. Rostrum proportions: rostral constriction absent (0), rostrum relatively short and rounded (1), or rostrum relatively long, slender, parallel-edged (2).

2. Premaxillary dentition: premaxillary fangs absent (0) or present (1).

3. Premaxillae separated from frontal by nasals (0), premaxilla meeting frontal at the level of the posterior margin of the external naris or between the external naris and the orbit (1), or premaxilla meeting frontal at the level of the anterior margin of the orbit (2).

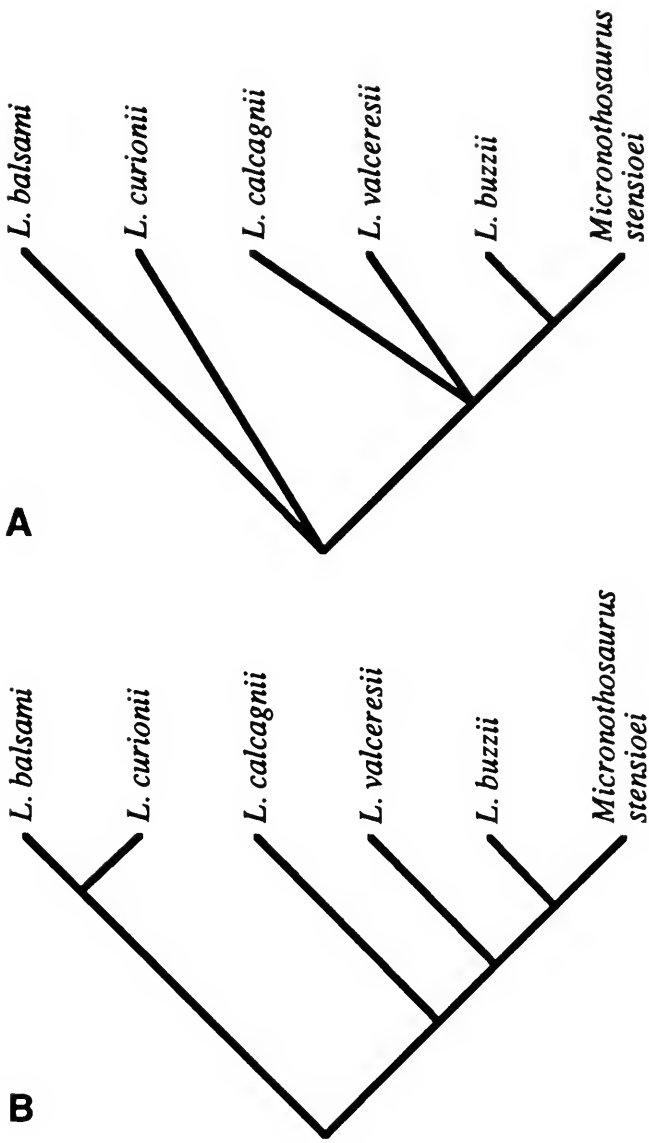

FIG. 42. **A.** Strict consensus tree (ten MPTs) for the interrelationships of species of *Lariosaurus*. **B.** 50% majority rule consensus tree (six trees out of ten MPTs) shows full resolution of lariosaur interrelationships. The analysis is based on the data presented in Table 5; search procedures are explained in the text.

4. Nasal without (0) or with (1) anterolateral process lining the entire medial margin of external naris.

5. Maxilla without (0) or with (1) depression at lateral margin of external naris, with a foramen at its bottom for the exit of a lateral branch of the superior alveolar nerve.

6. Anterior margin of internal naris positioned slightly (0) or distinctly (1) behind anterior margin of external naris (ratio obtained by dividing the distance from the snout to the anterior margin of the internal naris by the distance from the tip of the snout to the anterior margin of the external naris smaller than 1.2 [0] or larger than 1.2 [1]).

7. Length of nasal behind level of anterior margin of external naris less (0) or more (1) than twice the maximal width of nasal.

8. Dorsal exposure of prefrontal: large (0) or reduced (1).

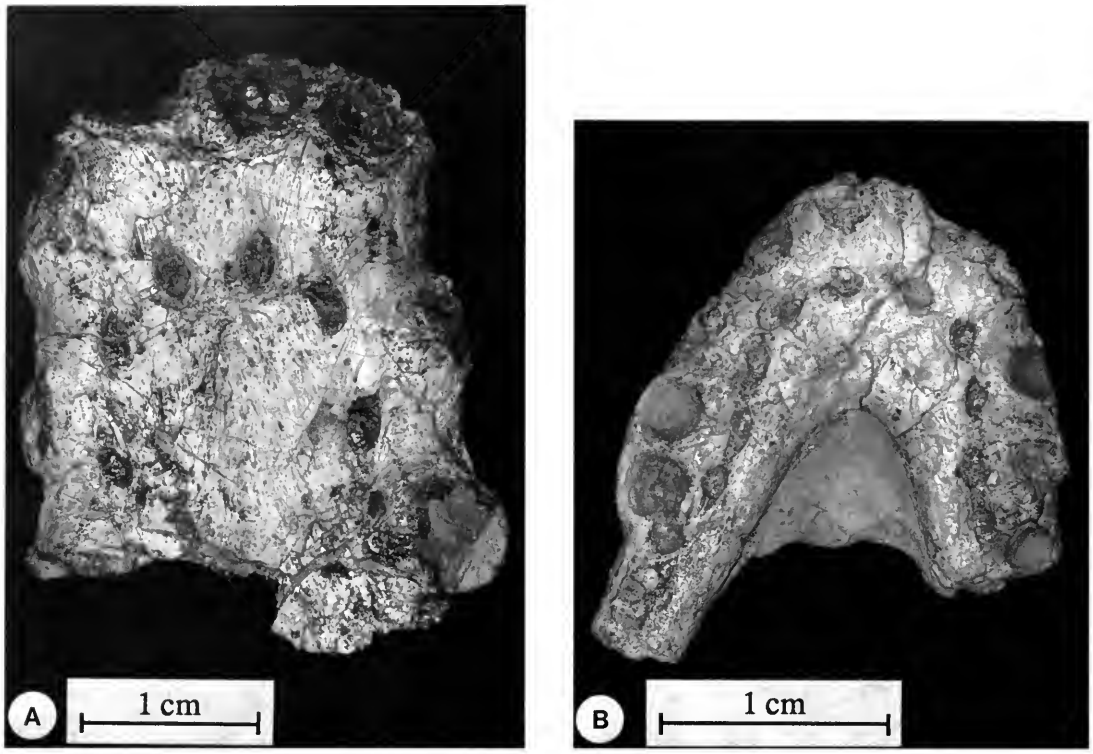

FIG. 43. Indeterminate remains of *Nothosaurus* sp. **A,** HUJ-Pal. 223, premaxillary rostrum, ventral view. **B,** HUJ-Pal. 1904, mandibular symphysis, dorsal view.

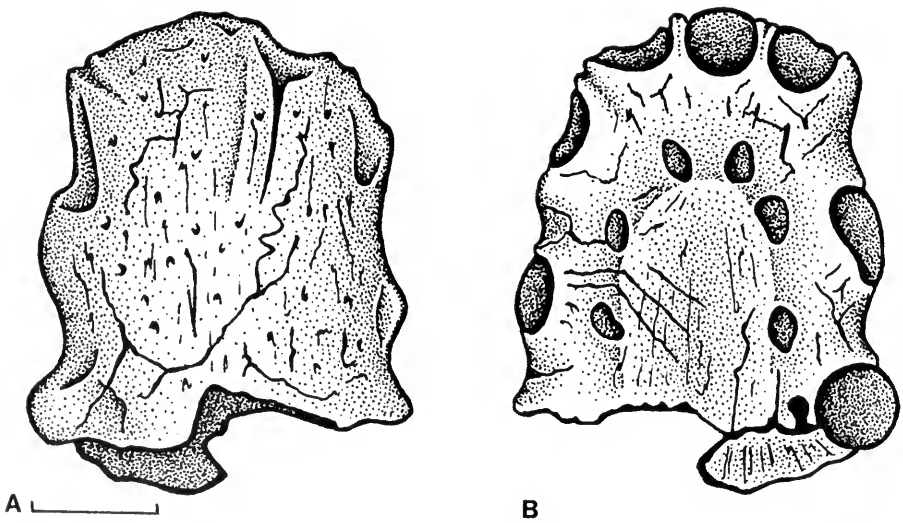

FIG. 44. A premaxillary rostrum of *Nothosaurus* sp. (HUJ-Pal. 223). **A,** dorsal view. **B,** ventral view. Scale bar = 10 mm.

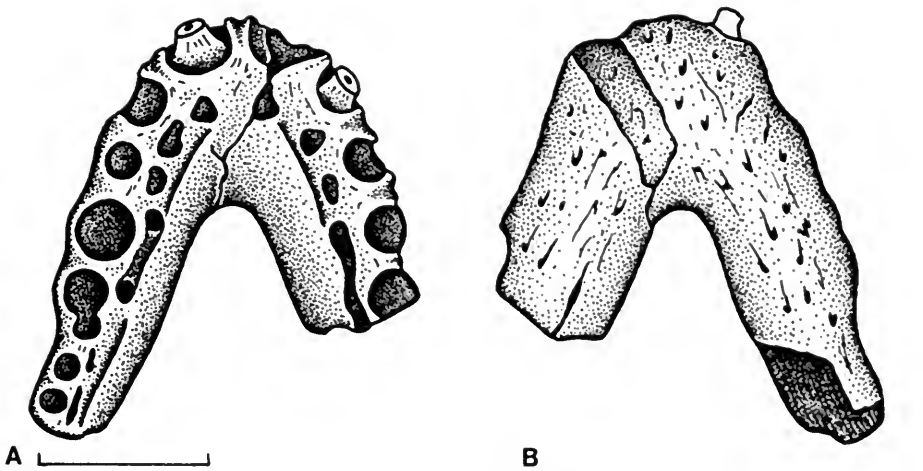

FIG. 45. A mandibular symphysis of *Nothosaurus* sp. (HUJ-Pal. 1904). **A,** dorsal view. **B,** ventral view. Scale bar = 10 mm.

9. Frontal: paired (0) or fused (1).
10. Postfrontal enters upper temporal fossa (0) or remains excluded therefrom.
11. Postfrontal tapering posteriorly (0) or broad posteriorly and interdigitating with parietal in a transversely oriented suture (1).
12. Postorbital forms part (0) or all (1) of the anterior margin of the upper temporal fossa.
13. Distance from posterior margin of external naris to anterior margin of orbit more (0) or less (1) than 1.5 times the width of the postorbital arch.

TABLE 6. Measurements (in millimeters) for neural arches of *Nothosaurus* sp. The height of the neural spine is defined as the distance from the roof of the neural canal to the tip of the neural spine. The total width is measured across the transverse processes.

specimen	total height	height of neural spine	total width
HUJ-Pal. 1500	32	23.5	42
HUJ-Pal. 1492	21.5	16	33.4
HUJ-Pal. 2008	--	--	31.6
HUJ-Pal. 796b	--	--	31
HUJ-Pal. 796a	--	--	29.5
HUJ-Pal. 2011	21.5	15	26.6
HUJ-Pal. 796c	16.3	9.9	22.1

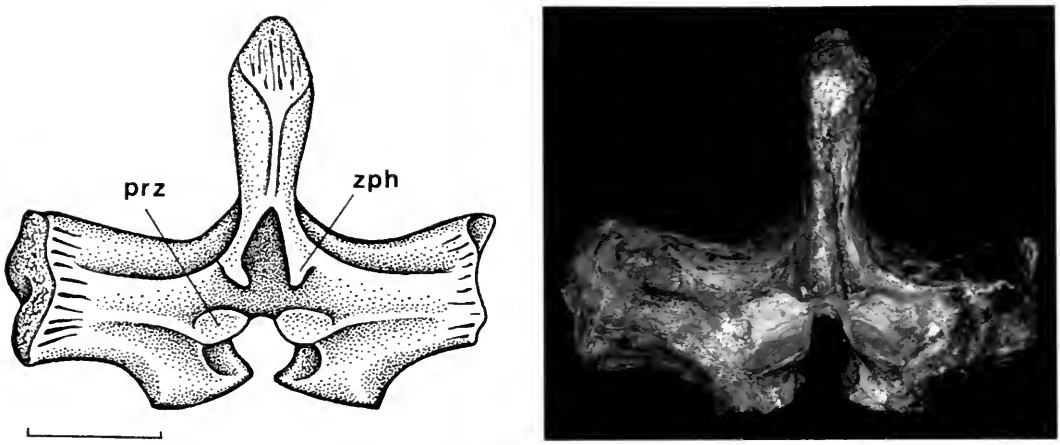

FIG. 46. An isolated neural arch of *Nothosaurus* sp. (HUJ-Pal. 1500), anterior view. Scale bar = 10 mm. Abbreviations: prz, prezygapophysis; zph, zygosphene.

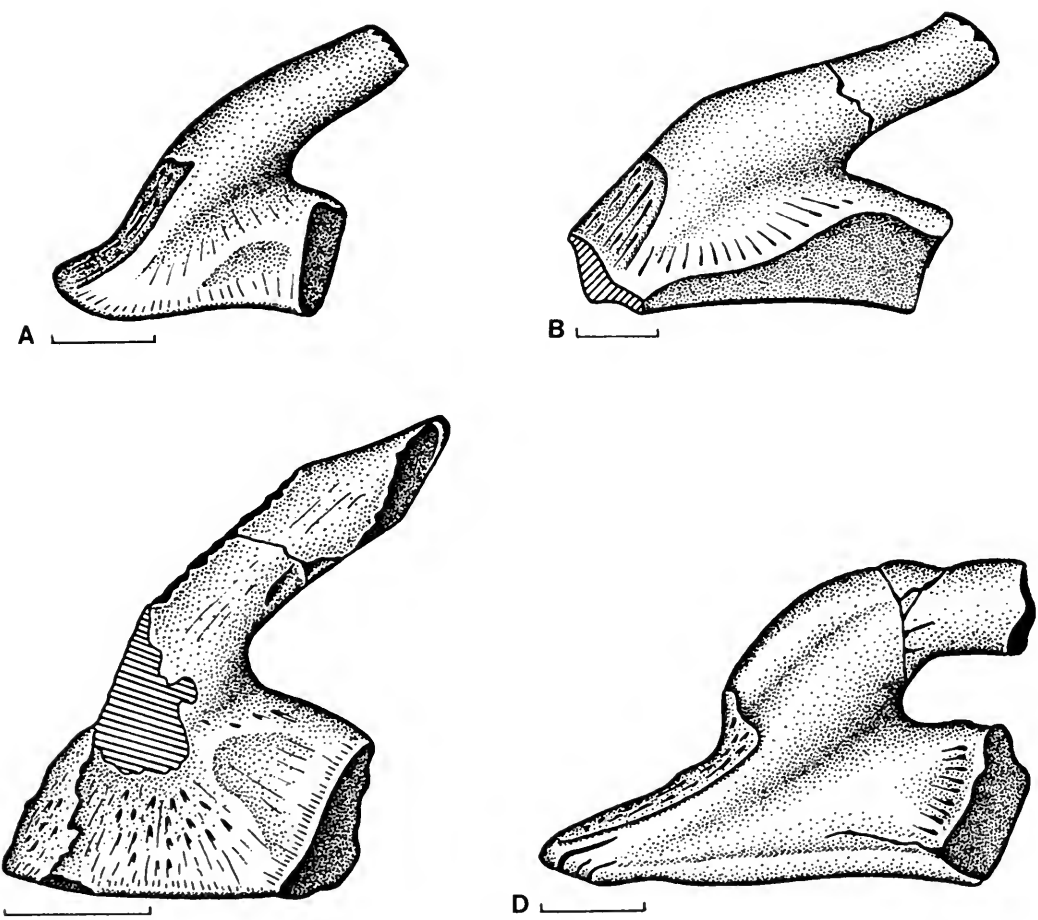

FIG. 47. A series of isolated scapulae of *Nothosaurus* sp. **A,** HUJ-Pal. 1111, right scapula, medial view; scale bar = 10 mm. **B,** HUJ-Pal. 2041, right scapula, medial view; scale bar = 5 mm. **C,** HUJ-Pal. 2063, left scapula, lateral view; scale bar = 20 mm. **D,** HUJ-Pal. 3818, left scapula, medial view; scale bar = 10 mm.

TABLE 7. Measurements (in millimeters) for coracoids of *Nothosaurus* sp.

specimen	total length	proximal width	minimal width	distal width
HUJ-Pal. 1998	81	39.3	22.1	--
HUJ-Pal. 739	75	--	16	36
HUJ-Pal. 1216	66.5	27	15.2	--
HUJ-Pal. 747	39.3	18.5	9.9	21.4
HUJ-Pal. 1131	21.8	9.5	6.0	8.3

14. Jugal present and entering orbit (0), present but excluded from posterior margin of orbit (1), or absent (2).
15. Posterior extent of maxillary toothrow: restricted to level in front of anterior margin of anterior third of upper temporal fossa (0), extending approximately to level of anterior one-third of longitudinal diameter of upper temporal fossa (1), or extending approximately to level of midpoint on longitudinal diameter of upper temporal fossa (2).
16. Condylobasal skull length divided by longitudinal diameter of upper temporal fossa: ratio >3 (0), 2.5–3.0 (1), or 2.3–2.5 (2).
17. Longitudinal diameter of upper temporal fossa equal to or less than two times (0) or more than two times (1) the longitudinal diameter of the orbit.
18. Anterior corner of upper temporal fenestra rounded (0) or constricted by distinct lateral convexity of parietal (1).
19. Maxillary fangs absent (0) or present (1).
20. Frontoparietal suture largely in front of or bridging the level of the anterior margin of upper

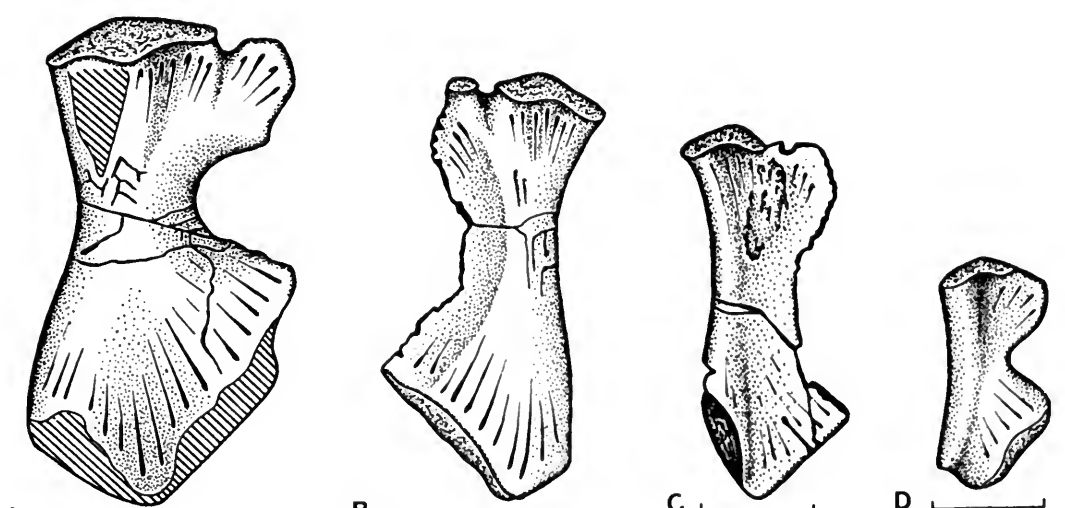

FIG. 48. A series of isolated coracoids of *Nothosaurus* sp. **A**, HUJ-Pal. 1998. **B**, HUJ-Pal. 739. **C**, HUJ-Pal. 1216. **D**, HUJ-Pal. 747. Scale bar = 20 mm.

TABLE 8. Measurements (in millimeters) for ilia of *Nothosaurus* sp.

specimen	maximal height	maximal width
HUJ-Pal. 23816	16.5	15
HUJ-Pal 109	55.5	46.0
HUJ-Pal. 85	58.5	45.2
HUJ-Pal. 114	63.3	45.8

temporal fossa (0), or located entirely behind (1) that level.
21. Parietal paired (0) or fused (1).
22. Parietal skull table unconstricted (0); weakly constricted (1); strongly constricted, at least posteriorly (2); or with a sagittal crest (3).
23. Pineal foramen close to the middle of the skull table (0), weakly displaced posteriorly (1), or strongly displaced posteriorly (2).
24. Occipital crest absent (0) or present (1).
25. Neural spines on dorsal vertebrae low (0) or tall (1).

The data were analyzed using the software package PAUP (version 3.1.1.) developed by David L. Swofford (Swofford, 1990; Swofford & Begle, 1993). All multistate characters were treated as unordered. The branch-and-bound search option was implemented in all searches. Synapomorphy listings for successively subordinated nodes is based on DELTRAN character optimization, because this will minimize synapomorphies diagnostic of any one level, which will be reversed (lost) at a subordinated level.

In a first run, all terminal taxa of the presumed monophyletic ingroup (Rieppel, 1997: Nothosauridae) were rooted on *Simosaurus* and the pachypleurosaur clade. One single MPT was obtained with a TL of 62 steps, CI of 0.677, and RI of 0.661. Nothosaur interrelationships are fully resolved, as shown in Figure 55.

Rooting all ingroup plus the two outgroup taxa on a hypothetical all-0 ancestor resulted in a total of two equal MPTs with TL = 64, CI = 0.656, and RI = 0.707, the only lack of resolution affecting the relative placement of the two outgroup taxa. Identical nothosaur interrelationships to those obtained in the previous search are supported by both MPTs. Removing the undescribed taxon from Winterswijk from the analysis and rooting the latter on the two outgroup taxa yielded three MPTs (TL = 59, CI = 0.721, RI = 0.660). *Germanosaurus* remains the sister taxon of *Nothosaurus*; *N. juvenilis* remains the sister taxon to all other species of *Nothosaurus*. The relationships of *N. edingerae* and *N. marchicus* remain unresolved with respect to a monophyletic clade including (*N. giganteus* (*mirabilis* (*haasi, tchernovi*))). Deleting the Winterswijk taxon and rooting both ingroup and outgroup taxa on an all-0 ancestor resulted in six MPTs (TL = 61, CI = 0.698, RTI = 0.721) with identical partial resolution of nothosaur relationships as indicated for the previous search and unresolved relationships of the two outgroup taxa with respect to the ingroup taxa. The position of the nothosaur taxa from the Muschelkalk of Makhtesh Ramon, deeply nested within the nothosaurs from the Germanic Muschelkalk, therefore seems well supported. In view of the relatively small number of characters and the relatively high level of homoplasy in the data set, the cladogram is very unstable. A tree one step longer than the MPT loses all resolution within the genus *Nothosaurus*!

On the basis of the given set of data (see Rieppel [1997a] for an extended data set), synapomorphies diagnostic for the Nothosauridae (*Germanosaurus* and *Nothosaurus*) are these: presence of a rostral constriction (1[1]); presence of premaxillary fangs (2[1]); reduced dorsal exposure of prefrontals (1[1]); and jugal excluded from posterior margin of the orbit (14[1]). The Nothosaurinae (comprising all species of *Nothosaurus,* plus *Lariosaurus,* which was not included in this analysis [Rieppel, 1997a, 1998]) are diagnosed by the presence of an anterolateral process of the nasal lining the medial margin of the external naris (4[1]); presence of a depression on the maxilla lateral to the external naris with a foramen at its bottom for the exit of a lateral branch of the superior alveolar nerve (5[1]); presence of maxillary fangs (19[1]); fused parietals (21[1]); strongly constricted parietal, at least posteriorly (22[2]); strong displacement of pineal foramen posteriorly (23[2]); and presence of occipital crest (24[1]). The Winterswijk taxon and all the species of *Nothosaurus* except *N. juvenilis* group together on the basis of these characteristics: nasal relatively short and broad (7[0]); postorbital forming all of the anterior margin of the upper temporal fossa

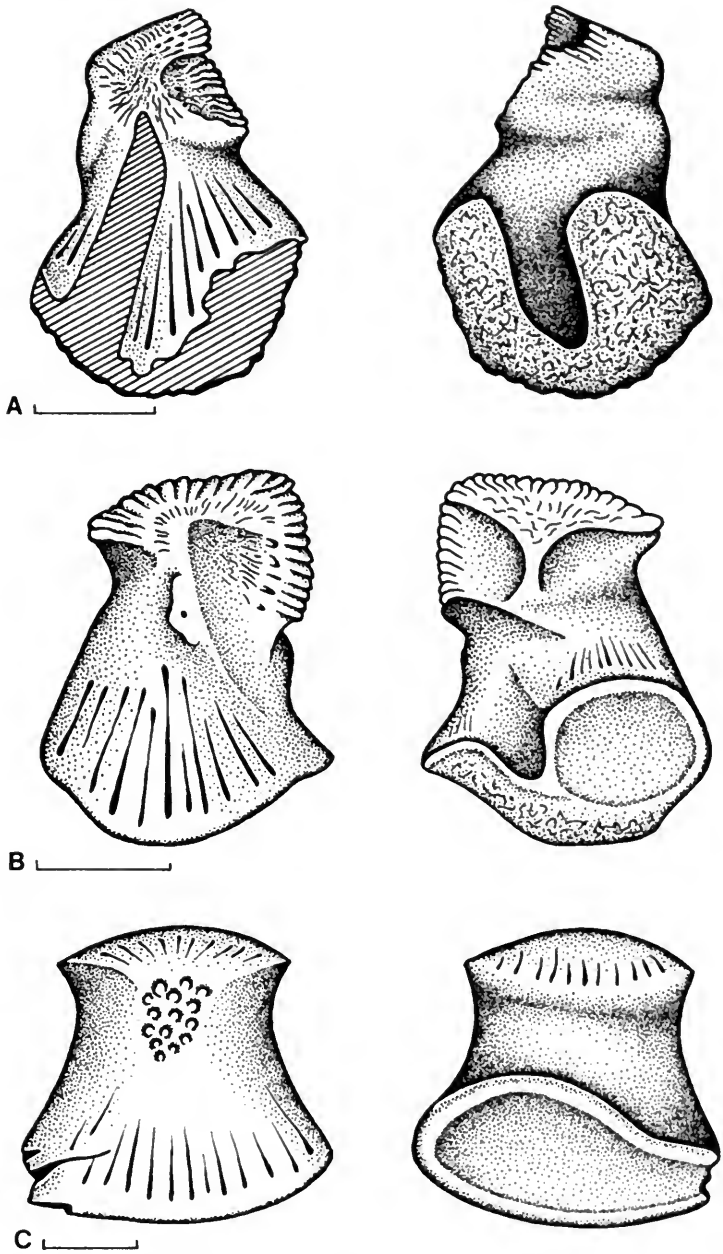

FIG. 49. A series of isolated ilia of *Nothosaurus* sp.; left column in medial view, right column in lateral view. **A**, HUJ-Pal. 114; scale bar = 20 mm. **B**, HUJ-Pal. 85; scale bar = 20 mm. **C**, HUJ-Pal. 3816; scale bar = 5 mm.

(12[1]); relatively broad postorbital arch (13[1]); and elongated upper temporal fossae (17[1]). *Nothosaurus marchicus* and *N. edingerae* are linked to the (*N. giganteus* (*mirabilis* (*haasi, tchernovi*))) clade by the maxillary toothrow extending to the level of the anterior third of the longitudinal diameter of the upper temporal fossa (15[1]). *Nothosaurus edingerae* groups with the (*N. giganteus* (*mirabilis* (*haasi, tchernovi*))) clade on the basis of the frontoparietal suture being located entirely behind the level of the anterior margin of the upper temporal fossa. Monophyly of the (*N.*

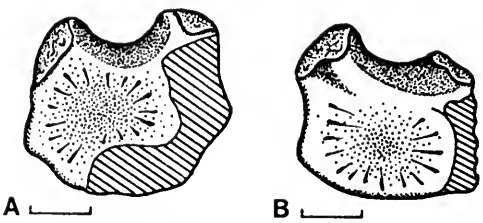

FIG. 50. Two isolated astragali of *Nothosaurus* sp. **A**, HUJ-Pal. 236. **B**, HUJ-Pal. 3606. Scale bar = 10 mm.

giganteus (*mirabilis* (*haasi, tchernovi*))) clade is based on the relatively long and slender nasals (7[1]), the postfrontal being broad posteriorly and interdigitating with the parietal in a transversely oriented suture, and the condylobasal skull length being 2.3–2.5 times the longitudinal diameter of the upper temporal fossa (16[2]). *Nothosaurus mirabilis* is the sister taxon of *N. haasi* and *N. tchernovi* on the basis of the relatively long, slender, and parallel-edged rostrum and the tall and slender neural spine in the dorsal vertebral column. Finally, the *Nothosaurus* from the Muschelkalk of Makhtesh Ramon are sister taxa, sharing the absence of the depression of the maxilla lateral to the external naris with a foramen at its bottom (5[0], reversed), and the absence of the jugal (14[2]).

The cladogram obtained for the species of *Nothosaurus* was used to test the match of successive sister-group relationships among the species of the genus *Nothosaurus* versus their stratigraphic appearance in the fossil record, following the method outlined by Norell and Novacek (1992). The result shows a poor, indeed statistically insignificant, correlation of age rank and clade rank for *Nothosaurus* species (Fig. 56). The Spearman rank correlation test yields a coefficient ρ, corrected for ties, of 0.524 (tied ρ-value: 0.138), which is not significant at $\alpha < 0.05$. The stratigraphic CI for the cladogram shown in Figure 55 is 0.667. Closer inspection of the match of clade rank and age rank for *Nothosaurus* species (Fig. 56) reveals the following problems. The correlation suffers, as most taxa make their first appearance either during the late Scythian or in the late Anisian. The clumping of first appearances during these two time intervals reflects the fact that the *Nothosaurus* species either appear in the Germanic basin or in the Makhtesh Ramon basin, which share a very similar geological history correlated with cyclical sea level changes. The times of first appearances coincide with cycles of marine transgressions that formed epicontinental seas during the late Scythian and in lower salinity levels (after a salinity crisis) during the late Anisian. Beyond the fact that for most species the time of first appearance coincides with the opening of appropriate habitats that also have fossilization potential, there are two taxa with distinctly delayed first appearances relative to their clade rank, namely *N. juvenilis* and *N. edingerae.*

Nothosaurus edingerae is known from the Gipskeuper only, and indeed represents the geologically latest occurrence of its genus. Its absence in the upper Muschelkalk, in which its sister taxa first appear, may be due to taphonomic bias, in view of the small size of the species. The more striking exception is *N. juvenilis* from the lower upper Muschelkalk, which is shown to be the sister taxon to all other species of *Nothosaurus,* including those from the lower Muschelkalk (for an alternative position of the species, based on a more restricted data set, see Rieppel & Wild, 1996). The position of *N. juvenilis* in the result of the present analysis can be explained by a more detailed discussion of the data basis. On the one hand, the material from Winterswijk shows a striking mixture of plesiomorphic (jugal entering posterior margin of orbit, pineal foramen positioned anteriorly, and restricted posterior extent of maxillary toothrow) and apomorphic characters (entire anterior margin of the upper temporal fossa formed by postorbital, postfrontal excluded from upper temporal fossa, and broad postorbital arch). On the other hand, two derived characters that exclude *N. juvenilis* from a higher clade rank (relatively broad postorbital arch, relatively long upper temporal fossae) in fact represent the relatively large size of the orbits autapomorphic for this species (Rieppel, 1994b), whereas the relatively posterior extent of the maxillary toothrow is coded as unknown for this species due to breakage. The relatively long and slender premaxillary rostrum, finally, shows up as convergent in *N. juvenilis* on grounds of global parsimony. The relative position of *N. juvenilis* with respect to other species of its genus may well change (Rieppel & Wild, 1996) as their morphology becomes better known.

The most important result of the cladistic analysis, however, is the monophyly of the (*N. giganteus* (*mirabilis* (*haasi, tchernovi*))) clade. The two diagnosable nothosaur species from the Muschelkalk of Makhtesh Ramon are sister taxa, as documented most notably by the loss of the jugal,

FIG. 51. A lower jaw fragment of an unidentified sauropterygian (Eosauropterygia indet., HUJ-Pal. uncatalogued).

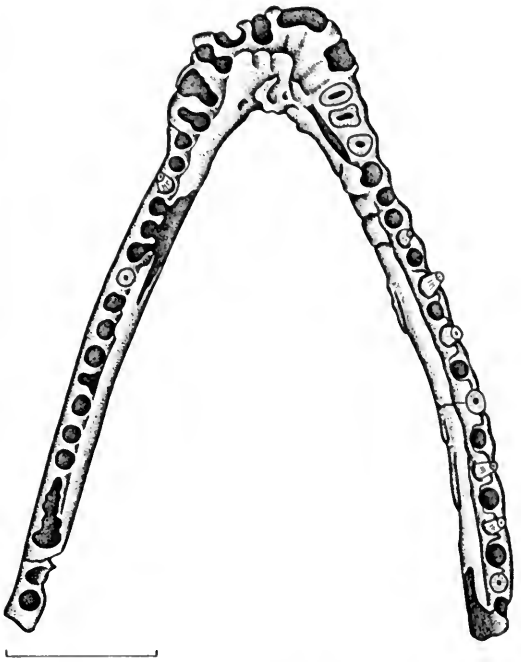

FIG. 52. A lower jaw fragment of an unidentified sauropterygian (Eosauropterygia indet., HUJ-Pal. uncatalogued). Scale bar = 5 mm.

and together the two form the sister taxon of *N. mirabilis*.

Stratigraphic and Geographic Distribution of the Genus *Nothosaurus*

The species of the genus *Nothosaurus* from the Germanic Muschelkalk have recently been reviewed by Rieppel and Wild (1996). The first diagnostic species of *Nothosaurus* to occur in the Germanic Triassic (upper lower Muschelkalk of the eastern Germanic basin) is *N. marchicus*. This does not take into account the fragmentary material from the lowermost Muschelkalk of Gogolin, Upper Silesia (Kunisch, 1888), which may also be referable to *N. marchicus*. *Nothosaurus juvenilis* comes from the lower upper Muschelkalk (mo_1, Anisian) of Wiesloch near Heidelberg (Rieppel, 1994b). The lower upper Muschelkalk (mo_1) is also the interval of the first occurrence of *N. giganteus* and *N. mirabilis*. Finally, *N. edingerae* comes from Gipskeuper (Rieppel & Wild, 1994). The correlation of the *Ceratites* beds of the Muschelkalk of Makhtesh Ramon, which have yielded *N. haasi* and *N. tchernovi*, was discussed in detail above. Straddling the Anisian–Ladinian boundary, these beds are equivalent to the mo_1 and/or mo_2 of the upper Muschelkalk of the Germanic Triassic. Other than its location in the Negev, *Nothosaurus* has been reported from outside the Germanic Triassic in Transylvania, Spain, Tunisia, and the Alpine Triassic.

The marine Middle Triassic (Anisian) deposits on the southern slope of the Plopis Mountains near Alesd, 22 miles east of Oradea, Transylvania (Romania), have yielded nothosaur dorsal vertebrae with a low neural spine, as well as a skull fragment described as *N. transsylvanicus* Jurcsak, 1976 (see also Jurcsak, 1977, 1978, 1982). The skull fragment represents a small species very close to, if not identical with, *N. marchicus*, as indicated by Jurcsak's (1973) original identification of the specimen as *Nothosaurus* cf. *procerus*. (*Nothosaurus procerus* Schröder, 1914, is a subjective junior synonym of *N. marchicus* Koken, 1893: Rieppel & Wild, 1996.) The only difference between *N. transsylvanicus* and the latter species relates to the proportions of the external nares. *Nothosaurus marchicus* is characterized by a relatively broad and rounded external naris: dividing

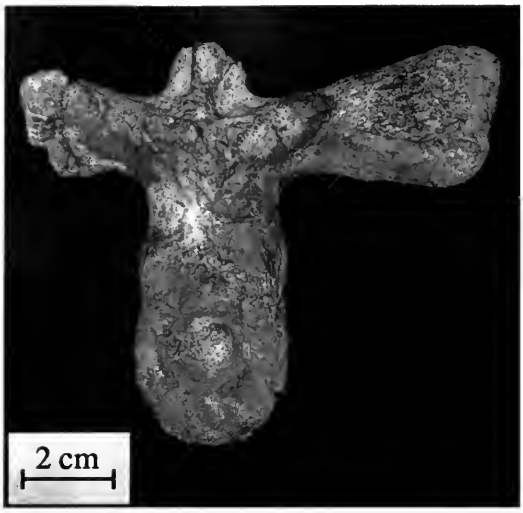

FIG. 53. A dorsal vertebra of an unidentified sauropterygian (Sauropterygia indet., HUJ-Pal. 824), anterior view.

the longitudinal diameter of the external naris by its transverse diameter yields a ratio of 1.0–1.6. In the holotype of *N. transsylvanicus,* the longitudinal diameter of the external naris is 13.6 mm on the left (12.7 mm on the right), the transverse diameter is 6.3 (6.7) mm, and the average quotient of the left and right measurements is 2.02, indicating a distinctly more elongated external naris. Jurcsak (1973) showed the nasal to be in contact with the prefrontal, thus separating the frontal from the maxilla in *N. transsylvanicus.* In all specimens of *N. marchicus* described by Schröder (1914, cf. *N. crassus, N. oldenburgi, N. procerus, N. procerus* var. *parva,* and *N. raabi*), the nasal is separated from the prefrontal by a frontal–maxillary contact. The holotype of *N. marchicus* can no longer be located today, but the latex peel of the counterslab supports Koken's (1893) description of a broad contact between prefrontal and nasal (Rieppel & Wild, 1996). This character is furthermore bilaterally asymmetrical in the skull of other *Nothosaurus* species (Rieppel, 1993b; Rieppel & Wild, 1996).

Other fossils from the Transylvanian Muschelkalk include a probable pachypleurosaur, a second, larger species of *Nothosaurus* (not represented by diagnostic material), *Tanystropheus,* numerous osteoderms of a cyamodontoid placodont identified as *Psephosaurus,* and an ichthyosaur (probably *Mixosaurus*). One vertebra from Alesd shows an elevated neural spine, recalling the structure of those of *N. mirabilis* (Jurcsak, 1977). This observation ties in with the singular occurrence of a long-snouted nothosaur skull in the basal middle Muschelkalk of the eastern Germanic basin (Rieppel & Wild, 1996, p. 64). In general, the faunal assemblage from Alesd is similar to the one recorded from the lower Muschelkalk of the Germanic Triassic, as well as to the faunal assemblage from the *Beneckeia* beds of Makhtesh Ramon (Parnes, 1962, p. 8). The fauna, including invertebrates, is characteristic of a nearshore assemblage that populated the coastal stretches along the Transylvanian Island (Huza et al., 1987).

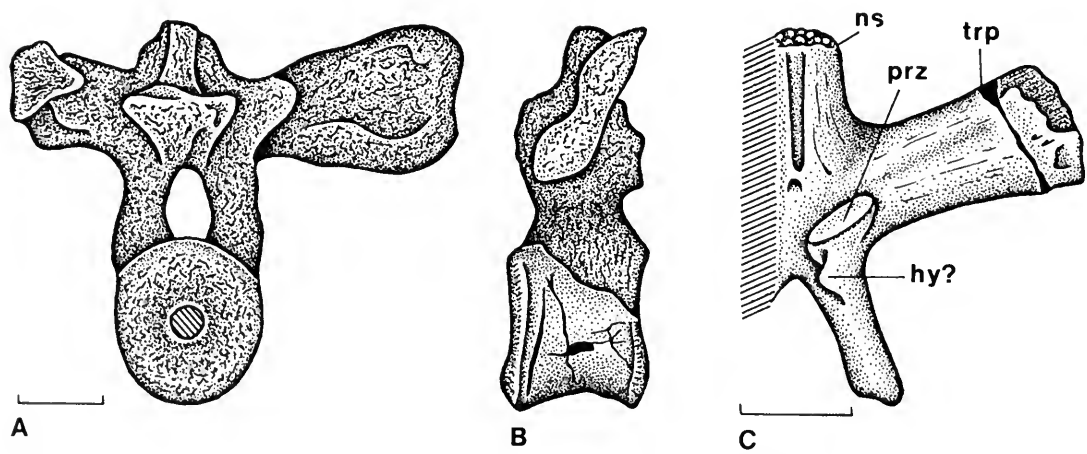

FIG. 54. Two dorsal vertebrae of unidentified sauropterygians (Sauropterygia indet.) **A,** HUJ-Pal. 824, anterior view. **B,** HUJ-Pal. 824, left lateral view. **C,** HUJ-Pal. 28, anterior view. Scale bar = 20 mm. Abbreviations: hy, hypantrum; ns, neural spine; prz, prezygapophysis; trp, transverse process.

TABLE 9. Data matrix for the analysis of the phylogenetic relationships of the species of the genus *Nothosaurus*.

Nothosaurus 1		1	2	3	4	5	6	7	8	9	10
1	Pachypleurosaurs	0	0	0&1	0	0	0	1	0	0&1	0
2	Simosaurus	0	0	1	0	0	1	0	0	1	0
3	Germanosaurus	1	1	2	0	0	1	1	1	0	0
4	N. edingerae	1	1	?	1	0	0	0	1	1	0
5	N. giganteus	1	1	1	1	1	0	1	1	1	?
6	N. juvenilis	2	1	0	1	1	0	1	1	1	0
7	N. marchicus	1	1	0	1	1	0	0	1	1	0&1
8	N. mirabilis	2	1	0&1	1	1	0	1	1	1	1
9	N. haasi	2	1	2	0	0	0	1	1	1	0
10	N. tchernovi	2	1	0	1	0	0	?	1	1	?
11	Winterswijk	1	1	0	1	1	0	0	1	1	1
12	Ancestor	0	0	0	0	0	0	0	0	0	0

Nothosaurus 2		11	12	13	14	15	16	17	18	19	20
1	Pachypleurosaurs	0	0	0	0	0	0	0	0	0	0
2	Simosaurus	0	0	0&1	0	2	1	0	0	0	1
3	Germanosaurus	0	0	1	1	0	?	0	0	0	0
4	N. edingerae	0	1	0	?	1	1	1	1	1	1
5	N. giganteus	1	1	1	1	1	2	1	1	1	1
6	N. juvenilis	0	0	0	1	?	1	0	0	1	0
7	N. marchicus	0	0&1	1	1	1	1	1	0&1	1	0
8	N. mirabilis	1	1	1	0&1	1&2	2	1	1	1	1
9	N. haasi	1	0	0	2	1	0	1	0	1	1
10	N. tchernovi	1	1	1	2	1	2	1	1	1	1
11	Winterswijk	0	1	1	0	0	1	1	1	1	0
12	Ancestor	0	?	0	0	0	?	0	0	0	0

Nothosaurus 3		21	22	23	24	25
1	Pachypleurosaurs	0	0	0	0	0
2	Simosaurus	1	1	0	0	0
3	Germanosaurus	0	1	1	0	0
4	N. edingerae	1	3	2	1	0
5	N. giganteus	1	2	2	1	0
6	N. juvenilis	1	2	2	1	0
7	N. marchicus	1	2	2	1	0
8	N. mirabilis	1	2	2	1	1
9	N. haasi	1	2	2	1	1
10	N. tchernovi	1	2	2	1	1
11	Winterswijk	1	2	1	1	0
12	Ancestor	0	0	0	0	0

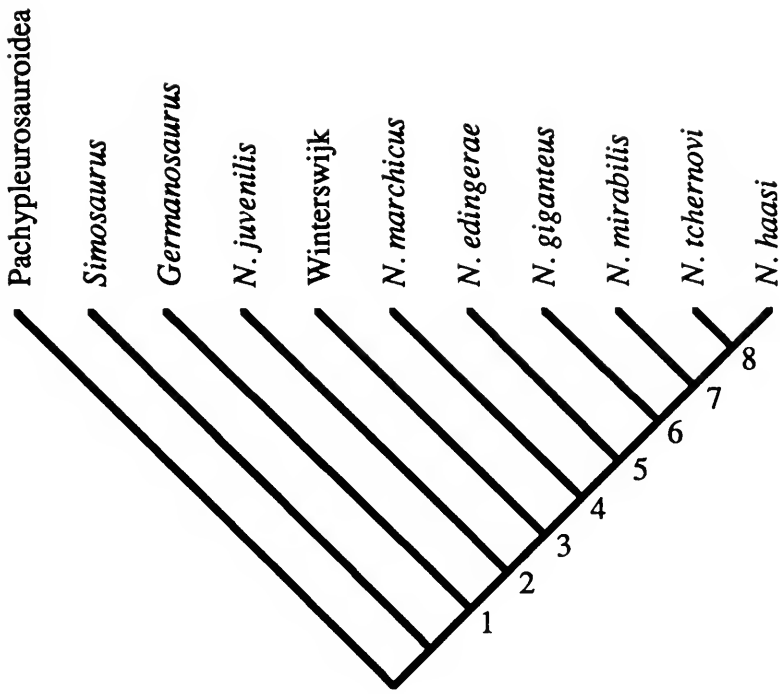

FIG. 55. Interrelationships of the Nothosauridae. Numbers along the axis of the cladogram indicate clade rank for the Nothosauridae. The cladogram represents the single most parsimonious solution in an analysis of nothosaur interrelationships rooted on the outgroup taxa *Simosaurus* and Pachypleurosauroidea. The analysis is based on the data presented in Table 9; search procedures are explained in the text.

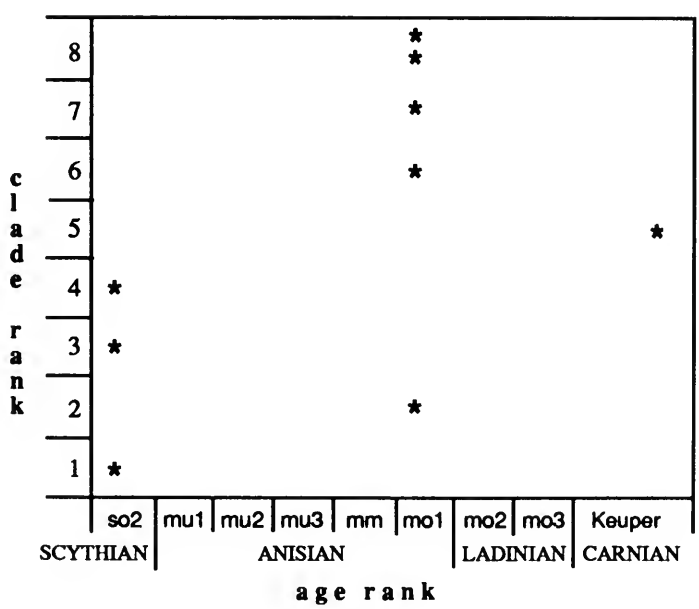

FIG. 56. Clade rank versus age rank for the Nothosauridae. The stratigraphy is calibrated on the Germanic Triassic. The occurrence of *Nothosaurus edingerae* (age rank 5) is in the Gipskeuper.

Vertebrate fossils have been reported from the Ladinian of the western Taurus, southwestern Turkey (Beltan et al., 1979). Apart from fishes (*Perleidus, Saurichthys*), the only tetrapods collected so far from this locality are cyamodontoid placodonts, represented by osteoderms and a partial vertebra, and tentatively identified as *Psephosaurus*. The invertebrate fauna indicates a close affinity to the Arabo-African platform, which is hardly surprising, given the geological origin of the Taurride carbonate platform (reviewed in Robertson & Dixon, 1984).

A rich sauropterygian fauna comes from the upper Muschelkalk (Ladinian) of northeastern Spain, with outcrops located about 100 km southwest of Barcelona in the vicinity of Mont-ral and Alcover (Sanz, 1976, 1983a–b; Alafont & Sanz, 1996; for a review see Rieppel & Hagdorn, in press). The peculiar preservation of vertebrate fossils at that locality renders the identification of taxa at the species level very difficult, if not impossible. The fauna includes a possible pachypleurosaur, *Lariosaurus,* an enigmatic skull identified as a pistosaur, an unidentified thalattosaur, and an endemic nothosaur, *N. cymatosauroides* Sanz, 1983a. The species is represented by the skull of a relatively small nothosaur with a relatively short, broad rostrum and upper temporal fossae that are 2.3 times longer than the longitudinal diameter of the orbit. A small cyamodontoid from Mont-ral–Alcover was provisionally identified as *Psephosaurus* or *Psephoderma.*

A rather poorly known sauropterygian fauna comes from the Muschelkalk of Djebel Rehach in southern Tunisia (Gorce, 1960; Lehman, 1965). Unfortunately, there is as yet no precise stratigraphic correlation of the occurrence of sauropterygians at Djebel Rehach, although the vertebrates derive from the basal layers of the outcrop of the Tunisian Muschelkalk (Gorce, 1960). Osteoderms of cyamodontoid placodonts from Djebel Rehach are too fragmentary to permit meaningful comparison with the cyamodontoids from Makhtesh Ramon. Gorce (1960) therefore argued for placing more emphasis on a comparison of nothosaurs occurring at both localities, but was herself unable to pursue such a comparison because the Israeli material had not been described by the time of her writing.

The material that formed the basis of Gorce's (1960) monograph comprises a fairly large number of fragmentary and rather poorly preserved sauropterygian remains (Rieppel, 1997b). The occurrence of a large nothosaur (*Nothosaurus* cf. *N. giganteus*) is documented by a partial premaxillary rostrum (Gorce, 1960, Pl. III, Fig. 3, Text Fig. 4), as well as by a skull fragment (Gorce, 1960, Pl. I., Fig. 1, Text Fig. 2). Bone is only preserved on the ventral surface of the latter, and shows an unpaired (fused) vomer. This skull fragment represents the only nothosaur with an unpaired (fused) vomer other than *N. haasi* from the Muschelkalk of Makhtesh Ramon, yet the two taxa differ widely in absolute size. It should be noted that in large skulls of *N. giganteus,* suture lines are often very difficult to identify, which may indicate partial or complete fusion of originally separate elements (Rieppel & Wild, 1996). The presence of *Nothosaurus* cf. *N. giganteus* at Djebel Rehach is further evidenced by a very large cervical centrum. The presence of a smaller nothosaur, perhaps comparable in adult size to *N. tchernovi* or *N. mirabilis,* is indicated by numerous other, smaller vertebral centra, some in articulation with each other and with ribs that show a characteristic bladelike distal expansion. No such ribs are known from other Triassic stem-group Sauropterygia. The neural spines of these vertebrae are all broken, but to judge from their slender base, they do not seem to have reached the height characteristic of *N. tchernovi* or *N. mirabilis.* One vertebra was singled out by Gorce (1960, Pl. III, Figs. 1–2, 7, Text Fig. 7; Lehman, 1965) as resembling those of *Pistosaurus.*

Nothosaurus is a comparatively rare faunal element in the Alpine Triassic. Aside from *N.* (*Paranothosaurus*) *giganteus* (Peyer, 1939; Dalla Vecchia, 1993; see discussion above), the few occurrences include an indeterminate lower jaw and an undescribed specimen from the Grenzbitumenzone (Anisian–Ladinian boundary) of the southern Alps, and an undescribed specimen resembling *N. marchicus* from the Ladinian of the eastern Alps (Bürgin et al., 1991; Furrer et al., 1992). Nothosaur remains have been collected in the uppermost Ladinian or lower Carnian of Fusea in the Friulian Alps, and an indeterminate nothosaur femur is reported (Sirna et al., 1994) from the *gracilis* Formation of Recoaro (Bithynian, lower Anisian).

Paleobiogeographic History of the Sauropterygians from Makhtesh Ramon

Formation of the southern branch of the Mesozoic Neotethys was initiated during the upper-

most Scythian. During the Middle Triassic (Anisian–Ladinian), the southern Tethyan margin was differentiated as an epicontinental shelf of Muschelkalk facies extending from the Levant of the eastern Mediterranean to the Iberian, Catalonian, Apulian, and Sardo-Provençal regions of the western Mediterranean (Hirsch, 1986; see also Hirsch, 1977, 1984; Dercourt et al., 1993). Fluctuations of transgression and regression lasting from the middle Anisian through the early Carnian resulted in local formations of Muschelkalk deposits on the northern Gondwanan shelf, ranging from Arabia to northeastern Spain (Hirsch, 1986). These deposits have been referred to collectively as the Sephardic faunal realm by Hirsch (1972, 1976, 1977, 1984, 1986; Marquez-Aliaga et al., 1986), who described the Mediterranean basins as being characterized by invertebrate (ammonoid and bivalve) and conodont faunas whose compositions differ radically from those of the Germanic Triassic (Hirsch, 1986, p. 223). The biota of the Mediterranean realm is described as being characterized by a large number of endemic taxa, which are found in association with Tethyan taxa but which are entirely absent in the Germanic Muschelkalk. These faunal associations indicate a wide-open connection between the Mediterranean faunal realm and the pelagic Tethys, whereas the Mediterranean faunal realm appears to have been separated from the Germanic basin (Hirsch, 1986, p. 220; see below for further discussion). However, a purely numerical, rather than cladistic, approach to faunal comparison was pursued (Hirsch, 1976, p. 547) supporting this concept of a separate southern Sephardic faunal, a concept that furthermore implies the rejection of the existence of a Burgundian Gate. The Burgundian Gate has been hypothesized to connect the Germanic Muschelkalk to the southern branch of the developing Neotethys, thus providing a gateway for faunal exchange between the Germanic basin, the Alpine intraplatform basins, and the Sephardic (Mediterranean) faunal province (Hirsch, 1986).

The concept of such a Sephardic faunal province contrasts with analyses of the paleobiogeographic history of the Germanic Muschelkalk fauna (Hagdorn, 1985, 1991; Urlichs & Mundlos, 1985; Mostler, 1993). During Anisian and Ladinian times, the open Tethys was located east of the Bohemian Massif and its southward continuation, the Vindelician Ridge, with a broad belt of shallow carbonate platforms intercalated between the emergent land masses and the open ocean (Marcoux et al., 1993). Triassic sedimentation patterns in western and Central Europe again reflect frequent sea-level oscillations (Ziegler, 1982). In the wake of a late Scythian (Röt) sea-level rise inducing marine transgressions, faunal elements characteristic of the Germanic Muschelkalk reached the Germanic basin through a northeastern gateway, the East Carpathian Gate. During the Pelsonian (middle Anisian), a second, southeastern gateway linked the Germanic basin to the northern branch of the Neotethys, the Silesian–Moravian Gate (Kozur, 1974; Ziegler, 1982; Hagdorn, 1985, 1991; Urlichs & Mundlos, 1985; Mostler, 1993; Rieppel, 1997a; Rieppel & Hagdorn, 1997). It was through these eastern and southeastern gateways that the lower Muschelkalk fauna established itself (Hagdorn, 1985, 1991; Urlichs & Mundlos, 1985; Szulc, 1991). During the middle Muschelkalk (middle to upper Anisian), the closure of the East Carpathian Gate and a shallowing of the Silesian–Moravian Gate provoked a salinity crisis that resulted in a much depleted fossil record (Ziegler, 1982; Hagdorn, 1985, 1991; Urlichs & Mundlos, 1985). The fossil record picks up again with the transition to the upper Muschelkalk, when a renewed marine transgression entered the Germanic basin through a southern gateway, the Burgundian Gate, linking the Germanic basin to the southern branch of the Neotethys (Kozur, 1974; Hagdorn, 1985; Urlichs & Mundlos, 1985). At the same time—the transition from the middle to the upper Muschelkalk—the Silesian–Moravian Gate disappeared, whereas the East Carpathian Gate was reestablished, but only to a limited extent (Kozur, 1974; Senkowiczowa & Szyperko-Sliwczynska, 1975; Urlichs & Mundlos, 1985; Hagdorn, 1991).

The question to be addressed at this point is how the Makhtesh Ramon fauna bears on these conflicting scenarios of the geological evolution of the western Tethyan realm. The Muschelkalk deposits of the Negev formed in a basin that resulted from subsidence, as plate movement during the preliminary phases of the opening of the Neotethys was primarily vertical (Garfunkel & Derin, 1984; Hirsch, 1984; May, 1991). At Makhtesh Ramon, the Muschelkalk deposits comprised shallow marine, lagoonal, and intertidal facies (Sestini, 1984), and vertebrate fossils have been recorded from two different layers within the entire sequence.

An earlier fauna, collected from the *Beneckeia* beds (Middle Member of the Gevanim Formation: Druckman, 1974), comprised labyrinthodont amphibians (Zanon, 1991), ?*P. mosis, Tanystropheus*

sp., and indeterminate *Nothosaurus* remains. Lithological, sedimentological, and paleontological clues indicate that the lower part of this member was deposited in a tidal flat environment, whereas shallow normal marine conditions prevailed during deposition of the upper part of the member (Druckman, 1974).

The younger fauna derives from the *Ceratites* beds (Lower Member of the Saharonim Formation: Druckman, 1974), and includes ?*Psephosaurus* osteoderms, *Tanystropheus,* and all the taxa described in this paper, with the exception of ?*P. mosis.* "The Lower Member of the Saharonim formation was deposited under normal, calm, shallow marine conditions as part of the ingression of the Saharonim Sea which prevailed in the area during the upper Anisian and lower to middle Ladinian" (Druckman, 1974, p. 35).

The only vertebrate fossils found between these faunal associations, i.e., in the Upper Member of the Gevanim Formation, are cyamodontoid (?*Psephosaurus*) osteoderms. The deposition environment for these strata was a marginal tidal flat (Druckman, 1974). It appears, therefore, that the occurrence of sauropterygians at Makhtesh Ramon is tied to shallow marine conditions. The stratification of vertebrate occurrences in the Muschelkalk of Makhtesh Ramon has to be accepted with some reservation, however, because the material has been assembled largely by surface collecting (with the exception of ?*P. mosis:* Brotzen, 1957).

In the Germanic Muschelkalk, different species of *Tanystropheus* occur at different times. The lower Muschelkalk yielded *T. antiquus* (possibly congeneric with *Macrocnemus:* Wild, 1987); the upper Muschelkalk, *T. conspicuus* (Wild, 1973). The *Tanystropheus* material from Makhtesh Ramon has not yet been described, but a fragmentary cervical vertebra, apparently from the *Ceratites* beds, was found to closely resemble those of *T. conspicuus* (Peyer, 1955; Wild, 1973, pp. 73, 152), a taxon from the upper Muschelkalk. Unfortunately, the *Tanystropheus* material from the *Beneckeia* beds has never been described and compared to *T. antiquus.*

In aggregate, the tetrapod fauna from the *Beneckeia* beds of Makhtesh Ramon (*Tanystropheus,* cyamodontoid placodonts [?*Psephosaurus*], and indeterminate "*Nothosaurus*") resembles the faunal association known from the Anisian of Alesd (Transylvania), which in turn resembles the fauna from the lower Germanic Muschelkalk. These very general faunal resemblances might lend some support to the paleobiogeographical reconstructions of Hirsch (1986; see also Marquez-Aliaga et al., 1986). Faunal elements found east of the Bohemian–Vindelician Massif in Transylvania might have spread northwest through the Silesian–Moravian Gate into the Germanic basin and southward into the eastern Mediterranean realm during the lower Anisian. In view of the still very incomplete knowledge of the Transylvanian fauna and its precise stratigraphic provenience, on the one hand, and the incomplete knowledge of the fauna from the *Beneckeia* beds of Makhtesh Ramon on the other, this scenario remains only weakly supported. In the absence of cladistic analysis of phylogenetic relationships among well-established faunal components, it may derive its main support from the absence of conflicting evidence.

Examined in isolation, cyamodontoid placodonts (represented as osteoderms) show an almost ubiquitous distribution. Their presence in the Anisian of Transylvania may indicate that they reached the Germanic basin through the Silesian–Moravian Gate during the lower upper Anisian (*C. tarnowitzensis* Gürich, 1884; lower Muschelkalk; lower Illyrian), whereas their presence in the Negev, Tunisia (Gorce, 1960), Turkey (Beltan et al., 1979), and Spain (Westphal, 1975; Rieppel & Hagdorn, 1997a) may indicate that they reached upper Muschelkalk deposits of the Germanic basin (*Cyamodus kuhnschnyderi* Nosotti & Pinna, 1993b) through the Burgundy Gate (H. Hagdorn, in litt., 12 November 1996). The enigma here is the problematic, and certainly incomplete, diagnosis of *Psephosaurus,* based on osteoderms from the upper Lettenkeuper (upper Ladinian), as opposed to *Cyamodus* from lower and upper Muschelkalk deposits, which is diagnosed on the basis of cranial material (Rieppel & Zanon, 1997). The use of placodonts in the analysis of Middle Triassic paleobiogeographic patterns in the western Tethyan realm requires a thorough revision of armored placodonts (cyamodontoids) at the species level and the analysis of phylogenetic relationships among those species.

The best known faunal elements from the Muschelkalk of Makhtesh Ramon are the nothosaurs (*Nothosaurus* and *Lariosaurus*) from the *Ceratites* beds, which, although endemic for this basin at the species level, bear close cladistic relationships to the upper Muschelkalk fauna from the Germanic Triassic. *Nothosaurus giganteus* first appears in the fossil record in the lower upper Muschelkalk (mo_1, upper Anisian), as does *N. mira-*

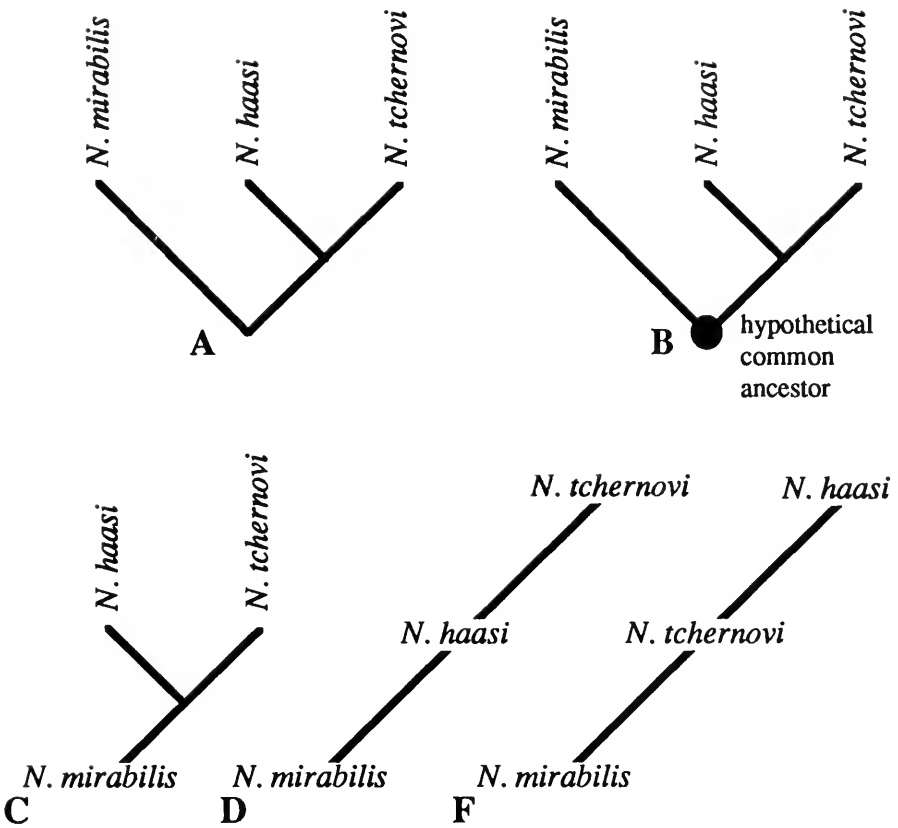

FIG. 57. **A.** Cladistic relationships of three species of *Nothosaurus*. **B–F.** Some possible ancestor–descendant relationships derived from cladogram **A.**

bilis, and both persist into the lower Keuper (Rieppel & Wild, 1996). The earliest occurrence of *N. giganteus,* or a very closely related species, in the Alpine Triassic is in the Grenzbitumenzone (Anisian–Ladinian boundary) of Monte San Giorgio (Peyer, 1939; a Bulgarian occurrence is not precisely dated: Rieppel & Wild, 1996). Other occurrences of *N. giganteus,* or a very closely related species, are known from the Ladinian of the southern Alps (Dalla Vecchia, 1993) and Djebel Rehach, Tunisia (Gorce, 1960). Diagnostic material of *N. mirabilis* is only known from the Germanic Triassic (upper Anisian and Ladinian). Cladistic analysis shows *N. haasi* and *N. tchernovi* to form a monophyletic clade, known only from the Makhtesh Ramon Muschelkalk, and together to be more closely related to *N. mirabilis* than to any other nothosaur species considered valid today (Rieppel & Wild, 1996).

Lariosaurus is the sister taxon of *Nothosaurus,* and its first geological occurrence is in the Grenzbitumenzone (Anisian–Ladinian boundary) of the southern Alps. The genus diversified in the Alpine Triassic (Rieppel, 1998), and it is also known from the Germanic basin (Keuper: Rieppel & Hagdorn 1997), from the Spanish Muschelkalk (Rieppel & Hagdorn, in press), and from the Makhtesh Ramon basin of the eastern Mediterranean. As shown above, cladistic analysis nests *L. stensioei* from Makhtesh Ramon within the other species of its genus.

Nothosaurs (*Nothosaurus, Lariosaurus*) from the *Ceratites* beds of Makhtesh Ramon therefore show exactly the mix of Germanic and Alpine elements contradicted by the concept of a Sephardic faunal realm (Hirsch, 1986). Affinities of the Makhtesh Ramon fauna with that of the upper Muschelkalk and lower Keuper of the Germanic and Alpine Triassic is further supported by the occurrence of *Simosaurus.* Other than its occurrence in Makhtesh Ramon, this genus is only known from the southern Germanic basin (Rieppel, 1994a) and the eastern Alps (Rieppel, 1996)

Cladistic analysis shows that *N. haasi* and *N.*

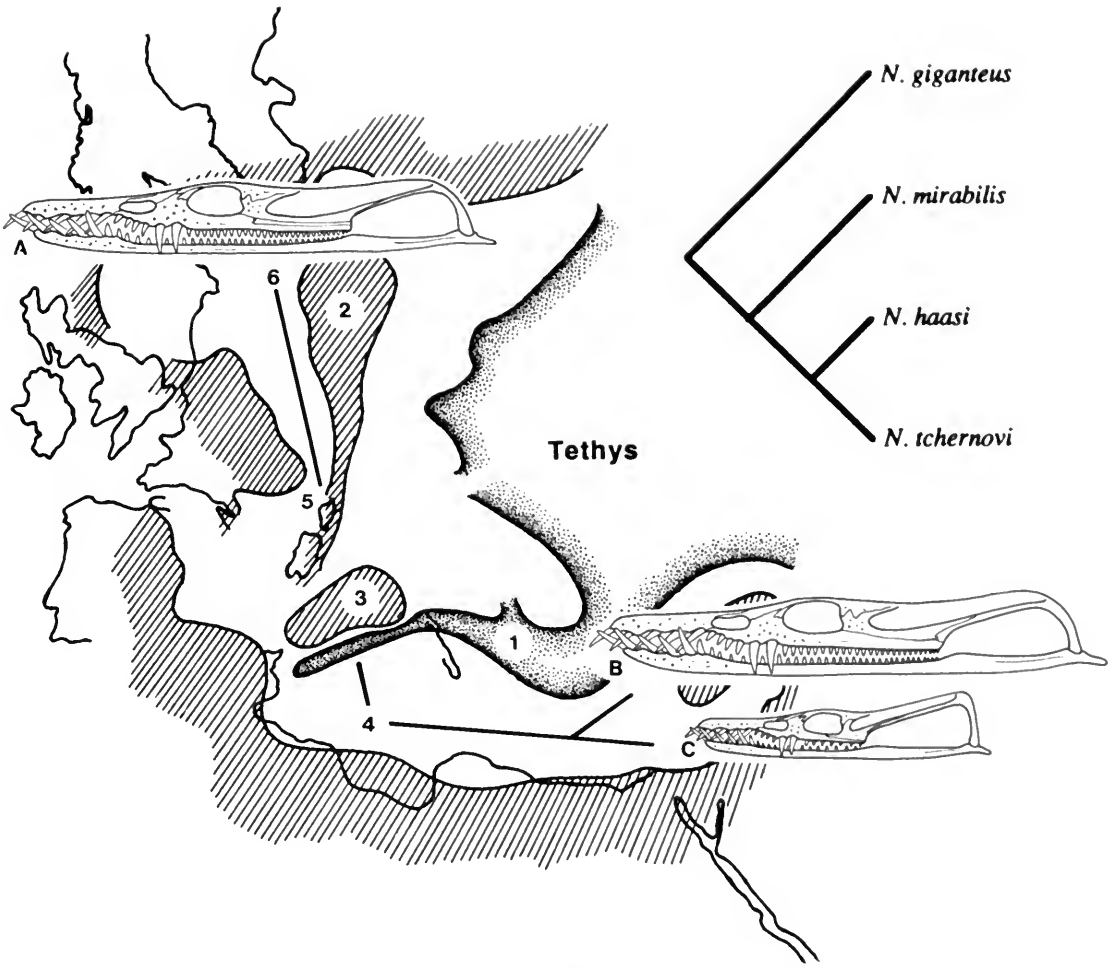

FIG. 58. Phylogenetic relationships and late Anisian paleobiogeography (Marcoux et al., 1993) of the nothosaurs from the Muschelkalk of Makhtesh Ramon, Negev, Israel. **A,** *Nothosaurus mirabilis.* **B,** *Nothosaurus tchernovi.* **C,** *Nothosaurus haasi.* Stippled: deep ocean basins; hatched, exposed land surface; 1, southern branch of Neotethys; 2, Bohemian–Vindelician Massif; 3, Apennine carbonate platform; 4, northern Gondwanan shelf (shallow platform); 5, Burgundy Gate; 6, Germanic basin.

tchernovi are more closely related to one another than either is to any other species of *Nothosaurus.* Successive sister taxa of the Makhtesh Ramon nothosaurs are *N. mirabilis* and *N. giganteus* from the upper Muschelkalk of the Germanic Triassic. Translating these cladistic relationships (Fig. 57A) into possible ancestor–descendant hypotheses (Figs. 57B–D), the conclusion must be that neither *N. haasi* nor *N. tchernovi* can possibly be construed as being ancestral to *N. mirabilis.* Conversely, *N. mirabilis* could potentially be ancestral to the *N. haasi–N. tchernovi* clade (Fig. 57C–D), or *N. mirabilis* and the *N. haasi–N. tchernovi* clade may share an as-yet-unknown common ancestor (Fig. 57B).

If *N. mirabilis* was ancestral to the *N. haasi–N. tchernovi* clade, this implies the southeastern migration of *N. mirabilis* through the Burgundian Gate across the southern Tethyan margin during late Anisian times. This scenario does not explain the occurrence of the nothosaurs in the upper Muschelkalk, following the salinity crisis that dominated the middle Muschelkalk. It would therefore seem more likely that *N. mirabilis* and the *N. haasi–N. tchernovi* clade shared an unknown common ancestor, distributed in the western Tethyan realm, along with other nothosaurs such as *Nothosaurus* cf. *N. giganteus.* On either side of the developing southern branch of the Neotethys, this hypothetical ancestor might have

given rise to *N. mirabilis* in the Germanic basin, on the one hand, and to the *N. haasi–N. tchernovi* clade on the eastern part of the northern Gondwanan shelf on the other (Fig. 58).

The faunal mix of sauropterygians in the Makhtesh Ramon Muschelkalk, with *Simosaurus,* a *Lariosaurus* cladistically nested within the other species of its genus from the Alpine Triassic, and *Nothosaurus* species most closely related to a Germanic taxon, does seem to indicate faunal exchange between the northern Gondwanan shelf, the Alpine intraplatform basins along the southeastern shelf of Europe, and the Germanic basin. This finding argues in favor of the existence of a Burgundian Gate during late Anisian and Ladinian times, linking the Germanic basin to the developing southern branch of the Neotethys. In view of the notorious incompleteness of the fossil record, more specific dispersal scenarios like the one developed above for some species of the genus *Nothosaurus* remain highly conjectural until similar patterns of phylogenetic relationships and geographic distribution can be independently established for different taxa. Cyamodontoid placodonts are the obvious candidates to be approached in a search for taxonomic congruence. The differences of faunal composition between the Germanic basin and the circum-Mediterranean realm, noted by the proponents of the concept of a separate Sephardic faunal province (Hirsch, 1972, 1976, 1977, 1984, 1986; Marquez-Aliaga et al., 1986) can perhaps best be explained with reference to different salinity tolerance of the taxa involved (Hagdorn, personal communication). Ammonoids and conodonts in particular show greater stenotopicity due to a lesser tolerance for salinity changes than the more tolerant bivalves and reptiles, which may have been more eurytopic, migrating more easily between habitats (F. Hirsch, in litt. 12 February 1997)

Summary and Conclusions

The Middle Triassic Muschelkalk of Makhtesh Ramon, Negev, has yielded a rich tetrapod fauna, including an indeterminate labyrinthodont amphibian (Zanon, 1991), *Tanystropheus,* cyamodontoid placodonts (*?Psephosaurus*), and sauropterygians. Eosauropterygia are the most frequently found vertebrate fossils; they comprise possible pachypleurosaurs, *Simosaurus* sp., at least three taxa of *Nothosaurus* (*Nothosaurus* cf. *N. giganteus, N. haasi,* and *N. tchernovi*), plus indeterminate nothosaur remains, and one lariosaur (*L. stensioei*). The use of cyamodontoids for historical biogeographical analysis remains impeded because the diagnosis of lower Muschelkalk taxa (*?Psephosaurus, Cyamodus*) remains incomplete.

At this time, cladistic relationships are resolved (yet poorly supported) only for nothosaurs (*Nothosaurus, Lariosaurus*). They indicate that the taxa from Makhtesh Ramon are most closely related to cladistically high-ranked taxa from the upper Muschelkalk of the Germanic basin (*N. giganteus* and *N. mirabilis*) or are nested within the hierarchical relationships of taxa known from the Alpine Triassic (*L. stensioei*). This pattern of cladistic relationships indicates paleobiogeographic affinities of the Makhtesh Ramon fauna with the Germanic and Alpine realm, supporting the hypothesis of a Burgundian Gate that connected the Germanic basin with the southern branch of the developing Neotethys.

In Makhtesh Ramon, the occurrence of eosauropterygians can be tied to a shallow marine habitat, characteristic of local, individualized basins that developed across the Gondwanan shelf as a result of fluctuating transgressions and regressions. *Nothosaurus haasi* and *N. tchernovi* are sister species and as such provide evidence for dichotomous speciation within the intraplatform basin habitat characteristic of the northern Gondwanan shelf (southern margin of the developing southern branch of the Neotethys). Cladogenesis of the *N. haasi–N. tchernovi* clade also indicates habitat partitioning between the two sister species resulting from that speciation event. The skulls of *N. haasi* and *N. tchernovi* differ not only in absolute size but also in osteological correlates, indicating different jaw mechanics. The skull of *N. tchernovi* is distinctly larger and retains proportions similar to those of *N. mirabilis,* with an elongated postorbital region, large upper temporal fenestrae, and numerous (>20) closely spaced teeth on the maxilla. The skull of *N. haasi* is much smaller and autapomorphic with respect to a relative shortening of the postorbital region of the skull and contains fewer (13) but more widely spaced teeth on the maxilla. Collectively, these characters indicate resource partitioning with respect to prey: i.e., different preferences for prey size and, perhaps, prey kind.

Acknowledgments

We thank Jim Clark (Washington), Hans Hagdorn (Ingelfingen), Francis Hirsch (Jerusalem),

and Hans-Dieter Sues (Toronto), who read an earlier draft of this manuscript or parts thereof, and offered much helpful advice and criticism. Peter Wagner and Chris Brochu helped with the Spearman rank correlation test. The painstaking printing of the photographs was done by Kimberly Mazanek of the Department of Photography at the Field Museum. This study was supported by U.S. National Science Foundation grant DEB-9419675 (to O.R.).

Literature Cited

ALAFONT, L. S., AND J. L. SANZ. 1996. Un nuevo Sauropterigio (Reptilia) en el Triasico de la Sierra de Prades (Tarragona). Cuadernos de Geologia Iberica, **20:** 313–329.

ARTHABER, G. 1924. Die Phylogenie der Nothosaurier. Acta Zoologica, Stockholm, **5:** 439–516.

BARDET, N., AND G. CUNY. 1993. Triassic reptile faunas from France. Paleontologia Lombarda, n.s., **2:** 9–14.

BAUR, G. 1889. *Palaeohatteria* Credner, and the Proganosauria. American Journal of Science, series 3, **37:** 310–313.

BELTAN, L., P. JANVIER, O. MONOD, AND F. WESTPHAL. 1979. A new marine fish and placodont reptile fauna of Ladinian age from southwestern Turkey. Neues Jahrbuch für Geologie und Paläontologie, Monatshefte, **1979:** 257–267.

BOULENGER, G. A. 1898. On a nothosaurian reptile from the Trias of Lombardy, apparently referable to *Lariosaurus*. Transactions of the Zoological Society of London, **14:** 1–10.

BROTZEN, F. 1955. Occurrence of vertebrates in the Triassic of Israel. Nature, **176:** 404–405.

———. 1957. Stratigraphical studies on the Triassic vertebrate fossils from Wadi Ramon, Israel. Arkiv för Mineralogi och Geologi, **2:** 191–217.

BÜRGIN, T., U. EICHENBERGER, H. FURRER, AND K. TSCHANZ. 1991. Die Prosanto-Formation—Eine fischreiche Fossil-Lagerstätte in der Mitteltrias der Sivretta-Decke (Kanton Gaubünden, Schweiz). Eclogae Geologicae Helvetiae, **84:** 921–990.

COX, L. R. 1924. A Triassic fauna from the Jordan Valley. Annals and Magazine of Natural History, series 9, **14:** 52–96.

———. 1932. Further notes on the Trans-Jordan Trias. Annals and Magazine of Natural History, series 10, **10:** 93–113.

CURIONI, G. 1847. Cenni sopra un nuovo saurio fossile dei monti di Perledo sul Lario e sul terreno che lo racchiude. Giornale del' J. R. Instituto Lombardo di Scienze, Lettre ed Arte, **16:** 159–170.

DALLA VECCHIA, F. M. 1993. Reptile remains from the Middle-Upper Triassic of the Carnic and Julian Alps (Friuli-Venezia Giulia, northeastern Italy). Gortania–Atti del Museo Friulano di Storia Naturale, **15:** 49–66.

DERCOURT, J., L. E. RICOU, AND B. VRIELYNCK, EDS. 1993. Atlas Tethys Paleoenvironmental Maps. Gauthier-Villars, Paris.

DRUCKMAN, Y. 1974. The stratigraphy of the Triassic Sequence in southern Israel. Geological Survey of Israel, Bulletin, **64:** 1–93.

FRAAS, E. 1896. Die Schwäbischen Trias-Saurier. E. Schweizerbart, Stuttgart.

FREUND, R., M. GOLDBERG, T. WEISSBROD, Y. DRUCKMAN, AND B. DERIN. 1975. The Triassic-Jurassic structure of Israel and its relation to the origin of the eastern Mediterranean. Geological Survey of Israel, Bulletin, **65:** 1–26.

FURRER, H., U. EICHENBERGER, N. FROITZHEIM, AND D. WÜSTER. 1992. Geologie, Stratigraphie und Fossilien der Ducankette und des Landwassergebiets (Silvretta-Decke, Ostalpin). Eclogae Geologicae Helvetiae, **85:** 246–256.

GARFUNKEL, Z., AND B. DERIN. 1984. Permian–early Mesozoic tectonism and continental margin formation in Israel and its implications for the history of the Eastern Mediterranean, pp. 187–201. *In* Dixon, J. E., and A. H. F. Robertson, eds., the Geological Evolution of the Eastern Mediterranean. Blackwell Scientific Publications, Oxford.

GORCE, F. 1960. Étude de quelques vertébrés du Muschelkalk du Djebel Rehach (Sud Tunisien). Mémoires de la Société Géologique de France, n.s., **88B:** 1–33.

GÜRICH, G. 1884. Über einige Saurier des oberschlesischen Muschelkalkes. Zeitschrift der Deutschen Geologischen Gesellschaft, **36:** 125–144.

HAAS, G. 1959. On some fragments of the dermal skeleton of Placodontia from the Trias of Aari en Naga, Sinai Peninsula. Kunglia Svenska Vetenskapsakademiensis Handlingar, series 4, **7:** 1–19.

———. 1963. *Micronothosaurus stensiöi*, ein neuer Nothosauride aus dem Oberen Muschelkalk des Wadi Ramon, Israel. Paläontologische Zeitschrift, **37:** 161–178.

———. 1967. On the vertebral centra of nothosaurs and placodonts from the Muschelkalk of Wadi Ramon, Israel. Colloque International, Centre National de la Recherche Scientifique, **163:** 329–334.

———. 1969. The armour of placodonts from the Muschelkalk of Wadi Ramon (Israel). Israel Journal of Zoology, **18:** 135–147.

———. 1970. Eine bemerkenswerte Interclavicula von (?)*Tanystropheus* aus dem Muschelkalk des Wadi Ramon, Israel. Paläontologische Zeitschrift, **44:** 207–214.

———. 1975. On the placodonts of the Wadi Ramon area Muschelkalk. Colloque International, Centre National de la Recherche Scientifique, **218:** 451–456.

———. 1980. Ein Nothosaurier-Schädel aus dem Muschelkalk des Wadi Ramon (Negev, Israel). Annalen des Naturhistorischen Museums Wien, **83:** 119–125.

———. 1981. A fragmentary skull of *Simosaurus* (Reptilia: Sauropterygia) from the Middle Triassic of the Makhtesh Ramon, Israel. Israel Journal of Zoology, **30:** 30–34.

HAGDORN, H. 1985. Immigration of crinoids into the German Muschelkalk basin, pp. 237–254. *In* Bayer, U., and A. Seilacher, eds., Sedimentary and Evolutionary Cycles. Springer, Heidelberg.

———. 1991. The Muschelkalk in Germany—An introduction, pp. 7–21. *In* Hagdorn, H., T. Simon, and J. Szulc, eds., Muschelkalk—A Field Guide. Goldschneck Verlag, Korb.

HIRSCH, F. 1972. Middle Triassic conodonts from Israel, southern France and Spain. Mitteilungen der Gesellschaft für Geologie und Bergbaustudien, **21:** 811–828.

———. 1976. Sur l'origine des particularismes de la faune du Trias et du Jurassique de la plate-forme africano-arabe. Bulletin de la Société Géologique de France, series 7, **18:** 543–552.

———. 1977. Essai de corrélation biostratigraphique des niveaux Méso- et Néotriasiques de facies "Muschelkalk" du domaine Sépharade. Cuadernos Geologia Iberica, **4:** 511–526.

———. 1984. The Arabian sub-plate during the Mesozoic, pp. 217–223. *In* Dixon, J. E., and A. H. F. Robertson, eds., The Geological Evolution of the Eastern Mediterranean. Blackwell Scientific Publications, Oxford.

———. 1986. The Gondwanian Triassic and Jurassic Tethys shelf: Sephardic and Ethiopian faunal realms, pp. 215–232. *In* McKenzie, K. G., ed., International Symposium on Shallow Tethys. Balkema, Rotterdam.

HUENE, F. V. 1948. Short review of the lower tetrapods, pp. 65–106. *In* Du Toit, A. L., ed., Robert Broom Commemorative Volume, Special Publication of the Royal Society of South Africa. Royal Society of South Africa, Cape Town.

———. 1952. Skelett und Verwandtschaft von *Simosaurus.* Palaeontographica, A, **102:** 163–182.

———. 1958. Aus den Lechtaler Alpen ein neuer *Anarosaurus.* Neues Jahrbuch für Geologie und Paläontologie, Monatshefte, **1958:** 382–384.

———. 1959. *Simosaurus guilielmi* aus dem unteren Mittelkeuper von Obersontheim. Palaeontographica, A, **113:** 180–184.

HUZA, R., T. JURCSAK, AND E. TALLODI. 1987. Fauna de reptile Triasice Din Bihor. Crisia, **17:** 571–578.

JAEKEL, O. 1907. *Placochelys placodonta* aus der Obertrias des Bakony. Resultate der wissenschaftlichen Erforschung des Balatonsees, I. Band. 1. Teil. Palaeontologischer Anhang. Victor Hornyanszky, Budapest.

JURCSAK, T. 1973. Date noi asupra reptilelor fosile de virsta Mesozoika din Transilvania. Nymphaea, **1:** 245–261.

———. 1976. Noi descoperini de reptile fossile in Triasicul de la Alesd. Nymphaea, **4:** 67–105.

———. 1977. Contributii noi privind placodontele si sauropterygienii din Triasicul de la Alesd (Bihor, Romania). Nymphaea, **5:** 5–30.

———. 1978. Rezultate noi in studiul saurienilor fosili de la Alesd. Nymphaea, **6:** 15–60.

———. 1982. Occurrences nouvelles des Sauriens mesozoiques de Roumanie. Vertebrata Hungarica, **21:** 175–184.

KOKEN, E. 1893. Beiträge zur Kenntnis der Gattung *Nothosaurus.* Zeitschrift der Deutschen Geologischen Gesellschaft, **45:** 337–377.

KOZUR, H. 1974. Probleme der Triasgliederung und Parallelisierung der germanischen und tethyalen Trias. Teil II: Anschluss der germanischen Trias an die internationale Triasgliederung. Freiberger Forschungshefte, Reihe C: Paläontologie, **2:** 51–77, Freiberg.

KUHN, O. 1969. Proganosauria, Bolosauria, Placodontia, Araeoscelidia, Trilophosauria, Weigeltisauria, Millerosauria, Rhynchocephalia, Protorosauria. Handbuch der Paläoherpetologie, Teil. 9. Gustav Fischer Verlag, Stuttgart.

KUHN-SCHNYDER, E. 1960. Über Placodontier. Paläontologische Zeitschrift, **34:** 91–102.

———. 1965. Der Typus-Schädel von *Cyamodus rostratus* Münster. Senckenbergiana Lethaea, **46a:** 257–289.

KUNISCH, H. 1888. Ueber eine Saurierplatte aus dem oberschlesischen Muschelkalke. Zeitschrift der Deutschen Geologischen Gesellschaft, **40:** 671–693.

LEHMAN, J. P. 1965. Les progrès récents de la Paléontologie des vertébrés du Trias au sud de la Méditerranée. Israel Journal of Zoology, **14:** 173–184.

MARCOUX, J., A. BAUD, L.-M. RICOU, M. GAETANI, L. KRYSTYN, Y. BELLION, R. GUIRAUD, C. MOREAU, J. BESSE, Y. GALLET, AND H. THEVENIAUT. 1993. Late Anisian (237 to 234 Ma), pp. 21–33. *In* Dercourt, J., L. E. Ricou, and B. Vrielynck, eds., Atlas Tethys Paleoenvironmental Maps. Gauthier-Villars, Paris.

MARQUEZ-ALIAGA, A., F. HIRSCH, AND A. LOPEZ-GARRIDO. 1986. Middle Triassic bivalves from the Hornos-Siles Formation (Sephardic Province, Spain). Neues Jahrbuch für Geologie und Paläontologie, Abhandlungen, **173:** 201–227.

MAY, P. R. 1991. The eastern Mediterranean basin: Evolution and oil habitat. The American Association of Petroleum Geologists Bulletin, **75:** 1215–1232.

MEYER, H. V. 1842. *Simosaurus,* die Stumpfschnauze, ein Saurier aus dem Muschelkalke von Luneville. Neues Jahrbuch für Mineralogie, Geognosie, Geologie und Petrefakten-Kunde, **1842:** 184–197.

MOSTLER, H. 1993. Das Germanische Muschelkalkbecken und seine Beziehungen zum tethyalen Muschelkalkmeer, pp. 11–14. *In* Hagdorn, H., and A. Seilacher, eds., Muschelkalk: Schöntaler Symposium 1991. Goldschneck Verlag, Korb.

MÜNSTER, G. 1834. Vorläufige Nachricht über einige neue Reptilien im Muschelkalke von Baiern. Neues Jahrbuch für Mineralogie, Geognosie, Geologie und Petrefaktenkunde, **1834:** 521–527.

———. 1839. Beiträge zur Petrefaktenkunde, mit XVIII nach der Natur gezeichneten Tafeln der Herren Hermann v. Meyer und Professor Rudolph Wagner. Buchner'sche Buchhandlung, Bayreuth.

NOPCSA, F. 1928. Palaeontological notes on reptiles. Geologica Hungaria, Ser. Palaeontologica, **1:** 3–84.

NORELL, M., AND M. NOVACEK. 1992. Congruence between superpositional and phylogenetic pattern: Comparing cladistic patterns with fossil records. Cladistics, **8:** 319–337.

NOSOTTI, S., AND G. PINNA. 1993a. New data on placodont skull anatomy. Paleontologia Lombarda, n.s., **2:** 109–130.

———. 1993b. *Cyamodus kuhn-schnyderi* n. sp., nouvelle espèce de Cyamodontidae (Reptilia, Placodontia) du Muschelkalk supérieur allemand. Comptes

Rendues à l'Académie des Sciences, Paris, **317:** 847–850.

———. 1996. Osteology of the skull of *Cyamodus kuhnschnyderi* Nosotti & Pinna, 1993 (Reptilia, Placodontia). Paleontologia Lombarda, n.s., **6:** 1–42.

Owen, R. 1860. Palaeontology. Adam and Charles Black, Edinburgh.

Parnes, A. 1962. Triassic ammonites from Israel. Geological Survey of Israel, Bulletin, **33:** 1–59.

———. 1965. Note on Middle Triassic ammonites from Makhtesh Ramon (southern Israel). Israel Journal of Earth-Sciences, **14:** 9–17.

———. 1975. Middle Triassic ammonite biostratigraphy in Israel. Geological Survey of Israel, Bulletin, **66:** 1–44.

———. 1986. Middle Triassic cephalopods from the Negev (Israel) and Sinia (Egypt). Geological Survey of Israel, Bulletin, **79:** 9–59.

Parnes, A., C. Benjamini, and F. Hirsch. 1985. New aspects of Triassic ammonoid biostratigraphy, paleoenvironments, and paleobiogeography in southern Israel. Journal of Paleontology, **59:** 656–666.

Peyer, B. 1935. Die Triasfauna der Tessiner Kalkalpen. VIII. Weitere Placodontierfunde. Abhandlungen der Schweizerischen Paläontologischen Gesellschaft, **55:** 1–26.

———. 1939. Die Triasfauna der Tessiner Kalkalpen. XIV. *Paranothosaurus amsleri* nov. gen. nov. spec. Abhandlungen der Schweizerschen Paläontologischen Gesellschaft, **62:** 1–87.

———. 1955. Demonstration von Trias-Vertebraten aus Palästina. Eclogae Geologicae Helvetiae, **48:** 486–490.

Peyer, B., and E. Kuhn-Schnyder. 1955. Placodontia, pp. 459–486. *In* Piveteau, J., ed., Traité de Paléontologie, vol. 5. Masson, Paris.

Pinna, G., and S. Nosotti. 1989. Anatomie, morfologia funzionale e paleoecologia del rettile placodonte *Psephoderma alpinum* Meyer, 1858. Memorie della Società Italiana di Scienze Naturali e del Museo Civico di Storia Naturale di Milano, **25:** 1–50.

Renesto, S. 1993. A juvenile *Lariosaurus* (Reptilia, Sauropterygia) from the Kalkschieferzone (uppermost Ladinian) near Viggiù (Varese, Northern Italy). Rivista Italiana di Paleontologia e Stratigrafia, **99:** 199–212.

Rieppel, O. 1989. A new pachypleurosaur (Reptilia: Sauropterygia) from the Middle Triassic of Monte San Giorgio, Switzerland. Philosophical Transactions of the Royal Society of London, B, **323:** 1–73.

———. 1993a. Status of *Psilotrachelosaurus toeplitschi* Nopcsa (Reptilia, Sauropterygia), from the Middle Triassic of Austria. Fieldiana (Geology), n.s., **27:** 1–17.

———. 1993b. The status of the nothosaurian reptile *Elmosaurus lelmensis*, with comments on *Nothosaurus mirabilis*. Palaeontology, **36:** 967–974.

———. 1994a. Osteology of *Simosaurus* and the interrelationships of stem-group Sauropterygia (Reptilia, Diapsida). Fieldiana (Geology), n.s., **28:** 1–85.

———. 1994b. The status of the sauropterygian reptile *Nothosaurus juvenilis* from the Middle Triassic of Germany. Paleontology, **37:** 733–745.

———. 1994c. The braincases of *Simosaurus* and *Nothosaurus:* Monophyly of the Nothosauridae (Reptilia: Sauropterygia). Journal of Vertebrate Paleontology, **14:** 9–23.

———. 1995a. The genus *Placodus:* Systematics, morphology, paleobiogeography and paleobiology. Fieldiana: Geology, n.s., **31:** 1–44.

———. 1995b. The status of *Anarosaurus multidentatus* von Huene (Reptilia, Sauropterygia), from the lower Anisian of the Lechtaler Alps (Arlberg, Austria). Paläontologische Zeitschrift, **69:** 289–299.

———. 1996. The status of the sauropterygian reptile *Partanosaurus zitteli* Skuphos from the Middle Triassic of the Austrian Alps, with comments on *Microleptosaurus schlosseri* Skuphos. Paläontologische Zeitschrift, **70:** 567–577.

———. 1997a. Revision of the sauropterygian reptile genus *Cymatosaurus* Fritsch, 1894, and the relationships of *Germanosaurus* Nopcsa, from the Middle Triassic of Europe. Fieldiana: Geology, n.s., **36:** 1–38.

———. 1997b. Sauropterygia from the Muschelkalk of Djebel Rehach, southern Tunisia. Neues Jahrbuch für Geologie und Paläontologie, Monatshefte, **1997:** 517–530.

———. 1998. The status of the sauropterygian reptile genera *Ceresiosaurus, Lariosaurus,* and *Silvestrosaurus* from the Middle Triassic of Europe. Fieldiana: Geology, n.s., **38:** 1–46.

Rieppel, O., and H. Hagdorn. 1997. Paleobiogeography of Middle Triassic Sauropterygia in Central and Western Europe, pp. 121–144. *In* Callaway, J. M., and E. L. Nicholls, eds., Sea Reptiles of the Past. Academic Press, San Diego.

———. In press. Fossil reptiles from the Spanish Muschelkalk (Mont-ral and Alcover, Province Tarragona). Historical Biology.

Rieppel, O., and K. Lin. 1995. Pachypleurosaurs (Reptilia: Sauropterygia) from the lower Muschelkalk, and a review of the Pachypleurosauroidea. Fieldiana: Geology, n.s., **32:** 1–44.

Rieppel, O., J. M. Mazin, and E. Tchernov. 1997. Speciation along rifting continental margins: A new nothosaur from the Negev (Israel). Comptes Rendues à l'Académie des Sciences, Paris, **325:** 991–997.

Rieppel, O., and R. Werneburg. 1998. A new species of the sauropterygian reptile genus *Cymatosaurus* from the lower Muschelkalk of Thuringia, Germany. Palaeontology, **41:** 575–589.

Rieppel, O., and R. Wild. 1994. *Nothosaurus edingerae* Schultze, 1970: Diagnosis of the species and comments on its stratigraphical occurrence. Stuttgarter Beiträge für Naturkunde, B, **204:** 1–13.

———. 1996. A revision of the genus *Nothosaurus* (Reptilia, Sauropterygia) from the Germanic Triassic, with comments on the status of *Conchiosaurus clavatus*. Fieldiana: Geology, n.s., **34:** 1–82.

Rieppel, O., and Zanon, R. T. 1997. The interrelationships of Placodontia. Historical Biology, **12:** 211–227.

Robertson, A. H. F., and J. E. Dixon. 1984. Introduction: Aspects of the geological evolution of the East-

ern Mediterranean, pp. 1–74. *In* Dixon, J. E., and A. H. F. Robertson, eds., The Geological Evolution of the Eastern Mediterranean. Blackwell Scientific Publications, Oxford.

SANDER, P. M. 1989. The pachypleurosaurids (Reptilia: Nothosauria) from the Middle Triassic of Monte San Giorgio (Switzerland), with the description of a new species. Philosophical Transactions of the Royal Society of London, B, **325:** 561–670.

SANZ, J. L. 1976. *Lariosaurus balsami* (Sauropterygia, Reptilia) de Estada (Huesca). Estudios Geologicos, **32:** 547–567.

———. 1983a. Los Nothosaurios (Reptilia, Sauropterygia) Espanoles. Estudios Geologicos, **39:** 193–215.

———. 1983b. Consideraciones sobre el genero *Pistosaurus*. El suborden Pistosauria (Reptilia, Sauropterygia). Estudios Geologicos, **39:** 451–458.

SCHRÖDER, H. 1914. Wirbeltiere der Rüdersdorfer Trias. Abhandlungen der Preussischen Geologischen Landesanstalt, Neue Folge, **65:** 1–98.

SCHULTZE, H.-P. 1970. Über *Nothosaurus*. Neubeschreibung eines Schädels aus dem Keuper. Senckenbergiana Lethaea, **51:** 211–237.

SEELEY, H. G. 1882. On *Neusticosaurus pusillus* (Fraas), an amphibious reptile having affinities with terrestrial Nothosauria and with marine Plesiosauria. Quarterly Journal of the Geological Society of London, **38:** 350–366.

———. 1889 (1890). Researches on the structure, organization, and classification of the fossil Reptilia. VI. On the anomodont Reptilia and their allies. Philosophical Transactions of the Royal Society of London, B, **180:** 215–296.

SENGÖR, A. M. C., Y. YILMAZ, AND O. SUNGURLU. 1984. Tectonics of the Mediterranean Cimmerides: Nature and evolution of the western termination of the Palaeo-Tethys, pp. 77–112. *In* Dixon, J. E., and A. H. F. Robertson, eds., The Geological Evolution of the Eastern Mediterranean. Blackwell Scientific Publications, Oxford.

SENKOWICZOWA, H., AND A. SZYPERKO-SLIWCZYNSKA. 1975. Stratigraphy and paleogeography of the Trias. Bulletin of the Geological Institute, Warszawa, **252:** 131–147.

SESTINI, G. 1984. Tectonic and sedimentary history of the NE African margin (Egypt-Lybia), pp. 161–175. *In* Dixon, J. E., and A. H. F. Robertson, eds., The Geological Evolution of the Eastern Mediterranean. Blackwell Scientific Publications, Oxford.

SHAW, S. H. 1947. Southern Palestine: Geological map on a scale of 1/250 000 with explanatory notes. Government of Palestine, Jerusalem.

SIRNA, G., F. M. DALLA VECCHIA, G. MUSCIO, AND G. PICCOLI. 1994. Catalogue of Paleozoic and Mesozoic vertebrates and vertebrate localities of the Tre Venezie area (northeastern Italy). Memorie di Scienze Geologiche, **46:** 255–281.

STORRS, G. W. 1991. Anatomy and relationships of *Corosaurus alcovensis* (Diapsida: Sauropterygia) and the Triassic Alcova Limestone of Wyoming. Bulletin of the Peabody Museum of Natural History, **44:** 1–151.

SUES, H.-D. 1987. Postcranial skeleton of *Pistosaurus* and interrelationships of the Sauropterygia (Diapsida). Zoological Journal of the Linnean Society, **90:** 109–131.

SWINTON, W. E. 1952. A nothosaurian vertebra from Israel. Annals and Magazine of Natural History, series 12, **15:** 875–876.

SWOFFORD, D. L. 1990. PAUP—Phylogenetic Analysis Using Parsimony, Version 3.0. Illinois Natural History Survey, Champaign, Ill.

SWOFFORD, D. L., AND D. P. BEGLE. 1993. PAUP—Phylogenetic Analysis Using Parsimony, Version 3.1. Laboratory of Molecular Systematics, Smithsonian Institution, Washington, D.C.

SZULC, J. 1991. The Upper Silesian Muschelkalk—A general setting, pp. 61–62. *In* Hagdorn, H., ed., Muschelkalk, A Field Guide. Korb (Goldschneck), Stuttgart.

TSCHANZ, K. 1989. *Lariosaurus buzzii* n. sp. from the Middle Triassic of Monte San Giorgio (Switzerland), with comments on the classification of nothosaurs. Palaeontographica, A, **208:** 153–179.

URLICHS, M., AND R. MUNDLOS. 1985. Immigration of cephalopods into the Germanic Muschelkalk Basin and its influence on their suture line, pp. 221–236. *In* Bayer, U., and A. Seilacher, eds., Sedimentary and Evolutionary Cycles. Springer Verlag, Heidelberg.

WESTPHAL, F. 1975. Bauprinzipien im Panzer der Placodonten (Reptilia triadica). Paläontologische Zeitschrift, **49:** 97–125.

WESTPHAL, F., AND I. WESTPHAL. 1967. Die Pflasterzahnsaurier (Placodontier) der Germanischen Trias. Der Aufschluss, **18:** 249–255.

WILD, R. 1973. Die Triasfauna der Tessiner Kalkalpen. XXIII. *Tanystropheus longobardicus* (Bassani). Schweizerische Paläontologische Abhandlungen. **95:** 1–162.

———. 1987. An example of biological reasons for extinction: *Tanystropheus* (Reptilia, Squamata). Mémoires de la Société Géologique de France, n.s., **150:** 37–44.

ZAK, I. 1986. The Triassic Period in southern Israel. Geological Survey of Israel, Bulletin, **79:** 1–8.

ZANON, R. T. 1991. *Negevodus ramonensis* Mazin, 1986, reinterpreted as a temnospondyl, not a placodont. Journal of Vertebrate Paleontology, **11:** 515–518.

ZIEGLER, P. A. 1982. Triassic rifts and facies patterns in Western and Central Europe. Geologische Rundschau, **71:** 747–772.

ZITTEL, K. A. V. 1887. Handbuch der Palaeontologie, I. Abtheilung. Palaeozoologie, III. Band. Vertebrata (Pisces, Amphibia, Reptilia, Aves). R. Oldenbourg, München und Leipzig.

Appendix I: Character Definitions for the Data Matrix Shown in Table 5

See Rieppel (1994a, 1997a, 1998) for a complete discussion of characters and for references.

1. Premaxillae are small (0) or large (1), forming most of snout in front of external nares.
2. Premaxilla is without (0) or with (1) postnarial process, excluding maxilla from posterior margin of external naris.
3. Snout is unconstricted (0) or constricted (1).
4. Temporal region of skull is relatively high (0) or strongly depressed (1).
5. Nasals are shorter (0) or longer (1) than frontal(s).
6. Nasals are not reduced (0), somewhat reduced (1), or strongly reduced or absent (2).
7. Nasals do (0) or do not (1) enter external naris.
8. Nasals meet in dorsomedial suture (0) or are separated from one another by nasal processes of the premaxillae extending back to the frontal bone(s) (1).
9. The lacrimal is present and enters the external naris (0), or it is present but remains excluded from the external naris by a contact of maxilla and nasal (1), or it is absent (2).
10. The prefrontal and postfrontal are separated by the frontal along the dorsal margin of the orbit (0), or a contact of prefrontal and postfrontal excludes the frontal from the dorsal margin of the orbit (1).
11. Dorsal exposure of prefrontal is large (0) or reduced (1).
12. Preorbital and postorbital regions of skull are of subequal length (0); preorbital region is distinctly longer than postorbital region (1); postorbital region is distinctly longer (2).
13. Upper temporal fossa are absent (0), present and subequal in size or slightly larger than the orbit (1), present and distinctly larger than orbit (2), or present and distinctly smaller than orbit (3).
14. Frontal(s) are paired (0) or fused (1) in the adult.
15. Frontal(s) are without (0) or with (1) distinct posterolateral processes.
16. Frontal is widely separated from the upper temporal fossa (0), narrowly approaches the upper temporal fossa (1), or enters the anteromedial margin of the upper temporal fossa (2).
17. Parietal(s) are paired (0), fused in their posterior part only (1), or fully fused (2) in adult.
18. Pineal foramen is close to the middle of the skull table (0), weakly displaced posteriorly (1), strongly displaced posteriorly (2), displaced anteriorly (3), or absent (4).
19. Parietal skull table is broad (0), weakly constricted (1), strongly constricted (at least posteriorly) (2), or forms a sagittal crest (3).
20. Postparietals are present (0) or absent (1).
21. Tabulars are present (0) or absent (1).
22. Supratemporals are present (0) or absent (1).
23. The jugal extends anteriorly along the ventral margin of the orbit (0), is restricted to a position behind the orbit but enters its posterior margin (1), or is restricted to a position behind the orbit without reaching its posterior margin (2).
24. The jugal extends backward no farther than to the middle of the cheek region (0) or nearly to the posterior end of the skull (1).
25. The jugal remains excluded from (0) or enters (1) the upper temporal arch.
26. Postfrontal is large and platelike (0), with distinct lateral process overlapping the dorsal tip of the postorbital (1) or postfrontal, with reduced lateral process and of hence a more elongated shape (2).
27. Lower temporal fossa is absent (0), present and closed ventrally (1), or present but open ventrally (2).
28. Squamosal descends to (0) or remains broadly separated from (1) ventral margin of skull.
29. Quadratojugal is present (0) or absent (1).
30. Quadratojugal has (0) or lacks (1) anterior process.
31. Occiput with paroccipital process which forms the lower margin of the posttemporal fossa and extends laterally (0), paroccipital processes trend posteriorly (1), or occiput is platelike with no distinct paroccipital process and with strongly reduced posttemporal fossae (2).
32. Squamosal is without (0) or with (1) distinct notch to receive distal tip of paroccipital process.
33. Mandibular articulations are approximately on a level with occipital condyle (0) or displaced to a level distinctly behind occipital condyle (1), or they are positioned anterior to the occipital condyle (2).

34. Exoccipitals do (0) or do not (1) meet dorsal to the basioccipital condyle.
35. Supraoccipital is exposed more or less vertically on occiput (0) or more or less horizontally at posterior end of parietal skull table (1).
36. Occipital crest is absent (0) or present (1).
37. Quadrate has straight posterior margin (0) or the quadrate shaft is deeply excavated (concave) posteriorly (1).
38. Quadrate is covered by squamosal and quadratojugal in lateral view (0) or exposed in lateral view (1).
39. Dorsal wing of epipterygoid is broad (0) or narrow (1).
40. Lateral conch on quadrate is absent (0) or present (1).
41. Palate is kinetic (0) or akinetic (1).
42. Basioccipital tubera are free (0) or in complex relation to the pterygoid, as they extend ventrally (1) or laterally (2).
43. Suborbital fenestra is absent (0) or present (1).
44. Pterygoid flanges are well developed (0) or strongly reduced (1).
45. Premaxillae enter internal naris (0) or are excluded (1).
46. Ectopterygoid is present (0) or absent (1).
47. Internal carotid passage enters basicranium (0) or quadrate ramus of pterygoid (1).
48. Retroarticular process of lower jaw is absent (0) or present (1).
49. Distinct coronoid process of lower jaw is absent (0) or present (1).
50. Surangular does not have (0) or has (1) strongly projecting lateral ridge defining the insertion area for superficial adductor muscle fibers on the lateral surface of the lower jaw.
51. Mandibular symphysis is short (0), somewhat enforced (1), or elongated and scoop like (2).
52. Splenial bone enters the mandibular symphysis (0) or remains excluded therefrom (1).
53. Teeth are set in shallow or deep sockets (0) or are superficially attached to bone (1).
54. Anterior (premaxillary and dentary) teeth are upright (0) or strongly procumbent (1).
55. Premaxillary and anterior dentary fangs are absent (0) or present (1).
56. One or two caniniform teeth are present (0) or absent (1) on maxilla.
57. The maxillary tooth row is restricted to a level in front of the posterior margin of the orbit (0), or it extends backward to a level below the posterior corner of the orbit and/or the anterior corner of the upper temporal fossa (1), or it extends backward to a level below the anterior one-third to one-half of the upper temporal fossa (2).
58. Teeth on pterygoid flange are present (0) or absent (1).
59. Vertebrae are notochordal (0) or nonnotochordal (1).
60. Vertebrae are amphicoelous (0), platycoelous (1), or other (2).
61. Dorsal intercentra are present (0) or absent (1).
62. Cervical intercentra are present (0) or absent (1).
63. Cervical centra are rounded (0) or keeled (1) ventrally.
64. Zygosphene–zygantrum articulation is absent (0) or present (1).
65. Sutural facets receiving the pedicels of the neural arch on the dorsal surface of the centrum in the dorsal region are narrow (0) or expanded into a cruciform or butterfly-shaped platform (1).
66. Transverse processes of neural arches of the dorsal region are relatively short (0) or distinctly elongated (1).
67. Vertebral centrum is distinctly constricted in ventral view (0) or with parallel lateral edges (1).
68. Distal end of transverse processes of dorsal vertebrae do not increase in diameter (0) or are distinctly thickened (1).
69. Zygapophyseal pachyostosis is absent (0) or present (1).
70. Pre-and postzygapophyses do not (0) or do (1) show an anteroposterior trend of increasing inclination within the dorsal and sacral region.
71. Cervical ribs are without (0) or with (1) a distinct free anterior process.
72. Pachyostosis of dorsal ribs is absent (0) or present (1).
73. The number of sacral ribs is two (0), three (1), or four or more (2).
74. Sacral ribs have (0) or lack (1) distinct expansion of distal head.
75. Sacral (and caudal) ribs or transverse processes are sutured (0) or fused (1) to their respective centrum.
76. Cleithrum is present (0) or absent (1).

77. Clavicles are broad (0) or narrow (1) medially.
78. Clavicles are positioned dorsally (0) or anteroventrally (1) to the interclavicle.
79. Clavicles do not meet in front of the interclavicle (0) or meet in an interdigitating anteromedial suture (1).
80. Clavicles lack (0) or have (1) anterolaterally expanded corners.
81. Clavicle is applied to the anterior (lateral) (0) or to the medial (1) surface of scapula.
82. Interclavicle is rhomboidal (0) or T-shaped (1).
83. Posterior process on (T-shaped) interclavicle is elongate (0), short (1), or rudimentary or absent (2).
84. Scapula is represented by a broad blade of bone (0), or with a constriction separating a ventral glenoidal portion from a posteriorly directed dorsal wing (1).
85. The dorsal wing or process of the eosauropterygian scapula tapers to a blunt tip (0) or is ventrally expanded at its posterior end (1).
86. Supraglenoid buttress is present (0) or absent (1).
87. One (0) or two (1) coracoid ossifications are present.
88. Coracoid has rounded contours (0), is slightly waisted (1), is strongly waisted (2), or has expanded medial symphysis (3).
89. Coracoid foramen is enclosed by coracoid ossification (0), or lies between coracoid and scapula (1).
90. Pectoral fenestration is absent (0) or present (1).
91. Limbs are short and stout (0) or long and slender (1).
92. Humerus is rather straight (0) or "curved" (1).
93. Deltopectoral crest is well developed (0) or reduced (1).
94. Insertional crest for latissimus dorsi muscle is prominent (0) or reduced (1).
95. Humerus has prominent (0) or reduced (1) epicondyles.
96. The ectepicondylar groove is open and notched anteriorly (0), open without anterior notch (1), or closed (i.e., ectepicondylar foramen present) (2).
97. Entepicondylar foramen is present (0) or absent (1).
98. Radius is shorter than ulna (0), longer than ulna (1), or approximately the same length (2).
99. Iliac blade is well developed (0), reduced but projecting beyond level of posterior margin of acetabular portion of ilium (1), reduced and no longer projecting beyond posterior margin of acetabular portion of ilium (2), or absent, i.e., reduced to a simple dorsal stub (3).
100. Pubis has convex (0) or concave (1) ventral (medial) margin.
101. Obturator foramen is closed (0) or open (1) in adult.
102. Thyroid fenestra is absent (0) or present (1).
103. Acetabulum is oval (0) or circular (1).
104. Femoral shaft is stout and straight (0) or slender and sigmoidally curved (1).
105. Internal trochanter is well developed (0) or reduced (1).
106. Intertrochanteric fossa is deep (0), distinct but reduced (1), or rudimentary or absent (2).
107. Distal femoral condyles are prominent (0) or do not project is markedly beyond shaft (1).
108. Anterior femoral condyle relative to posterior condyle is larger and extends further distally (0) or is smaller/equisized and of subequal extent distally (1).
109. The perforating artery passes between astragalus and calcaneum (0) or between the distal heads of tibia and fibula proximal to the astragalus (1).
110. Astragalus lacks (0) or has (1) a proximal concavity.
111. Calcaneal tuber is absent (0) or present (1).
112. Foot is short and broad (0) or long and slender (1).
113. Distal tarsal 1 is present (0) or absent (1).
114. Distal tarsal 5 is present (0) or absent (1).
115. Total number of tarsal ossifications is four or more (0), three (1), or two (2).
116. Metatarsal 5 is long and slender (0) or distinctly shorter than the other metatarsals and with a broad base (1).
117. Metatarsal 5 is straight (0) or "hooked" (1).
118. Mineralized sternum is absent (0) or present (1).
119. The medial gastral rib element always has only a single (1) lateral process, or may have a two-pronged lateral process (1).
120. Ulna is slender (0) or broadened (1) at mid-diaphysis.
121. Ulna lacks (0) or has (1) a distinctly broadened proximal head.
122. Hyperphalangy is absent (0) or present (1) in manus.

A Selected Listing of Other *Fieldiana: Geology* Titles Available

Status of the Pachypleurosauroid *Psilotrachelosaurus toeplitschi* Nopcsa (Reptilia: Sauropterygia), from the Middle Triassic of Austria. By Olivier Rieppel. *Fieldiana: Geology*, n.s., no. 27, 1993. 17 pages, 9 illus.

Publication 1448, $10.00

Osteology of *Simosaurus gaillardoti* and the Relationships of Stem-Group Sauropterygia. By Olivier Rieppel. *Fieldiana: Geology*, n.s., no. 28, 1994. 85 pages, 71 illus.

Publication 1462, $18.00

The Genus *Placodus*: Systematics, Morphology, Paleobiogeography, and Paleobiology. By Olivier Rieppel. *Fieldiana: Geology*, n.s., no. 31, 1995. 44 pages, 47 illus.

Publication 1472, $12.00

Pachypleurosaurs (Reptilia: Sauropterygia) from the Lower Muschelkalk, and a Review of the Pachypleurosauroidea. By Olivier Rieppel and Lin Kebang. *Fieldiana: Geology*, n.s., no. 32, 1995. 44 pages, 28 illus.

Publication 1473, $12.00

A Revision of the Genus *Nothosaurus* (Reptilia: Sauropterygia) from the Germanic Triassic, with Comments on the Status of *Conchiosaurus clavatus*. By Olivier Rieppel and Rupert Wild. *Fieldiana: Geology*, n.s., no. 34, 1996. 82 pages, 66 illus.

Publication 1479, $17.00

Revision of the Sauropterygian Reptile Genus *Cymatosaurus* v. Fritsch, 1894, and the Relationships of *Germanosaurus* Nopcsa, 1928, from the Middle Triassic of Europe. By Olivier Rieppel. *Fieldiana: Geology*, n.s., no. 36, 1997. 38 pages, 16 illus.

Publication 1484, $11.00

The Status of the Sauropterygian Reptile Genera *Ceresiosaurus*, *Lariosaurus*, and *Silvestrosaurus* from the Middle Triassic of Europe. By Olivier Rieppel. *Fieldiana: Geology*, n.s., no. 38, 1998. 46 pages, 21 illus.

Publication 1490, $15.00

Order by publication number and/or ask for a free copy of our price list. All orders must be prepaid. Illinois residents add current destination tax. All foreign orders are payable in U.S. dollar-checks drawn on any U.S. bank or the U.S. subsidiary of any foreign bank. Prices and terms subject to change without notice. Address all requests to:

FIELD MUSEUM OF NATURAL HISTORY
Library—Publications Division
Roosevelt Road at Lake Shore Drive
Chicago, Illinois 60605-2498, U.S.A.

Field Museum of Natural History
Roosevelt Road at Lake Shore Drive
Chicago, Illinois 60605-2496
Telephone: (312) 922-9410